UNIVERSITY OF CALIFORNIA SAN DIEGO

Spatiotemporal regulation of axonal growth and protein synthesis by BDNF in hippocampal neurons

A dissertation submitted in partial satisfaction of the requirements for the degree Doctor of Philosophy

in

Neurosciences

by

Orlangie Natera

Committee in charge:

Professor William Mobley, Chair
Professor Brenda Bloodgood
Professor Jens Lykke-Andersen
Professor Gentry Patrick
Professor Binhai Zheng

2018

The Dissertation of Orlangie Natera is approved, and it is acceptable in quality and form for publication on microfilm and electronically:

_____

_____

_____

_____

Co-Chair

_____

Chair

University of California San Diego

2018

DEDICATION

To my niece, Amaia Natera, for being my main source of inspiration and hope.

Y a mis padres, Orlando y Angela, por su amor y apoyo incondicional.

TABLE OF CONTENTS

LIST OF ABBREVIATIONS

4E-BP	Initiation factor 4E-binding protein
AC	Axonal compartment
ActD	Actinomycin-D
AHA	Azidohomoalanine
AKT	Protein kinase B
ANOVA	Analysis of variance
Arc	Activity-regulated cytoskeleton-associated protein
Bcl2	B-cell lymphoma 2 apoptosis regulator
BDNF	Brain-derived neurotrophic factor
CFOS	FBJ osteosarcoma oncogene
CHX	Cycloheximide
CNS	Central nervous system
CREB	Cyclic AMP responsive element binding protein
DIV	Days *in vitro*
DRG	Dorsal root ganglion
EIF4E	Eukaryotic initiation factor 4E
Elk1	ETS-domain containing transcription factor
ERK	Extracellular signal-regulated kinase
FoxO	Forkhead box transcription factor, class O
FUNCAT	Fluorescent non-canonical amino acid tagging

GTPase	Guanosine triphosphate hydrolase
IEG	Immediate early gene
LIMK1	LIM-domain kinase 1
MAP1B	Microtubule-associated protein 1B
MAPK	Mitogen-activated protein kinase
MEF2	Myocyte enhancer factor 2
MTOR	Mechanistic target of rapamycin
MTORC1	Mechanistic target of rapamycin complex 1
NFAT	Nuclear factor of activated T-cells
NGF	Nerve growth factor
NT-3	Neurotrophin 3
NT-4	Neurotrophin 4
P75	Low-affinity neurotrophin receptor p75
PC12	Pheochromocytoma-derived cell line
PDMS	Polydimethylsiloxane
PI3K	Phosphatidylinositol-3-kinase
PLCγ	Phospholipase Cγ
PNS	Peripheral nervous system
PTB	Phosphotyrosine-binding domain
PTEN	Phosphatase and tensin homolog
RGC	Retinal ganglion cell
Rheb	Ras homolog enriched in brain

RSK	90 kDa ribosomal protein S6 kinase
S6K	70 kDa ribosomal protein S6 kinase
SC	Somatodendritic compartment
SCG	Superior cervical ganglion
SH2	Src-homology 2
SNAP25	Synaptosomal-associated protein 25
SRF	Serum response factor
TrkA	Tyrosine kinase receptor A
TrkB	Tyrosine kinase receptor B
TrkC	Tyrosine kinase receptor C
TSC2	Tuberous sclerosis complex subunit 2

LIST OF FIGURES

LIST OF TABLES

ACKNOWLEDGEMENTS

First, I wish to express my immense gratitude to my advisor, Dr. William Mobley, for his continuous guidance and support over the course of my PhD. His keen intellect, patience, and kindness were instrumental for the completion of this work.

I would like to give special thanks to Dr. Brenda Bloodgood and Dr. Gentry Patrick for their extensive help, encouragement and guidance throughout all these years. I would also like to thank Dr. Binhai Zheng and Dr. Jens Lykke-Andersen for their invaluable insight and support as part of my doctoral committee.

I would also like to acknowledge present and former members of the Mobley lab for their support and camaraderie. In particular, I am extremely thankful to Dr. Mariko Sawa for her great mentorship and support, both scientifically and personally— this dissertation would not have been completed without her help. I also thank Ann Becker for all her assistance, patience and friendship throughout all my years in the lab. Also, April Weissmiller, for her help and guidance during my first years in the lab.

Special thanks to Erin Gilbert in the UCSD Neuroscience department for her unwavering support and kindness.

I would also like to acknowledge my former mentors at NIH— Dr. Barry Kaplan, Dr. Aschrafi and Anthony Gioio— for their excellent training, mentorship and contribution to my professional development.

In addition, I wish to thank various friends and family members who have been a great source of strength and moral support throughout all these years. I thank Stephanie Alfonso and her family for all their love and support. Joshua François, thanks for being a wonderful friend and for all your help. My dear friend Vonmarie Martinez, thanks for your encouragement and love and for not giving up on me— I could not have done this without you. Finally, I wish to express my greatest gratitude to my dear parents, my brother Orlando, my abuela, my aunt and cousins for their unconditional love and support and for providing me the strength to endure the most difficult times.

Chapter 1, in part, is currently being prepared for submission for publication of the material. Natera-Naranjo, O and Mobley, W.C. The dissertation author was the primary investigator and author of this material.

Chapter 2, in full, is currently being prepared for submission for publication of the material. Natera-Naranjo, O and Mobley, W.C. The dissertation author was the primary investigator and author of this material.

VITA

2004-2008	Bachelor of Science in Chemistry University of Puerto Rico, Mayagüez, PR
2008-2010	Post-baccalaurate Research Fellow, National Institute of Mental Health, NIH, Bethesda, MD
2010-2018	Doctor of Philosophy in Neurosciences University of California, San Diego

PUBLICATIONS

Natera-Naranjo, O., and Mobley, W.C. 2019 (manuscript *in preparation*)

Le, M.H., Weissmiller, A.M., Monte, L., Lin, P.H., Hexom, T.C., **Natera, O**., Wu, C., and Rissman, R.A. 2016. "Functional Impact of Corticotropin-Releasing Factor Exposure on Tau Phosphorylation and Axon Transport." *PLoS One* 11 (1):e0147250.

Weissmiller, A. M., **Natera-Naranjo, O.**, Reyna, S.M., Pearn, M.L., Zhao, X., Nguyen, P., Cheng, S., Goldstein, L.S., Tanzi, R.E., Wagner, S.L., Mobley, W.C., and Wu, C. 2015. "A γ-secretase inhibitor, but not a γ-secretase modulator, induced defects in BDNF axonal trafficking and signaling: evidence for a role for APP." *PLoS One* 10 (2):e0118379.

Aschrafi, A., Kar, A.N., **Natera-Naranjo, O**., MacGibeny, M.A., Gioio, A.E., and Kaplan, B.B. 2012. "MicroRNA-338 regulates the axonal expression of multiple nuclear-encoded mitochondrial mRNAs encoding subunits of the oxidative phosphorylation machinery." *Cell Mol Life Sci* 69 (23):4017-27.

Natera-Naranjo, O., Kar, A.N., Aschrafi, A., Gervasi, N.M., Macgibeny, M.A., Gioio, A.E., and Kaplan, B.B. 2012. "Local translation of ATP synthase subunit 9 mRNA alters ATP levels and the production of ROS in the axon." *Mol Cell Neurosci* 49 (3):263-70.

Natera-Naranjo, O., Aschrafi, A., Gioio, A.E., and Kaplan, B.B. 2010. "Identification and quantitative analyses of microRNAs located in the distal axons of sympathetic neurons." *RNA* 16 (8):1516-29.

Aschrafi, A., **Natera-Naranjo, O.**, Gioio, A.E., and Kaplan, B.B. 2010. "Regulation of axonal trafficking of cytochrome c oxidase IV mRNA." *Mol Cell Neurosci* 43 (4): 422-30.

Aschrafi, A., Schwechter, A.D., Mameza, M.G., **Natera-Naranjo, O.**, Gioio, A.E., and Kaplan, B.B. 2008. "MicroRNA-338 regulates local cytochrome c oxidase IV mRNA levels and oxidative phosphorylation in the axons of sympathetic neurons." *J Neurosci* 28 (47):12581-90.

ABSTRACT OF THE DISSERTATION

Spatiotemporal regulation of axonal growth and protein synthesis by BDNF in hippocampal neurons

by

Orlangie Natera

Doctor of Philosophy in Neurosciences

University of California San Diego, 2018

Professor William Mobley, Chair

Over the past few decades, brain-derived neurotrophic factor (BDNF)— a member of a small family of secreted proteins called neurotrophins— has emerged as a crucial regulator of almost all stages of neuronal circuit development, including axonal specification and neurite growth. Nonetheless, details regarding the spatiotemporal regulation of BDNF-induced axonal growth and underlying mechanisms remain poorly understood. Here, we show that BDNF signals locally in distal axons of hippocampal neurons to rapidly increase axonal elongation rates, whereas BDNF signaling in somatodendritic compartments does not

increase distal axon growth. We found that BDNF signals through TrkB receptors in axons to locally activate the mTOR/S6K signaling pathway and intra-axonal protein synthesis. Our findings point to a mechanism whereby local BDNF signaling in axons induces: (1) an early growth response, noticeable within the first 10 min of axonal exposure to BDNF, which requires intra-axonal protein synthesis and local mTOR activity, and (2) a sustained growth response, which occurs 60 min or longer after initial exposure to BDNF, and requires new transcription and translation in neuronal cell bodies. Given the requirement for new transcription to sustain BDNF-induced axonal growth, in Chapter 3 we explored transcriptional changes following BDNF stimulation of hippocampal neurons in mass cultures or compartmentalized microfluidic cultures. We describe dynamic changes in the expression of select transcripts resulting from global and/or axonal BDNF signaling. Taken together, these results provide mechanistic insights into BDNF-induced axonal growth in hippocampal neurons.

Chapter 1: Introduction

Introduction and Background

One longstanding goal of neuroscience has been to understand how billions of neurons– and trillions of connections– organize themselves into intricate circuits that govern behavior. Neuronal circuit formation requires the precise coordination of numerous events during the early stages of a species' development and throughout its lifespan. In one initial event, neurons form and extend long protrusions called axons to contact targets far away from the cell body. Axonal growth is crucial for the initial establishment of neuronal polarity and proper wiring of neuronal circuits. Thus, understanding the mechanisms involved in axonal growth is critical to understanding how neuronal circuits develop, in both normal and pathological contexts.

To establish and maintain connections, axons rely on extracellular cues to guide their path and regulate their growth. One prominent example of such cues is the family of secreted peptides known as neurotrophic factors, or neurotrophins.

1.1 Discovery of neurotrophins: historical perspective

The identification of the first neurotrophin, nerve-growth factor (NGF), thoroughly revolutionized the fields of neuroscience and cell biology— from the era of its discovery during the 1950s to date. For a long period of time, biologists believed the processes of cell growth and differentiation— including the growth of neuronal axons over long distances— were entirely regulated by cell-intrinsic mechanisms. The discovery of NGF challenged this idea: it provided the first evidence that cells could produce and release molecules as

extracellular cues to influence growth and differentiation in targeting cells within relatively short range. This discovery completely changed our understanding, and consequent future lines of research, on how the nervous system develops and how cells communicate between each other.

During the early 1950s, scientists Stanley Cohen and Rita Levi-Montalcini isolated a biochemical extract, from particular mouse tumors, that greatly enhanced nerve growth in chick sympathetic and sensory neurons, both *in vivo* and *in vitro* (Cohen et al., 1954). To further isolate and characterize the growth-inducing factor, they used snake venom, a substance rich in nucleic acid-degrading enzymes: if the growth-promoting factor was a nucleic acid, as opposed to a protein, its activity would be suppressed by snake venom. To their surprise, the snake venom by itself promoted nerve growth to a similar or greater extent than the tumor extract (Cohen and Levi-Montalcini 1956)— a finding that strengthened Levi-Montalcini's belief on the existence of a diffusible molecule capable of inducing nerve growth. In a series of subsequent experiments, they established that the growth-promoting factor was a protein— which became known as nerve-growth factor (NGF)— secreted from mouse tumors, snake venom glands, and mouse salivary glands; the latter provided a rich source of NGF, which facilitated its biochemical purification and characterization (Cohen 1960). Although promising to the authors, these results were initially met with plentiful skepticism from most of the scientific community: NGF's described mode of action— a diffusible protein that was secreted from one tissue to reach and alter function in a different tissue within relatively close range— was unprecedented and thus deemed unlikely. In

addition, NGF's particularly disparate sources (i.e. mouse tumors, snake venom, and mouse salivary glands) made researchers doubt its physiological relevance.

Nonetheless, Cohen, Levi-Montalcini and colleagues persisted in their research and "it was in this skeptical atmosphere that NGF asserted its vital role in the life of its target cells," as Levi-Montalcini later described (Levi-Montalcini 1986). Over the next few years, they discovered that NGF was not` just a *tropic* factor— one secreted by target tissue that induces growth towards such region— but also a *trophic* factor— one required for neuronal survival and maintenance of connections with their innervated target(s). That NGF was essential for neuronal survival became evident after injecting mice with anti-NGF antiserum almost completely destroyed their sympathetic nervous system (Levi-Montalcini and Booker 1960). The existence and relevance of NGF gradually gained acceptance from the scientific community and opened the path to new avenues of research. Since the discovery of NGF, over 50 growth factors have been identified in diverse tissues, with crucial roles in normal cellular growth (e.g. during development) and, importantly, in instances of abnormal growth — namely, cancer. Not surprisingly, Cohen and Levi-Montalcini were awarded the Nobel Prize in Physiology or Medicine in 1986, in recognition of their discoveries of growth factors.

Despite all its notable, increasing roles in the peripheral nervous system and non-neuronal cells, NGF's action in the brain is surprisingly limited to a small subset of forebrain neurons— which led scientists to believe there were likely other molecules with similar functions in the central nervous system. In the early 1980s, a protein with high structural

similarity to NGF was isolated from pig brains (Barde et al., 1982) and named brain-derived neurotrophic factor, or BDNF. Henceforth, the family of neurotrophins was established, with other members including neurotrophin 3 (NT-3) and neurotrophin 4 (NT-4, also known as NT-5). Extensive research over the past six decades has shown that neurotrophins play crucial roles in the development and maintenance of both central and peripheral vertebrate nervous systems. Furthermore, abnormal neurotrophin signaling has been implicated in the pathophysiology of many diseases, including neurodegenerative and neuropsychiatric disorders, obesity, various types of cancers, among others (Chao et al., 2006; Gupta et al., 2013; Mitre et al., 2016). Thus, understanding the molecular mechanisms involved in neurotrophin signaling has been and remains a very active and important research focus.

1.2 Neurotrophin signaling mechanisms and functions: brief overview

Neurotrophin signaling through Trk receptors

Neurotrophins bind to and signal through two types of cell surface receptors: the pan-neurotrophin receptor p75 and the tropomyosin-related kinase (Trk) family of receptor tyrosine kinases. Each neurotrophin binds to specific members of the Trk family: NGF binds to TrkA, BDNF and NT4/5 bind to TrkB, and NT-3 preferentially binds to TrkC, but can also bind to TrkA and TrkB. All neurotrophins can unselectively bind to p75, a member of the tumor-necrosis factor family of receptors that lacks enzymatic activity but can recruit signaling adaptor proteins and function as a co-receptor for Trk's (Chao 2003; Sofroniew, Howe and Mobley 2001). The presence of p75 increases the affinity of Trk receptors for

their primary ligands— namely, TrkA and TrkB show much higher selectivity for NGF and BDNF, respectively. In general, differential expression patterns of both receptor types throughout the nervous system confer responsiveness to specific neurotrophins (Huang and Reichardt 2003; Sofroniew et al., 2001).

Although much remains to be clarified, research efforts over the past several decades have helped us gain significant insight into the mechanisms of neurotrophin signaling through Trk receptors. In general, ligand binding to Trk extracellular regions induces receptor dimerization, which in turn, activates intracellular tyrosine kinase domains (Huang and Reichardt 2003). Consequently, Trk receptors autophosphorylate (trans-phosphorylate) several tyrosine residues at specific conserved locations. Autophosphorylation of some residues serves to potentiate kinase activity, whereas others create docking sites for signaling proteins containing Src-homology 2 (SH2) or phosphotyrosine-binding (PTB) domains (Lemmon and Schlessinger 2010; Longo and Massa 2013). Most research has focused on studying the binding of adaptor and signaling proteins at two sites in particular, Y490 and Y785 (numbering for TrkA), and the cascade of signaling events that occur in return. For example, phosphorylated Y490 (or the homologous residues on TrkB/C) recruits the PTB-containing adaptor proteins Shc and Frs2, which in turn recruit other adaptor proteins, ultimately resulting in the activation of the Ras-mitogen-activated protein kinase (MAPK) and phosphatidylinositol 3-kinase (PI3K) signaling pathways— which play central roles in cellular survival and growth, further discussed below (Reichardt 2006). Autophosphorylation of Y785 leads to recruitment and activation of phospholipase Cγ

(PLCγ), which induces a cascade of intracellular events, including calcium release from internal stores and activation of several Ca2+-regulated kinases (Sofroniew, Howe and Mobley 2001). In the context of BDNF/TrkB signaling, activation of the PLCγ pathway has been shown to be particularly important for synaptic plasticity in the hippocampus (Minichiello 2009).

In response to extracellular stimuli such as neurotrophins, the PI3K and MAPK signaling pathways coordinately regulate fundamental intracellular processes such as gene transcription and translation, cell morphogenesis, growth and survival (Manning and Toker 2017; Mendoza, Er and Blenis 2012; Roskoski 2012). The best-known PI3K substrate is protein kinase B, most commonly known as Akt; when phosphorylated, Akt regulates the activity of numerous downstream targets, including Forkhead Box O (FoxO) transcription factors, tuberous sclerosis complex 2 (TSC2) and the mechanistic target of rapamycin complex 1 (mTORC1), among many others (Manning and Toker 2017). Similarly, MAPK1 and MAPK3— commonly known as the extracellular signal-regulated kinases ERK2 and ERK1, respectively— phosphorylate hundreds of cytosolic and nuclear substrates with diverse functions; these include cytosolic targets such as TSC2 and p90 ribosomal S6 kinases (RSKs), and nuclear transcription factors including cFOS, NFAT, MEF2 and Elk1 (Cargnello and Roux 2011; Roskoski 2012).

Trk-mediated endocytosis and retrograde neurotrophin signaling

Similar to other receptor tyrosine kinases, upon activation, Trk receptors are internalized from the plasma membrane and sorted into different types of endosomal compartments, from which receptors can be targeted to different intracellular destinations (Le Roy and Wrana 2005; Raiborg and Stenmark 2009). This type of receptor-mediated endocytosis was initially believed to serve as a means of signal attenuation, wherein ligand-activated receptors were removed from the cell membrane to ultimately be degraded intracellularly in lysosomes (Dobrowolski and De Robertis 2012; Sorkin and von Zastrow 2009). Further studies helped reveal other roles for receptor-mediated endocytosis extending beyond signal termination to intracellular signal propagation and maintenance. Some of the first evidence suggesting that endosomes could serve as signaling platforms came from studies performed using the pheochromocytoma-derived cell line (PC12). These studies showed that NGF-bound, phosphorylated TrkA receptors could be found in intracellular vesicles along with various associated signaling proteins, including PLCγ and members of the Ras-MAPK pathway (Grimmes et al., 1996; Howe et al., 2001). The formation of this type of endocytic vesicles containing ligand-receptor complexes— now known as *signaling endosomes*— allows continued activation of RTKs and downstream signaling molecules intracellularly, and provides a mechanism to propagate and regulate signals within specific spatial domains (Hoeller, Volarevic and Dikic 2005; Terenzio, Schiavo and Fainzilber 2017).

Receptor-mediated endocytosis and endosome trafficking have been shown to play a major role in long-range neurotrophin signaling. In neuronal circuits, neurotrophins are often released from post-synaptic targets located far (up to hundreds of centimeters away) from

the cell bodies of their innervating neurons (Zweifel, Kuruvilla and Ginty 2005). To transmit these signals to the soma, neurotrophins bind to and activate Trk receptors on distal axonal terminals. Subsequently, activated Trk receptors are internalized from the axonal plasma membrane into signaling endosomes, which undergo motor-mediated retrograde transport along microtubules towards neuronal cell bodies (Ascano, Bodmer and Kuruvilla 2012; Cosker and Segal 2014). In the soma, signaling molecules carried within signaling endosomes— or newly-activated upon their arrival— can translocate to the nucleus to induce transcriptional programs that mediate diverse cellular responses (Delcroix et al., 2003; Harrington and Ginty 2013).

Most insights into the mechanisms of endosomal-based retrograde neurotrophin signaling have come from studies of NGF/TrkA signaling in sympathetic and sensory neurons. The use of compartmentalized neuronal cultures, or *ex vivo* sciatic nerve preparations, helped provide initial, compelling evidence for the formation and retrograde transport of Trk signaling endosomes in axons (Delcroix et al., 2003; Ehlers et al., 1995; Kuruvilla, Ye and Ginty 2000; Tsui-Pierchala and Ginty 1999; Riccio et al., 1997; Watson et al., 2001; Ye et al., 2003). Compartmentalized neuronal cultures used in most of these studies were prepared using Campenot devices consisting of three chambers separated by Teflon dividers, where dissociated neurons are seeded in a central chamber and axons extend to the side chambers (Campenot 1977). The central and side chambers— which harbor neuronal cell bodies and axons, respectively— maintain fluidic separation and, thus, can be treated and analyzed individually. Application of NGF exclusively to axons of

compartmentalized SCG or DRG cultures for periods of 20-30 min increased the levels of phosphorylated TrkA, Erk1/2, Erk5 and Akt in both cell body and axonal chambers, and the transcription factor CREB in cell bodies, which strongly suggested that NGF/TrkA signaling complexes form in distal axons and signal retrogradely to cell bodies (Howe and Mobley 2005; Kuruvilla, Ye and Ginty 2000; Riccio et al., 1997; Watson et al., 2001; Ye et al., 2003). In addition, using pharmacological or genetic manipulations, several groups provided strong evidence that internalization and motor-based retrograde transport of phosphorylated-Trk (pTrk)-containing vesicles are required for the activation of downstream signaling events in cell bodies (Heerssen et al., 2004; Riccio et al., 1997; Tsui-Pierchala and Ginty 1999; Watson et al., 2001; Ye et al., 2003).

The mechanisms involved in Trk endosome formation, sorting and signaling are poorly understood and remain an active topic of investigation. Over the past two decades, significant effort has been dedicated to investigating the nature and role of the various adaptor and effector proteins that associate with Trk endosomes. Of note, various members of the Rab family of small GTPases, which play essential roles in endosomal formation and sorting, have been identified in Trk endosomes (Bucci, Alifano and Cogli 2014; Delcroix et al., 2003; Wang, Liang and Li 2011). In their active state (GTP-bound), each Rab protein can interact with distinct sets of effector proteins and recruit these to endosomes; the effectors include proteins that promote fusion with other compartments (e.g. lysosome, plasma membrane), proteins involved in motor transport, among others (Barford, Deppmann and Winckler 2017). For example, several Rabs can interact directly or indirectly with different

subunits of the dynein motor complex (Horgan and McCaffrey 2011), which have also been found in Trk endosomes and demonstrated to be essential for their retrograde transport from axons (Cosker and Segal 2014; Delcroix et al., 2003; Heerssen, Pazyra and Segal 2004; Mitchell et al, 2012). [Evidence from studies in neurons and PC12 cells indicates that TrkA is trafficked in signaling endosomes containing the early-endosomal protein Rab5, the late-endosomal protein Rab7, and/or the recycling endosome protein Rab11 (Delcroix et al., 2003; Harrington et al., 2011; Mitchell et al., 2012; Suo et al., 2014; Valdez et al., 2007; Ye, Lehigh and Ginty 2018). These findings raise the possibility that the population of Trk signaling endosomes is heterogeneous, i.e. molecularly distinct (Barford, Deppmann and Winckler 2017; Zahavi, Maimon and Perlson 2017), and could possibly have different functional targets.]

Importantly, constituents of the PI3K, MAPK and PLCγ signaling pathways associate with pTrk-endosomes (Delcroix et al., 2003; Harrington et al., 2011), making possible for endosomal signaling to occur within axons during transport. Recent analyses of endosomal transport dynamics further support a model in which Trk-endosomes signal along the axon. In these studies, endosomal transport was visualized by live-imaging in compartmentalized neuronal cultures after addition of fluorescently-tagged NGF particles to the axonal compartment (Cui et al., 2007) or labelling of surface Trk receptors in axonal compartments prior to NGF stimulation (Ye, Lehigh and Ginty 2018). Their findings revealed that NGF/TrkA endosomes undergo fast axonal transport (>1μm/s), mostly in a retrograde direction, and pause frequently along the axon for variable durations. One

exciting possibility is that pausing during transport facilitates highly localized signaling from proteins within endosomes to downstream effectors encountered *en route*. Whether neurotrophin signaling mechanisms and functions in axons are different from those in cell bodies remains unclear.

The best-studied function of retrograde neurotrophin signaling is the regulation of neuronal survival, especially in the peripheral nervous system. Different populations of sensory, sympathetic, among other neurons entirely depend on neurotrophin signaling to survive during embryonic development and for continued survival throughout adulthood, in the case of some neuronal subpopulations (Huang and Reichardt 2001). Although the mechanisms remain to be fully elucidated, neurotrophin-induced survival is mediated at least in part through the activation of nuclear transcription factors, including CREB, NFAT and MEF2D (Ascano, Bodmer and Kuruvilla 2012; Cox et al., 2008; Kim et al., 2014; Riccio et al., 1997; Watson et al., 2001). When activated, these factors induce the transcription of anti-apoptotic genes such as Bcl2, thereby promoting survival (Bonni et al., 1999; Cosker et al., 2013; Pazyra-Murphy et al., 2009). Retrograde neurotrophin signaling has also been shown to regulate various other functions, such as axonal growth and synapse formation (Harrington and Ginty 2013). NGF effects on sympathetic and sensory axonal growth are also mediated, at least in part, by the activation of transcription factors in the nucleus, namely CREB, SRF (serum response factor) and NFAT (Bodmer et al 2011; Lonze et al., 2002; Wickramasinghe et al., 2008). Importantly, most of our current insights into the mechanisms of retrograde neurotrophin signaling have come from studies of NGF/TrkA

using neuronal cell lines and/or sympathetic and sensory neurons. The mechanisms and functions of retrograde signaling for other neurotrophins, such as BDNF/TrkB, are much less understood.

1.3 BDNF signaling and functions in the central nervous system

Of the neurotrophin family, BDNF is the most widely expressed neurotrophin in the central nervous system (CNS) and it has recently emerged as a key regulator of brain function. Research efforts over the past two decades have uncovered a role for BDNF signaling in a myriad of processes during neuronal circuit development and maintenance—ranging from neural stem cell differentiation to synaptic strengthening (Park and Poo 2012). Given its wide-ranging actions in the developing and mature CNS, BDNF has been implicated in various neurological and psychiatric diseases. Abnormal BDNF signaling has been associated with the pathology of neurodegenerative disorders, e.g. Alzheimer's disease and Huntington's disease (Nagahara and Tuszynski 2011; Mitre, Mariga and Chao 2016); neuropsychiatric disorders, including depression, schizophrenia and drug addiction (Autry and Monteggia 2012); neurodevelopmental disorders, such as autism spectrum disorders (Bourgeron 2015) and Down syndrome (ref); among others. Targeted delivery of BDNF to specific regions within the brain and CNS is expected to become a future potential treatment strategy for some of these diseases and for axonal regeneration after injury (Anastasia and Hempstead 2014; Mitre, Mariga and Chao 2016).

BDNF/TrkB signaling mechanisms

Numerous studies have explored the signal transduction pathways that mediate BDNF effects using cultures of dissociated CNS neurons (e.g. hippocampal, cortical, cerebellar, spinal motor neurons) or synaptosomal fractions isolated from rodent brains. In these cultures, bath application of BDNF induces many intracellular signaling events within minutes, including phosphorylation and activation of TrkB, Erk1/2, Erk5, RSK1/2, Akt, PLCγ, and the transcription factor CREB (further discussed below) to promote neuronal survival (Kharebava et al 2008; Wang, Su and Xia 2006; Zheng et al., 2008), dendritic growth and branching (Guo et al., 2014; Ji et al., 2010), neurotransmitter release (Jovanovic et al., 2000), and various other functions. The kinetics of these BDNF-induced phosphorylation events vary across studies and are likely sensitive to several factors (e.g. cell type, experimental conditions). Importantly, several studies have provided evidence that select downstream signaling pathways are preferentially activated after TrkB-mediated endocytosis. In cultures of hippocampal, cortical or spinal neurons, treatment with pharmacological inhibitors of dynamin (and/or other proteins involved in receptor endocytosis) selectively reduced the intensity and duration of BDNF-induced activation of Akt, yet had no apparent effects on TrkB or Erk1/2 activation (Cheng et al., 2008; Zahavi et al., 2018), suggesting that endocytosis is required for sustained PI3K/Akt signaling downstream of TrkB activation. In a different study, inhibition of TrkB endocytosis in cultured cortical neurons, via a dominant-negative mutant form of dynamin or pharmacological inhibition of surface receptor internalization, attenuated BDNF-induced Erk2 activation and completely abolished Erk5 activation and nuclear translocation in response to BDNF (Wang, Su and Xia 2006). Together these findings indicate that BDNF

activates TrkB and downstream signaling pathways in CNS neurons and that TrkB-mediated internalization enables sustained signaling activity for certain molecules intracellularly.

Accumulating evidence suggests that BDNF is secreted from both pre- or post-synaptic terminals and acts on local TrkB receptors in a paracrine or autocrine fashion to regulate various neuronal functions (Park and Poo 2012; Sasi et al., 2017). In contrast to NGF/TrkA signaling in the PNS, the mechanisms and functions of retrograde BDNF/TrkB signaling are much less understood. Studies using compartmentalized cultures of sympathetic and sensory neurons with the Campenot chamber system helped provide the basis for most of our understanding of the mechanisms of retrograde neurotrophin signaling. Unlike PNS neurons, CNS neurons cannot be readily cultured using Campenot devices (Kim and Jaffrey 2016); thus, initially, the mechanisms of retrograde BDNF/TrkB signaling could not be explored using similar approaches to the ones used to study NGF signaling. The development of a microfluidic platform for compartmentalized culture of CNS neurons (Taylor et al., 2005) provided the opportunity to explore the mechanisms of retrograde BDNF/TrkB signaling in CNS neurons. Compartmentalized microfluidic cultures are established using a polydimethylsiloxane (PDMS) device consisting of two chambers interconnected by long microgrooves— where neurons are seeded in one chamber and only axons can fit through the microgrooves and extend to the other chamber (Figure 2.1A). This platform allows fluidic isolation of axonal and somatodendritic compartments, which can be exposed to different media conditions to resemble physiologically-relevant events.

In hippocampal microfluidic cultures, fluorescently-tagged BDNF molecules added exclusively to axonal compartments undergo internalization and retrograde transport from distal axons towards cell bodies (Weissmiller et al., 2015), similar to observations in sympathetic and sensory neurons (Cui et al., 2007; Lehigh and Ginty 2018). Furthermore, application of BDNF to the axonal compartment of hippocampal or cortical microfluidic cultures leads to activation of CREB or Erk5 in cell bodies (Bronfman et al., 2014; Li et al., 2017; Weissmiller et al., 2015; Zhou et al., 2012), suggesting that BDNF signals retrogradely from axonal terminals to induce transcriptional changes in the nucleus. In accordance with these findings, TrkB-endosomes isolated from mouse brain lysates were shown to associate with pErk1/2, Rab7, subunits of the dynein complex, and the SNAP25-binding protein Snapin, which was identified as an adaptor protein that recruits dynein to TrkB-endosomes (Zhou et al., 2012). Although these studies have helped identify some of the players involved in BDNF signaling, details of the mechanisms by which these players signal in distinct subcellular compartments to mediate specific cellular responses remain unclear. In particular, the local signaling events that take place in axons downstream of TrkB activation remain largely unexplored.

Regulation of transcription and translation downstream of BDNF/TrkB signaling

Similar to other growth factors and cytokines, BDNF signaling through TrkB and downstream pathways elicits dynamic changes in gene expression that drive various neuronal responses (Lonze and Ginty 2002; Tasdemir-Yilmaz and Segal 2016). Deciphering the nature and sequence of BDNF-induced signaling events and corresponding

transcriptional responses has been incredibly challenging. These responses are context-specific and highly dynamic— sensitive to many factors, including (1) neuronal subtype, e.g. retinal vs. hippocampal (Ito and Enomoto 2016); (2) developmental stage (young vs. mature); (3) subcellular location of signal origin, e.g. dendritic spines vs. distal axonal terminals (Zahavi, Maimon and Perlson 2017); (4) stimulus temporal pattern, i.e. transient vs. sustained (Yosef and Regev 2011); among others.

Seminal work by Finkbeiner and colleagues identified the transcription factor cAMP response element-binding protein (CREB) as a principal downstream effector of TrkB signaling and mediator of BDNF-induced changes in gene expression (Finkbeiner et al., 1997). The authors showed that exposure of cultured young cortical neurons to BDNF rapidly stimulated CREB phosphorylation (within 15 min) and transcription of the immediate early gene *cFOS* through at least two different pathways: one that depended on ERK2 and RSK2 activation, and another that depended on the activation of PLCγ and the calcium/calmodulin-dependent kinase IV (CaMKIV). More recently, several other groups have also reported increased CREB phosphorylation and activation in cultured cortical, hippocampal or cerebellar neurons after BDNF exposure for 15-30 min (Guo et al., 2014; Jia et al., 2007; Weissmiller et al., 2015; Zheng et al., 2008). In addition, a few studies described the involvement of a different transcription factor in BDNF-induced transcription: exposure of cultured cortical or hippocampal neurons to BDNF for 15-30 min promoted the activation and nuclear translocation of the transcription factor NFATc through a mechanism that required PLCγ signaling downstream of TrkB activation (Graef et al., 2003; Groth and

Mermelstein 2003). Thus, it is likely that BDNF-induced transcriptional programs result from the combined action of several transcription factors activated by downstream signaling cascades, particularly the Ras/MAPK and PLCγ pathways.

Given the elaborate regulation of transcriptional responses, it is perhaps not surprising that our current understanding of BDNF-induced transcriptional programs is very limited. Most insights into the changes in gene expression that occur in response to BDNF signaling have come from studies employing cultures of dissociated primary neurons. In these cultures, during early developmental stages (days *in vitro,* DIV 0~4), cells are simultaneously undergoing numerous physiological processes— not necessarily neuronal-specific, including differentiation, migration and growth— which complicates the study of the transcriptional changes that mediate specific cellular responses. Many studies have instead focused on exploring the transcriptional changes that mediate BDNF effects in synaptic formation and/or function using 'mature' neuronal mass cultures, e.g. DIV≥10 (Alder et al., 2003; Adams et al., 2011; Melo et al., 2013; Schratt et al., 2004). In one important study, Schratt and colleagues (2004) investigated mRNA species whose translation was enhanced after exogenous application of BDNF to cultured cortical neurons at two different developmental stages, DIV 4 or DIV 14. Upon 20 min of BDNF treatment, different subsets of mRNAs were newly-associated with polysomes isolated from neurons at the two different developmental stages. In DIV 4 neurons, several of the mRNAs identified encoded for proteins involved in axonal growth or guidance, including MAP1B and Limk1; whereas in DIV 14 neurons, BDNF up-regulated many mRNAs encoding for proteins

associated with synaptic function, including glutamatergic receptors and the calcium/ calmodulin−dependent protein kinase II (CamKII). Of note, some of these genes were induced in a rapamycin-sensitive manner, suggesting involvement of Akt/mTORC1 signaling downstream of BDNF to regulate the translation of select mRNAs (Schratt et al., 2004). This study provides strong evidence supporting the notion that BDNF induces differential effects on transcription at different developmental stages.

In addition to differential effects based on developmental stage, changes in gene expression in response to environmental stimuli follow prototypical temporal patterns in most cells. For example, some transcripts exhibit transient, 'impulse'-like changes— where their levels rise or decrease abruptly after the stimuli, maintain a new level for a certain period of time (from minutes to several hours) and typically return to original levels (Yosef and Regev 2011). Commonly, gene products induced early in response to extracellular stimuli influence the expression of other downstream targets, which may also exhibit transient changes in expression or sustained new patterns of expression required for long-term cellular effects (Yosef and Regev 2011). Consequently, quantitative analyses of stimulus-induced transcriptional changes will likely differ depending on the amount of time between initial exposure to a stimulus until cellular RNA extraction. Indeed, BDNF has been found to induce different transcriptional programs in cultured hippocampal or cortical neurons (DIV 10-14) after short- versus long-term exposure to BDNF. Short-term treatment with BDNF (from 20 min to 3 h) has been shown to mainly up-regulate the expression of immediate early genes (IEGs), including *Arc* and *cFOS* (Alder et al., 2003; Cohen et al.,

2011; Ring et al., 2006), which, in turn, are thought to promote the expression of 'late-response' genes (Amit et al., 2007; Roskoski 2012). Accordingly, long-term BDNF exposure (from 3 up to 24 h) induces the expression of many mRNAs with wide-ranging functions, including some IEGs but also ion channels, transmembrane receptors, signaling proteins, cytoskeletal proteins, among many others (Adams et al., 2011; Alder et al., 2003; Ring et al., 2006). It is unclear whether continual BDNF stimulation or sustained activation of signaling pathways were required for the observed long-term changes in gene expression.

A number of studies have also explored BDNF effects in gene expression at the translational level. Short-term BDNF exposure (30-60 min) stimulates global protein synthesis in neuronal mass cultures, synaptosomal fractions and hippocampal slices, as measured by the incorporation of radio-labeled methionine or a methionine analog into newly-synthesized proteins (Bowling et al., 2016; Briz et al., 2015; Dieterich et al., 2010; Genheden et al., 2015; Takei et al., 2004; Yin, Edelman and Vanderklish 2002). Although the mechanisms have not yet been fully elucidated, BDNF is thought to stimulate protein synthesis largely through activation of mTORC1 downstream of the PI3K/Akt pathway and RSKs downstream of the MAPK pathway (Leal, Comprido and Duarte 2014). This is supported by experimental evidence indicating that BDNF indeed activates mTOR and downstream effectors— namely, the translational regulators ribosomal protein S6 kinase (p70-S6K), eukaryotic initiation factor 4E (eIF4E) and eIF4E-binding protein (4E-BP)— in cultured cortical neurons and synaptosomal fractions (Takei et al 2001; Takei et al., 2004; REF). Other studies have found that BDNF activates the MAP kinase-interacting kinase

MNK1 and the p90 ribosomal S6 kinases RSK1/2 in cultured cortical neurons, and that these kinases also play a role in BDNF-induced protein synthesis (Genheden et al., 2015; Kharebava et al 2008).

Using quantitative proteomic approaches, researchers have attempted to characterize BDNF-induced changes to the neuronal proteome in mixed cultures of cortical/hippocampal neurons (Genheden et al., 2015; Liao et al., 2007) and adult hippocampal slices (Bowling et al., 2016). In response to 2 hours of BDNF stimulation (bath-applied), numerous proteins were up- or down-regulated in cultured cortical neurons (DIV10), including cytoskeletal (e.g. Map1B), synaptic (e.g. SNAP25), and other proteins (Genheden et al., 2015). Similarly, in synaptosome fractions derived from cultured cortical neurons (DIV15), hundreds of proteins were up-regulated after short-term treatment with BDNF, including multiple members of the translational machinery and synaptic proteins (Liao et al., 2007). In addition, Bowling and colleagues found significant differences in BDNF-induced proteomic changes in embryonic hippocampal cultures (DIV10) vs. adult hippocampal slices, especially in the expression of proteins involved in neurotransmission and other synaptic functions (Bowling et al., 2016), further supporting that BDNF-induced transcriptional effects are differentially regulated throughout development.

Together, these observations indicate that gene expression is temporally regulated at both transcriptional and translational levels by BDNF to alter neuronal function. Nonetheless, many questions remain to be explored, including which signaling events

mediate the observed effects and whether BDNF induces differential transcriptional effects depending on the subcellular location of signal initiation.

Regulation of axonal growth by BDNF

Elucidating the the complex spatiotemporal dynamics of BDNF signaling and resulting cellular responses has been a main goal in the field; this will help us better understand BDNF effects on neuronal development and function in both normal and pathological contexts. *In vitro* models have proven invaluable for studying the different roles BDNF plays in regulating neuronal development. One defining event in neuronal development is the establishment of neuronal polarity— commonly divided into five well-described, morphologically distinct stages (Polleux and Snider 2010; Yogev and Shen 2017). A great deal of experimental evidence supports a role for BDNF in nearly all stages underlying the establishment of neuronal polarity: immature neurite formation and extension (stages 1& 2; DIV 0-2), axonal initiation or specification (stage 3; DIV 2-4), axonal and dendritic growth and branching (stage 4; DIV 4-15), and spine morphogenesis and synaptic formation (stage 5; DIV≥15) (Park and Poo 2012).

Similar to NGF, which was first identified for its growth-promoting action, a number of studies have provided evidence that BDNF promotes neurite growth in various types of neurons (Table 1.1). Most of these studies have been performed using mass cultures of neurons DIV 0-4, wherein it is difficult to unambiguously distinguish immature neurite growth from growth during and/or after axon initiation. In addition, the effects on growth

have been examined after relatively long periods (over 24 h) of simultaneous BDNF exposure to different subcellular compartments— somatodendritic and axonal. These studies helped shed light into some of the mechanisms involved in BDNF-induced neurite growth but many important questions emerged that have yet to be addressed.

Of particular importance is understanding the intricate details regarding the regulation of neurite and axon growth by BDNF. After axonal initiation, axons continue to extend far distances from their emanating cell body and are influenced by cues within their local microenvironment. Whether BDNF modulates axonal growth particularly after initiation, when the source of the signal is likely to be local, remains unclear. Understanding the precise spatiotemporal coordination of cellular events induced by BDNF signaling to modulate axonal growth will help us better understand the intricate mechanisms that govern circuit formation.

Acknowledgements: Chapter 1, in part, is currently being prepared for submission for publication of the material. Natera-Naranjo, O and Mobley, W.C. The dissertation author was the primary investigator and author of this material.

Table 1.1 BDNF and axonal growth— summary of select studies

Growth factor(s)	Model organism/ cell type	Culture conditions	Growth assay	Effects	Mechanistic insights/ additional comments	Ref†
BDNF (*in vitro*, 20ng/mL; *in vivo*, 200ng/ µL)	*Xenopus* RGC (*in vivo,* stage 43/44 tadpoles)	*In vitro*: mass cultures ±BDNF at time of plating. *In vivo*: BDNF inject. optic tectum, target region of RGC axons	*In vitro*: axon length measured 4 d after treatment. *In vivo*: axon morphology analysis every 2 h after injection.	*In vitro*: BDNF increased mean axonal length by ~40% over 4 days. *In vivo*: BDNF increased axon arborization.	Target-derived BDNF is important for axonal arborization *in vivo*.	1
BDNF (25ng/ mL) NGF (10ng/ mL)	P1 rat superior cervical ganglia (SCG) neurons	Campenot chamber cultures infected with TrkB-expressing virus on DIV 5-6; axotomy 48 h later.	Axonal regrowth post-axotomy measured every 24 h over 4 d, after adding NGF **or** BDNF to opposing side compartments.	Neurotrophins promoted axonal regrowth into respective compartments; NGF-induced growth>BDNF -induced growth.	BDNF-induced growth (over 4 days) was mediated by PI3K and MEK signaling.	2
BDNF (200ng/ mL)	E15 rat thalamic neurons	Thalamic explant cultures DIV7; ±BDNF at time of plating	Total axonal length measured 7 d after treatment (± BDNF)	BDNF increased ave. axonal length by 50-60% compared to control		3
BDNF (100ng/ mL)	E18 rat hippocam-pal neurons	Mass cultures DIV3; ±BDNF at time of plating	Length of longest neurite recorded 3 d after treatment (± BDNF)	BDNF increased axonal length by 50-60%, reported as percent of control.	BDNF induces growth by mechanism involving GSK3ß and CRMP-2.*[A]	4
BDNF (25ng/ mL) IGF-1 (25ng/ mL)	P4 mouse corticospi-nal motor neurons (CSMN)	Mass cultures DIV2; ±BDNF at time of plating	Axonal length and branching measured 2 d after treatment	IGF increased CSMN axonal length by~100%; BDNF induced branching.	IGF-induced axonal growth mediated by PI3K and ERK.	5

Table 1.1 BDNF and axonal growth— summary of select studies, *continued*

Growth factor(s)	Model organism/ cell type	Culture conditions	Growth assay	Effects	Mechanistic insights/ additional comments	Ref†
BDNF (50ng/ mL)	E18 rat hippocam-pal neurons	Mass cultures ±BDNF at DIV2-3	Length of longest neurite was recorded 12-18 h after treatment (±BDNF)	BDNF increased axonal length by 20-30%; length data reported relative control.	BDNF induces growth through a mechanism involving ß-catenin.*A	6
BDNF (1nM, equivalent to 25ng/ mL)	E18 rat hippocam-pal neurons	Mass cultures DIV3; *Acute* BDNF (1nM) application or *gradual* (10-fold) increases in BDNF concentration (from 0.0001 to 1nM) every 30 min	Length of MAP2-positive neurites was recorded 3 d after treatment.	Acute BDNF treatment increased neurite length by ~90%; gradual BDNF treatment increased branching points by ~150%.	Acute and gradual BDNF application elicited transient and sustained activation of TrkB and downstream signaling, respectively.*B	7
BDNF (50µg/mL in micropipe tte)	E18 rat hippocam-pal neurons	Mass cultures DIV1-2	BDNF was delivered via a micropipette placed ~100 µm away from growth cone. Live-imaging of neurite.	BDNF significantly increased neurite growth: ~10µm/45 min compared to ~1µm/45 min in control .	BDNF induces neurite outgrowth and subsequent axonal specification.	8
BDNF (50ng/ mL)	E18 rat hippocam-pal neurons	Mass cultures DIV3; ±BDNF on DIV2	Length of Tau-positive neurites was measured 20 h after treatment.	BDNF increased axonal length by ~45% compared to control; data reported relative to control.	BDNF stimulates growth through a mechanism involving LIMK1 activation.*A	9

Table 1.1 BDNF and axonal growth— summary of select studies, *continued*

Growth factor(s)	Model organism/ cell type	Culture conditions	Growth assay	Effects	Mechanistic insights/ additional comments	Ref†
BDNF (25ng/ mL)	E18 rat hippocam-pal neurons	Mass cultures DIV3-4; ±BDNF on DIV3	Average neurite length measured 24 h after ±BDNF treatment.	BDNF caused a ~33% increase in neurite length.	BDNF-induced neurite growth involves Tau5 upregulation, microtubule polymerization .*C	10
BDNF (100ng/ mL)	E16 mouse hippocam-pal neurons	Mass cultures DIV3; ±BDNF at time of plating	Length of longest neurite was recorded 3 days after treatment (± BDNF)	BDNF increased axonal length by ~45% compared to control.	BDNF induces growth through a mechanism involving signaling by Dock3, GSK3ß, and CRMP2.*A	11
BDNF (50ng/ mL)	P0-2 mouse cortical neurons	Mass cultures, ±BDNF on DIV3	Average neurite length measured 24 h after BDNF treatment.	BDNF increased neurite length by ~50% compared to control.	*C	12
BDNF or NT-3 (50µg/mL in a micropipe tte)	E15 mouse hippocam-pal neurons	Mass cultures DIV2-3	Neurotrophins were delivered via micropipette placed ~100µm away from growth cone of longest neurite; growth was monitored by live-imaging	BDNF and NT-3 increased axonal elongation to a similar extent (~12µm/45 min) compared to control (~5µm/45min)	Local application of neurotrophins induces neurite growth.	13

*A Biochemical and/or immunocytochemical analyses of signaling events were performed within the first 5- to 90-min period following stimulation with neurotrophin(s). Effects on growth were assayed at least 12 h after stimulation, as indicated. *B Transient (peaking at ~15-30 min, returning to baseline by 2 h) versus sustained (increasing gradually within the first 60 min and remaining elevated for up to 8 h). *C Analyses include combined measurements of all neurites, dendrites and/or axons.

†References: (1) Cohen-Cory and Frazer, 1995. (2) Atwal et al., 2000. (3) Hanamura et al., 2004. (4) Yoshimura et al., 2005. (5) Ozdinler and Macklis 2006. (6) David et al., 2008. (7) Ji et al., 2010. (8) Nakamuta et al., 2011. (9) Dong et al., 2012. (10) Chen et al., 2012. (11) Namekata et al., 2012. (12) Kao et al., 2017. (13) Takano et al., 2017.

Chapter 2:
BDNF rapidly enhances axonal growth via intra-axonal protein synthesis and local mTOR signaling

2.1 Introduction

During neuronal circuit formation, axons have to navigate through molecularly complex environments wherein they heavily rely on extracellular cues to reach their final synaptic targets. Understanding the mechanisms involved in the regulation of axonal growth has been the focus of extensive research— ranging from the characterization of extracellular signals that promote or inhibit growth to defining the intracellular events that occur in response to these signals with temporal specificity. Neurotrophins are a small family of secreted peptides that play essential roles in the development and function of both PNS and CNS circuits. Brain-derived neurotrophic factor (BDNF) is the most abundant neurotrophin in the brain, widely expressed in various brain regions from early embryonic stages throughout adulthood, most notably in the hippocampus (Hofer et al., 1990).

Despite remarkable progress uncovering a role for BDNF in nearly every aspect of circuit development, the complex mechanisms underlying BDNF signaling and resulting cellular responses remain poorly understood. This has been particularly challenging because BDNF actions span wide spatial and temporal scales, at both tissue and cellular levels. Within the nervous system, BDNF and its main receptor TrkB are expressed in different neuronal populations— signaling mechanisms and functions may vary across different circuits. At the cellular level, BDNF can signal in an autocrine fashion in single dendritic spines to induce synaptic changes within minutes (Harward et al., 2016); whereas target-derived BDNF can signal retrogradely from distal axon terminals to cell bodies over the course of hours to days to promote survival and other functions (Park and Poo 2012). In

general, long-term trophic effects of neurotrophins are thought to depend on new gene expression, whereas more rapid actions (e.g. morphogenetic changes, modulation of neuronal excitability) are thought to be transcription-independent and result from the modulation of existing cytoplasmic effectors (Poo 2001). However, more recent research efforts have uncovered a role for intra-axonal protein synthesis in localized cytoskeletal regulation and other basic cellular processes (Terenzio, Schiavo and Fainzilber 2017). Thus, it has become clear that protein synthesis can be spatially regulated in neurons to satisfy 'instant' protein demands at specific subcellular locations. Currently, there is limited knowledge regarding the coordinate regulation of protein synthesis in axons and cell bodies by BDNF to generate various cellular responses.

During development, BDNF has been shown to play a major role in the regulation of axonal and dendritic growth in different types of neuronal populations (see Table 1.1; Park and Poo 2012). Most previous studies have explored these effects using neuronal mass cultures— generally consisting of dissociated neurons plated at low density over a small surface— wherein all neuronal sub-compartments are simultaneously subjected to any changes in the extracellular environment. Many important questions have emerged as we have gained new insight into BDNF functions in nervous system development. For example, before neurite differentiation, does BDNF induce growth of all immature neurites indiscriminately? Can BDNF signal locally in axons to influence axonal growth, or does the signal have to originate in cell bodies? Axonal elongation rates are systematically regulated during different stages of neuronal polarization, e.g. axonal specification, pathfinding and

terminal branching (Polleux and Snider 2010). BDNF has been shown to induce growth during axonal specification (Cheng et al., 2011); however, it is unclear whether it stimulates growth during the next elongation phases, i.e. target pathfinding, terminal branching. Understanding the precise spatial and temporal regulation of axonal elongation by BDNF is crucial for our understanding of neuronal circuit formation.

Recreating *in vitro* the complex environment and trajectory that axons undergo *in vivo* remains a highly challenging task for neuroscientists. In the present study, we examined the spatiotemporal dynamics of BDNF-induced axonal growth in hippocampal neurons using a compartmentalized microfluidic culture platform, which allowed us to mimic some aspects of *in vivo* subcellular environments. We show that axonal stimulation with BDNF increases axonal elongation rates within minutes; in contrast, BDNF stimulation of cell bodies for up to 2 hours does not induce axonal growth. These effects are mediated by local activation of TrkB, mTORC1/S6K signaling pathway and axonal protein synthesis. We describe a mechanism whereby BDNF signals from axons and coordinately regulates transcription in cell bodies and translation, in both cell bodies and axons, with temporal specificity to promote axonal growth.

2.2 Results

BDNF locally induces hippocampal axon growth

To investigate whether BDNF could act locally on axonal terminals to promote growth, we cultured embryonic hippocampal neurons in microfluidic devices that allow fluidic isolation of the somatodendritic and axonal compartments— thus allowing corresponding local microenvironments to be selectively manipulated (Fig. 2.1A). On DIV 6-8, we monitored the growth of distal axons located in the axonal compartment (AC) using time-lapse imaging. Axonal growth was measured as the change in axonal length over time — i.e. the displacement of the center of the growth cone relative to a stationary point on the axonal shaft (Δlength; Fig. 2.1A). Growth was characterized by intermittent phases of growth cone extension, pausing, and retraction, consistent with previous findings from studies performed using embryonic cortical slices (Skaliora et al., 2000) and *in vitro* models (Koch et al., 2012; Mondal et al., 2014). Accordingly, our growth measurements reflect the net effect of extension, pausing, and retraction following addition of BDNF or the vehicle control.

Upon selective addition of BDNF to the AC, we observed a rapid, significant increase in axonal growth: within the first 10 min of BDNF(AC) stimulation, relative axonal length increased by 109 ± 18% compared to 15 ± 14% in control conditions ($p<0.0001$, two-tailed unpaired *t*-test; Fig. 2.1C). After 60 min of BDNF(AC) treatment, the average change in axonal length was over 3 times greater than that measured in vehicle-treated control axons

— 36.1 ± 3.9 versus 10.0 ± 2.5 μm, respectively (p<0.0001, two-tailed unpaired t-test). To test whether axonal elongation varied with ligand concentration, we compared the growth response using two different concentrations of BDNF, 10 ng/mL and 100 ng/mL. There was no significant difference between axonal growth rates when 10 vs. 100 ng/mL of BDNF were added to axonal compartments, suggesting that maximal BDNF-induced growth was achieved with concentrations as low as 10 ng/mL.

To explore the temporal dynamics of early BDNF-induced growth, we analyzed time-lapse image sequences of axons, in intervals of 1-2 minutes, for the initial 30-min period following BDNF (or vehicle) addition to the AC. Quantitative analysis of growth cone trajectories after control treatment revealed regular alternating periods of forward movement (Δlength>0 between sequential intervals), pausing (Δlength=0), and retraction (Δlength<0). In the presence of BDNF, growth cones displayed longer periods of forward movement along with less frequent pausing, when compared to control (Fig. 2.1D). Remarkably, BDNF-induced increase in axonal length was already apparent 5.5 min after stimulation compared to control treatment (p=0.0008, two-tailed unpaired t-test with Welch's correction; Fig. 2.1D, inset), suggesting that axonally-applied BDNF can rapidly alter axonal elongation periods in a way that results in an immediate increase in axonal length compared to control.

To further characterize growth dynamics in the presence or absence of BDNF, we next analyzed axonal growth speed. Under control conditions, the average growth cone speed was 0.20 ± 0.02 μm/min— ranging from 0.05 ± 0.08 to 0.32 ± 0.08 μm/min

throughout a 30-min period— with alternating increases and decreases in speed observed at intervals as short as 2-3 minutes (Fig. 2.1E). These values are consistent with previously reported axonal growth rates measured *in vitro* (Deglincerti et al., 2015; Gomis-Ruth et al., 2014; Mita et al., 2016; Mondal et al., 2014; Zhang et al., 2013; Zhang et al., 2017). The average growth speed during the first 30 min-period after BDNF treatment was significantly higher than that of vehicle-treated axons: 0.65±0.06 versus 0.20±0.02 μm/min, respectively ($p<0.0001$, two-tailed unpaired *t*-test). Following BDNF(AC) addition, growth cone speed increased continually in intervals of 1.5-2 min, with transient decreases observed every 10-12 min (Fig. 2.1E). More in-depth analysis revealed that after BDNF treatment the cumulative fraction of axons moving at speeds≤0 μm/min— i.e. pausing or retracting— was significantly lower than that observed after control treatment (16.5 ± 2.1 versus 40.0 ± 3.7%, respectively; $p<0.0001$, two-tailed unpaired *t*-test). In addition, BDNF(AC) treatment markedly increased the cumulative fraction of axons moving at speeds ≥0.3 μm/min, compared to vehicle treatment (69.7 ± 5.4 versus 30.1 ± 4.0%, respectively; $p<0.0001$, two-tailed unpaired *t*-test). Together, these results show that BDNF locally stimulates axonal elongation by rapidly increasing growth cone forward-moving speed and decreasing the frequency of pausing and retraction.

Previous studies demonstrating a role for BDNF in neurite outgrowth have almost exclusively employed mass cultures (Chapter 1; Table 1.1), in which all subcellular compartments— somatodendritic and axonal— have been simultaneously exposed to BDNF. Given our findings that axonal growth was induced with axonally-applied BDNF, we next

asked whether BDNF applied to the somatodendritic compartment could also induce axonal growth. To this end, we added BDNF exclusively to the somatodendritic compartment (SC) and monitored growth in the AC using live-imaging. Interestingly, BDNF(SC) treatment did not significantly increase axonal growth compared to control over a 60-min period (Fig. 2.1 F-G). These findings suggest that BDNF can elicit different growth responses depending on the subcellular location where the signal originates.

Figure 2.1 BDNF acts locally in hippocampal axons to rapidly induce growth

(A) Schematic overview of two-chamber microfluidic culture devices— top and side views (not drawn to scale). Primary rat hippocampal neurons (E18) were seeded in the somatodendritic compartment (SC); axons extended through microgrooves into the axonal compartment (AC). To ensure fluidic isolation between compartments, culture media volume was maintained at a slightly lower level on the AC than SC, indicated by red curved dashed line (see Methods section). (**B,F)** Representative phase-contrast time-lapse images of distal axon terminals and growth cones captured before and after selective addition of BDNF (10 ng/mL) to the AC (**B**) or to the SC (**F**), respectively. Pseudo-colored outlines are shown to emphasize growth cone movement over time. Timestamps are indicated in minutes; BDNF was added at t= 0 min. Scale bars, 10 μm. (**C,G)** Change in relative axonal length (Δlength) was measured, as shown in **A,** in consecutive 10-min intervals throughout a 60-min period. See Methods section for more details (Chapter 5). Data represent mean values ± SEM; n = 20-50 axons per condition, 4-6 chambers, from ≥3 independent experiments. **p<0.001, ***p<0.0001, two-tailed unpaired t-test; *** p<0.0001, two-tailed unpaired t-test with Welch's correction for 60-min time point. (**D**) Axonal growth cone displacement after stimulation with BDNF (or control) at t= 0 min. Empty symbols correspond to individual growth cones; colored lines represent average displacement (n =12-15 growth cones per condition, per time-point). (**E**) Graph of growth cone speed as a function of time for the initial 30-min period after treatments. Speed values were calculated for 10-30 axonal trajectories per condition, at 12 different time points. Mean ± SEM; *p<0.05, **p<0.005, ***p<0.0001, Kruskal-Wallis test with Dunn's *post-hoc* analysis for multiple comparisons.

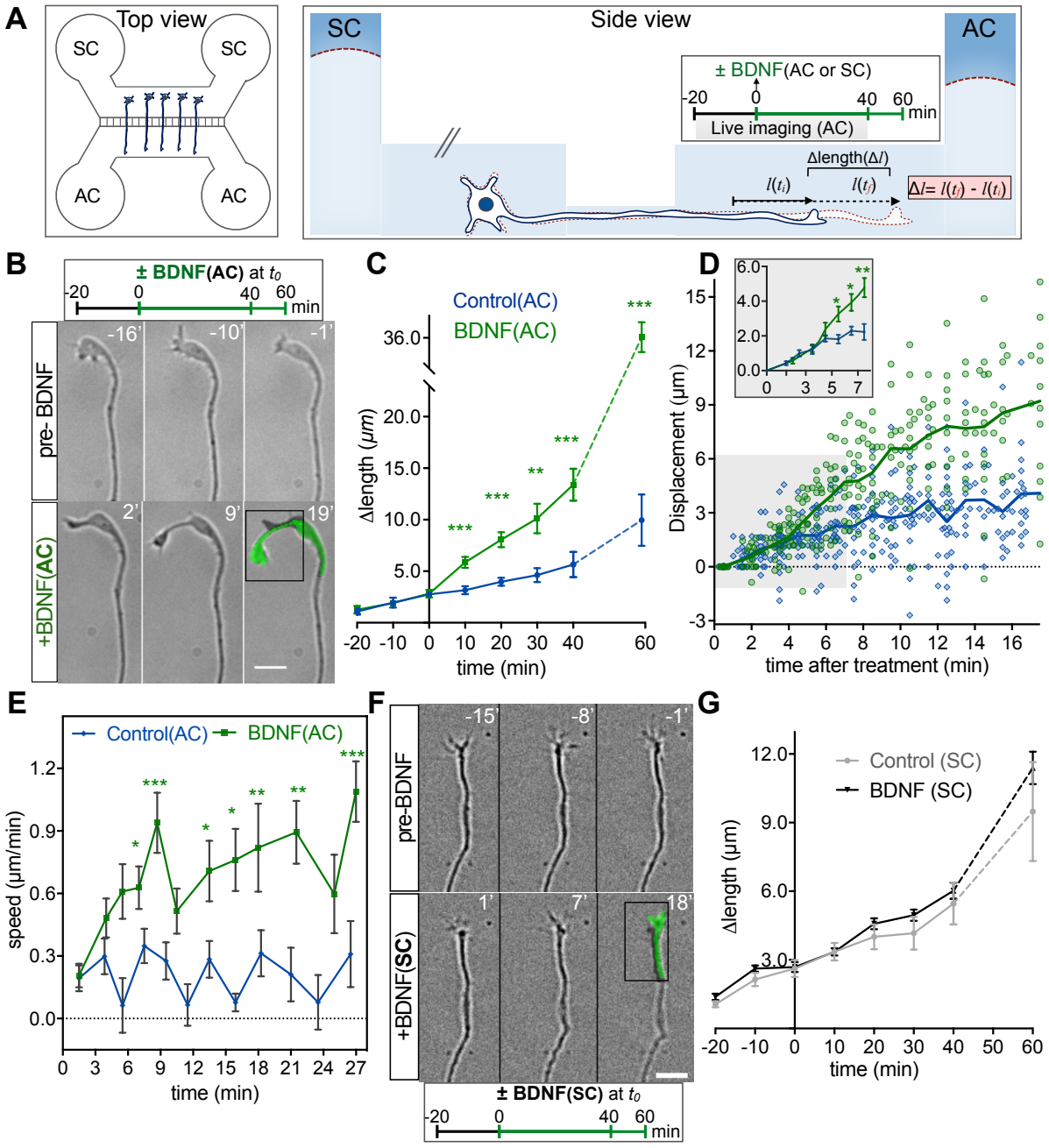
A
Top view
SC
SC
AC
AC
Side view
SC
AC
± BDNF(AC or SC)
-20
0
40
60
min
Live imaging (AC)
Δlength(Δl)
l(ti)
l(tf)
Δl= l(tf) - l(ti)
B
± BDNF(AC) at t0
-20
0
40
60
min
pre- BDNF
+BDNF(AC)
-16'
-10'
-1'
2'
9'
19'
C
Control(AC)
BDNF(AC)
Δlength (μm)
time (min)
D
Displacement (μm)
time after treatment (min)
E
Control(AC)
BDNF(AC)
speed (μm/min)
time (min)
F
pre-BDNF
+BDNF(SC)
-15'
-8'
-1'
1'
7'
18'
± BDNF(SC) at t0
-20
0
40
60
min
G
Control (SC)
BDNF (SC)
Δlength (μm)
time (min)

BDNF activates TrkB and downstream signaling pathways in hippocampal axons

To explore the possible mechanisms by which BDNF promotes axonal growth, we next investigated downstream signaling events induced by BDNF in hippocampal axons. First, we examined TrkB activation by measuring phosphorylated TrkB levels in axonal compartments of microfluidic cultures. As revealed by immunofluorescence, phospho-TrkB (pTrkB) was visualized as small puncta scattered throughout proximal/middle and distal axonal regions, including growth cones. Morphometric analysis of high-resolution confocal images revealed that BDNF(AC) treatment significantly increased the density of pTrkB-positive puncta throughout the axon, including the growth cone (Fig. 2.2 B,C). In addition, fluorescence intensity for pTrkB immunoreactivity significantly increased following BDNF(AC) treatment. BDNF-induced increases in pTrkB puncta density and fluorescence intensity were blocked when axons were preincubated with a specific TrkB antagonist, ANA-12 (Cazorla et al., 2011), prior to BDNF treatment (Fig. 2.2 B,C). These data are evidence that BDNF induced activation of TrkB in axons.

Activation of TrkB elicits a cascade of intracellular signaling events including activation of the well-known PI3K/AKT and Ras/MAPK pathways. These pathways have been shown to play essential roles in the control of cell growth— tightly coupled to the regulation of protein synthesis by downstream signaling molecules, such as the ribosomal protein S6 kinase, S6K (also known as p70-S6K). Although S6K was first identified on the basis of its ability to phosphorylate ribosomal protein S6, additional substrates have been identified including other regulators of protein synthesis, such as the eukaryotic initiation

factor 4B (Magnuson et al., 2012). Importantly, recent studies have pointed to S6K as a regulator of axonal formation and regeneration (Gong et al., 2015; Yang et al., 2014). Thus, we next examined S6K activation downstream of BDNF-TrkB signaling in hippocampal axons. Prior to BDNF addition, phospho-S6K (pS6K) immunoreactivity was observed in dense puncta within axons, whereas few if any puncta were detected in neuronal somas. This finding is consistent with previous observations (Choi et al., 2008; Nie et al., 2010) and suggests a subcellular distribution for pS6K that favors axons. Similar to the response observed for pTrkB, BDNF(AC) significantly increased pS6K immunofluorescence in axons, compared to control. In addition, we observed a significant increase in colocalization between pS6K and pTrkB-positive puncta after BDNF(AC) treatment, as revealed by quantitative analysis of Spearman's rank correlation and Mander's colocalization coefficients (Fig. 2.2 D,F).

The increased colocalization of pS6K and pTrkB raised the possibility that TrkB may signal locally in axons to directly or indirectly activate S6K. To explore this, we incubated axons with the TrkB antagonist ANA-12 prior to BDNF(AC) treatment, then analyzed pS6K immunofluorescence and colocalization with pTrkB. Preincubation with ANA-12 prevented the increases in pS6K immunoreactivity and colocalization with pTrkB (Fig. 2.2 D,F). Indeed, ANA-12 caused a small but significant reduction in axonal pS6K whether or not BDNF was added, suggesting that TrkB activation is upstream of endogenous activation of S6K. Together, these findings show that BDNF acts through TrkB to activate S6K in hippocampal axons.

Figure 2.2 BDNF locally activates TrkB and S6K in hippocampal axons

(**A**) Schematic model of BDNF/TrkB signaling pathway and downstream effectors. Diagram of treatment protocol applied to axons in microfluidic cultures of hippocampal neurons (DIV8). Axonal compartments (AC) were pretreated with the TrkB antagonist ANA-12 (10 μM) or vehicle (0.01% DMSO) for 30 min, followed by BDNF (50 ng/mL) or control treatment for 60 min. (**B**) Representative confocal images of phospho-TrkB (pTrkB) immunofluorescence in axonal compartments of microfluidic cultures after indicated treatments (pseudo-colored; scale bar, 2 μm). (**C**) Quantification of pTrkB puncta density and fluorescence intensity. Values represent mean ± SEM; n = 20-30 axons per condition, 3-4 chambers from three independent experiments. *p<0.05, ***p<0.0001, Kruskal-Wallis test with Dunn's *post-hoc* analysis for multiple comparisons. (**D**) Representative confocal images of pTrkB (green) and pS6K (red) immunofluorescence and corresponding plots of signal intensity across drawn lines, shown in white. Overlapping intensity peaks indicate higher colocalization between signals. (**E-F**) BDNF(AC) treatment significantly increased pS6K fluorescence intensity and pTrkB/pS6K colocalization in axons. (**F**) Graphs show quantification of Spearman's rank correlation and Mander's colocalization coefficients. Data represent mean ± SEM; n = 31-33 axons per condition, 3-4 chambers, 2 independent experiments. Statistical analysis was performed using One-way ANOVA with Tukey's test of multiple comparisons: asterisks (*) represent significant difference between treatment vs. vehicle, *p<0.05, **p<0.005, ***p<0.0005; pound signs (#) show significant difference when compared to BDNF(AC), $^{\#\#}$p<0.001, $^{\#\#\#}$p<0.0001.

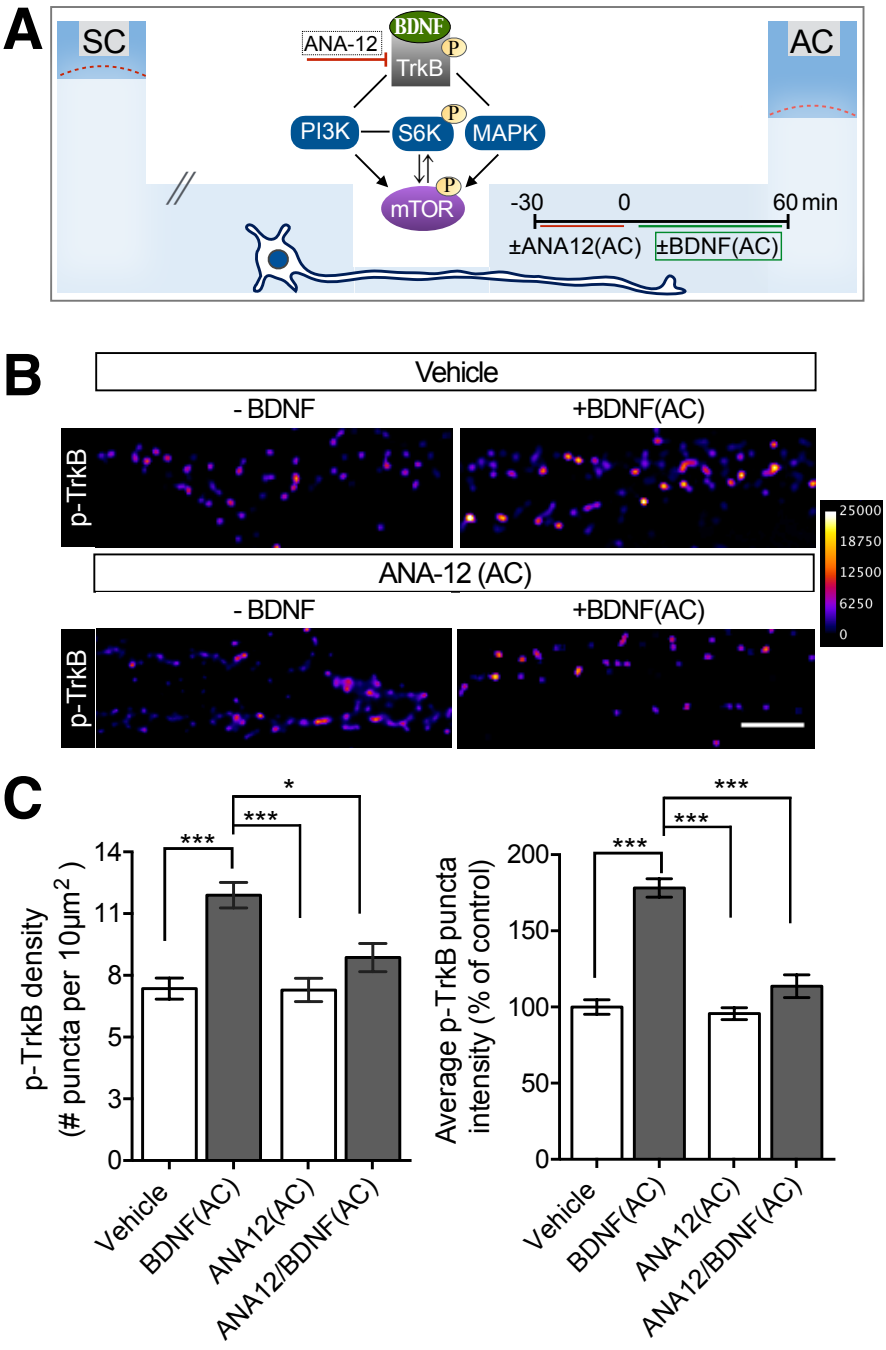
A
SC
AC
ANA-12
BDNF
P
TrkB
PI3K
S6K
MAPK
mTOR
-30
0
60 min
±ANA12(AC)
±BDNF(AC)
B
Vehicle
- BDNF
+BDNF(AC)
p-TrkB
25000
18750
12500
6250
0
ANA-12 (AC)
C
p-TrkB density
(# puncta per 10μm²)
Average p-TrkB puncta
intensity (% of control)
Vehicle
BDNF(AC)
ANA12(AC)
ANA12/BDNF(AC)

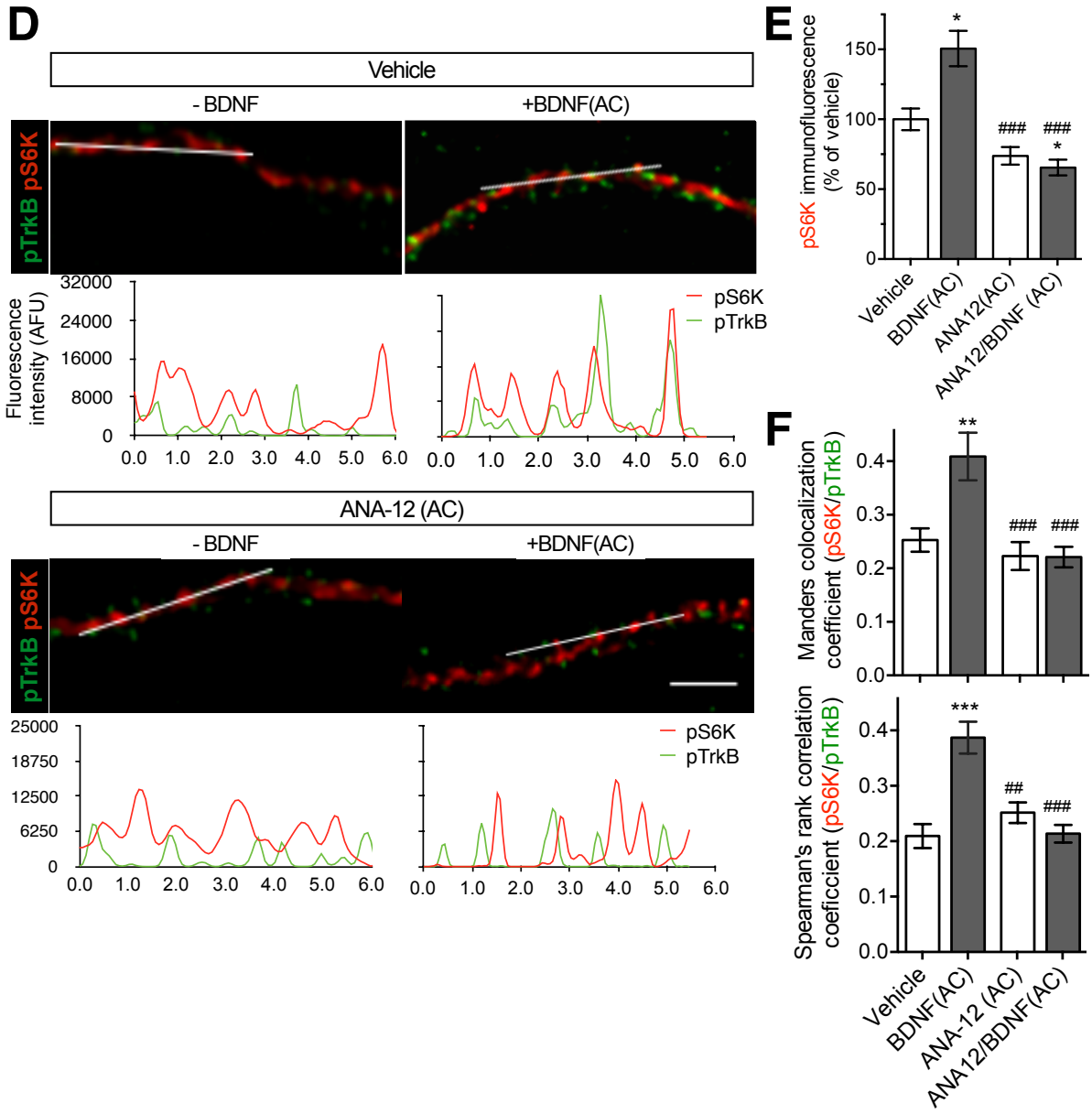

Figure 2.2 BDNF locally activates TrkB and S6K in hippocampal axons, *continued*

BDNF locally activates mTORC1 signaling in hippocampal axons

TrkB-mediated activation of S6K prompted us to examine the activation of other molecules along the mTORC1/S6K signaling axis— especially considering its prominent role in the regulation of cell growth and/or size. The mechanistic target of rapamycin (mTOR) is a serine/threonine kinase that signals through two distinct protein complexes— mTOR complex 1 (mTORC1) and 2 (mTORC2)— to influence almost all aspects of cellular function. By sensing growth factor, nutrient, and energy availability, mTOR regulates major biosynthetic pathways to control cell growth and survival (Saxton and Sabatini 2017). Upon activation, mTORC1 stimulates protein synthesis mainly via one key downstream effector— the eukaryotic initiation factor 4E-binding protein 1 (4EBP1), which normally binds to eIF4E with high affinity to suppress translation. mTORC1-mediated phosphorylation of 4EBP1 prompts its dissociation from the eIF4E-mRNA complex, thereby enabling cap-dependent translation initiation (Ma and Blenis 2009). Accordingly, increased phospho-4EBP1 levels— particularly at residues Ser65 and Thr70— are routinely used as a marker for mTOR activity, upstream of new protein synthesis. In addition, downstream of mTORC1 activation, S6K phosphorylates mTOR at Ser2448 through a possible feedback loop. Although the functional significance of this feedback phosphorylation remains unclear, the levels of phospho-mTOR (p-mTOR, S2448) serve as an additional readout for mTOR/S6K activity (Chiang and Abraham 2005; Magnuson et al., 2012).

To explore the activation of mTOR by local BDNF signaling in axons, we measured the levels of p-mTOR (S2448) and p4EBP1 (S65/T70) in axons grown in microfluidic

chambers, using immunocytochemistry. Upon BDNF(AC) treatment, the density of both p-mTOR and p4EBP1 puncta significantly increased in axons (Fig. 2.3 B-D). In addition, the intensity for p4EBP1 immunoreactivity increased by ~100% after BDNF, compared to control. We then examined p4EBP1 immunoreactivity in axons that were incubated with ANA-12 prior to BDNF addition. Under these conditions, BDNF failed to increase axonal p4EBP1 puncta density or fluorescence intensity (Fig. 2.3 C,D), suggesting that the increase in p4EBP1 occurs downstream of TrkB activation. Next, we verified that BDNF-induced increase in axonal p4EBP1 was indeed mediated by mTOR using Torin— a new generation, highly potent mTOR inhibitor. As expected, pretreatment of axons with Torin completely prevented the increase in p4EBP1 induced by BDNF (Fig. 2.3E). Taken together, these results demonstrate that BDNF signals locally through TrkB to activate the mTOR signaling pathway in hippocampal axons.

BDNF-induced axonal growth requires local mTOR activity

In addition to its conserved roles in eukaryotic cellular metabolism, mTOR has emerged as an important regulator of processes specific to neuronal function, such as axonal regeneration. For instance, several studies have shown that genetic up-regulation of mTOR activity— via upstream inhibitors (e.g. PTEN) or activators (i.e. Rheb)— enhances regeneration after injury in various types of CNS neurons (Abe et al., 2010; Kim et al., 2012; Geoffroy et al., 2016; Park et al., 2008). Additional insight into the role of mTOR in axonal growth has come from experiments using the drug rapamycin to pharmacologically block mTOR activity. Namely, several studies showed that rapamycin treatment blocked

stimulus-induced axonal growth of cortical or DRG neurons, although it did not appear to affect basal growth or axonal regrowth after injury (Hengst et al., 2009; Mita et al., 2015; Saijilafu et al., 2013; Zhang et al., 2013).

Thus, we reasoned that local mTOR activation by BDNF/TrkB signaling might play a role in BDNF-induced axonal growth. To investigate this, we blocked mTOR activity in axons using Torin, which has been shown to inhibit rapamycin-resistant functions of mTOR (Thoreen et al., 2009), and then monitored axonal growth. Compared to control conditions, Torin(AC) treatment did not affect axonal growth over a 40-min recording period: the average growth speed for Torin-treated axons was 0.17 ± 0.08 (n = 38) versus 0.23 ± 0.09 μm/min for vehicle-treated axons (n = 42; Kolmorogov-Smirnov test of cumulative distributions, p=0.72). This result is consistent with previous reports described earlier, and suggests that inhibiting local mTOR activity using Torin does not alter basal axonal growth rate. In marked contrast, Torin(AC) blocked BDNF-induced axonal growth at all time points after the first 10 min (Fig. 2.3 F, G). Interestingly, Torin did not block the very early period of BDNF-induced growth, suggesting that mTOR activity may not be needed for this epoch. Taken together, these results suggest that BDNF-induced axonal growth is mediated, at least in part, by local mTOR signaling.

Figure 2.3 BDNF locally activates mTORC1 in axons to stimulate growth

(**A**) Schematic model of BDNF/TrkB and mTOR/S6K signaling pathways. Diagram of treatment protocol applied to axons in microfluidic cultures of hippocampal neurons (DIV8). Axonal compartments were pretreated with either TrkB antagonist ANA-12 (10 μM), mTOR inhibitor Torin1 (1 μM) or vehicle (0.01% DMSO) for 30 min, followed by BDNF (50 ng/mL) or control treatment for 60 min. (**B**) Representative thresholded images of phospho-mTOR (p-mTOR, S2448) immunofluorescence in axons and quantitative analysis of p-mTOR-positive puncta density. Scale bar, 5 μm. n = 29 (BDNF), n = 25 (control) axons were analyzed from two independent experiments. Values represent mean ± SEM; ***p<0.0001; two-tailed unpaired t-test. (**C**) Pseudo-colored confocal images of phospho-4EBP1 (S65/T70) immunofluorescence in axons grown in microfluidic chambers after specified treatments (scale bar, 2 μm). (**D**) Quantification of p4EBP fluorescence intensity and puncta density. 20-30 axons were analyzed per condition from three independent experiments; values represent mean ± SEM. *p<0.05, **p<0.005; Kruskal-Wallis test with Dunn's *post-hoc* test of multiple comparisons. (**E**) BDNF-induced increase in axonal p4EBP was blocked by Torin pretreatment. n = 11-24 axons per condition from two independent experiments; values represent mean ± SEM. ***p=0.0001; One-way ANOVA with Tukey's *post-hoc* test of multiple comparisons. (**F-G**) Torin(AC) treatment blocks BDNF-induced axonal growth. (**F**) Representative phase-contrast, time-lapse images of distal axon terminals and growth cones. Timestamps are indicated in minutes; BDNF was added at *t*= 0 min. Scale bar, 5 μm. (**G**) Quantification of Δlength per 10-min intervals. Data represent mean ± SEM; n = 16-34 axons per condition from two independent experiments. Statistical analysis performed using One-way ANOVA with Tukey's *post-hoc* test of multiple comparisons: asterisks represent difference between BDNF(AC) vs. vehicle control, *p<0.05, **p<0.005; pound signs (#) represent difference between Torin/BDNF vs. vehicle control, $^{\#}$p<0.01.

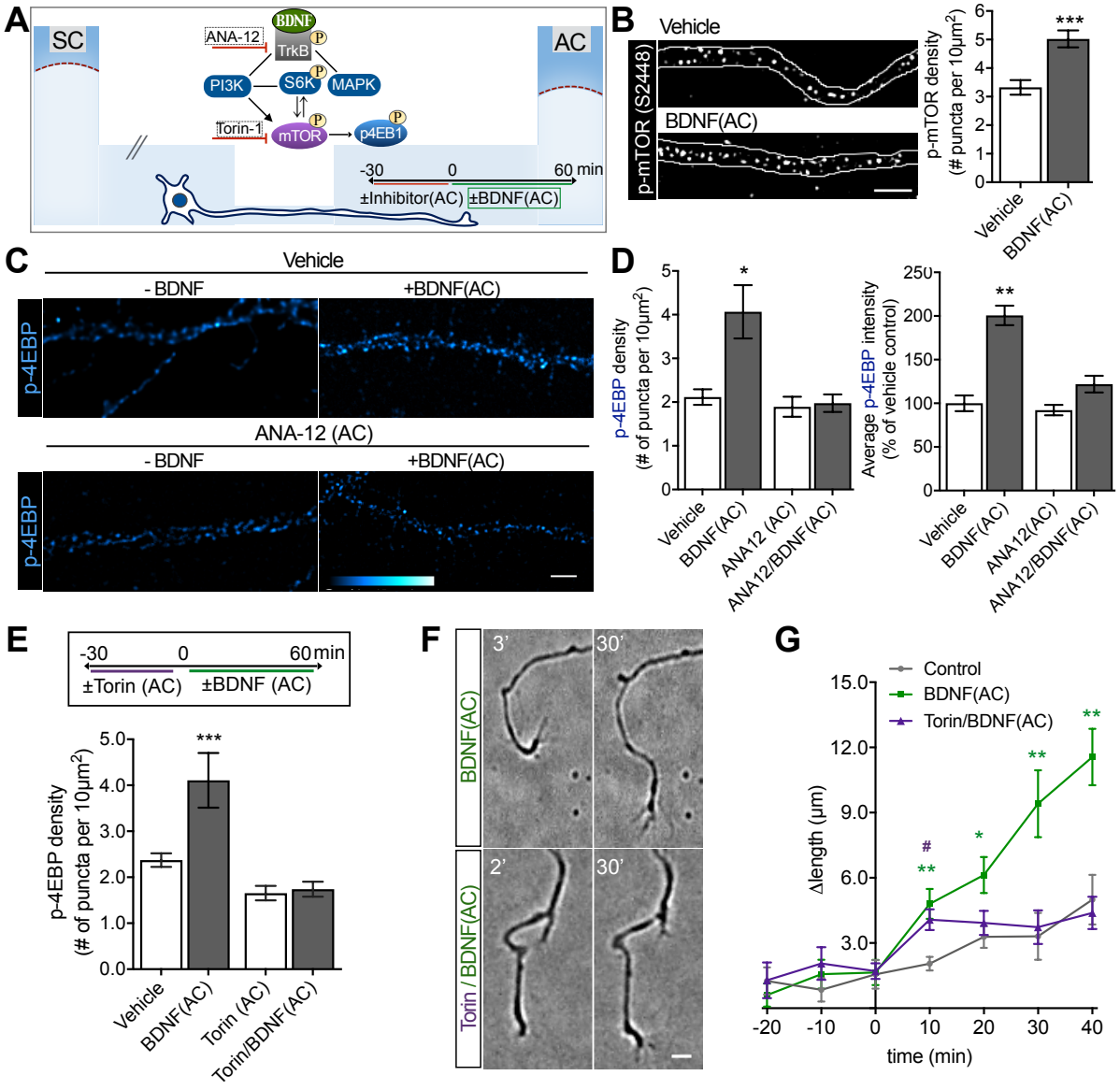
A
SC
AC
BDNF
TrkB
ANA-12
PI3K
S6K
MAPK
Torin-1
mTOR
p4EB1
-30
0
60 min
±Inhibitor(AC)
±BDNF(AC)
B
Vehicle
BDNF(AC)
p-mTOR (S2448)
p-mTOR density
(# puncta per 10μm²)
Vehicle
BDNF(AC)
C
Vehicle
- BDNF
+BDNF(AC)
p-4EBP
ANA-12 (AC)
- BDNF
+BDNF(AC)
p-4EBP
D
p-4EBP density
(# of puncta per 10μm²)
Vehicle
BDNF(AC)
ANA12 (AC)
ANA12/BDNF(AC)
Average p-4EBP intensity
(% of vehicle control)
Vehicle
BDNF(AC)
ANA12(AC)
ANA12/BDNF(AC)
E
-30
0
60 min
±Torin (AC)
±BDNF (AC)
p-4EBP density
(# of puncta per 10μm²)
Vehicle
BDNF(AC)
Torin (AC)
Torin/BDNF(AC)
F
BDNF(AC)
Torin / BDNF(AC)
3'
30'
2'
30'
G
Control
BDNF(AC)
Torin/BDNF(AC)
Δlength (μm)
time (min)

BDNF-induced growth of hippocampal axons requires local protein synthesis

Thus far, our findings point to local mTOR activation downstream of BDNF/TrkB signaling in axons. In particular, the local activation of S6K and inhibition of 4EBP1 strongly suggest activation of mTORC1 to stimulate protein synthesis. Increasing evidence from a number of studies indicate that various stimuli can induce local protein synthesis in axons. Moreover, the local translation of multiple axonally-localized mRNAs has been shown to be important for axonal growth and/or function in different contexts— i.e. nervous system development, regeneration and maintenance (Costa and Willis 2017; Jung et al., 2012; Rangaraju et al., 2017). Since both mTOR signaling and local protein synthesis have previously been implicated in axonal growth, we hypothesized that BDNF effects on axonal growth were mediated by local protein synthesis.

First, we sought to verify whether local BDNF signaling in hippocampal axons stimulates intra-axonal protein synthesis. Previous studies have shown that bath-applied BDNF promotes protein synthesis in cultured cortical neurons and hippocampal slices (Schratt et al., 2004; Dieterich et al., 2010; Genheden et al 2015; Bowling et al, 2016). To visualize BDNF-induced protein synthesis in axons, we employed the fluorescent non-canonical amino acid tagging (FUNCAT) method (Dieterich et al., 2010) using microfluidic cultures. Briefly, we first depleted axons off methionine by replacing the growth medium in axonal compartments (AC) with methionine-free medium. Then, we selectively added the methionine analog L-azidohomoalanine (AHA) to ACs, in the presence or absence of BDNF (Fig. 2.4A). Finally, we visualized new protein synthesis by labelling AHA-containing

proteins using a specific fluorescent tag. As expected, we observed a significant increase of ~120% in the density of AHA-positive puncta in axons treated with BDNF(AC), compared to control (Fig. 2.4B). These findings, together with the observed activation of S6K and inhibition of 4EBP1, provide evidence that local BDNF signaling stimulates *de novo* protein synthesis in hippocampal axons. Notably, using this experimental paradigm, AHA-positive puncta were not detected in the somatodendritic compartment throughout the duration of the experiment: if axonally-synthesized proteins are retrogradely transported to cell bodies in response to BDNF during this period, they failed to reach detectable levels.

To directly test the hypothesis that BDNF effects on axonal growth were mediated by local protein synthesis, we used the translation inhibitors cycloheximide (CHX) or anisomycin to pharmacologically block protein synthesis in axons grown in microfluidic chambers. First, we assessed whether blocking local protein synthesis had any effect on basal axonal growth by treating the axonal compartment with CHX (5μg/mL) for 30 min, then monitoring growth over the next 30-60 min. On average, the change in axonal length (Δlength) over a 45-min period was significantly lower for CHX-treated axons than for vehicle-treated controls ($\Delta l_{Control}$ = 2.6 ± 0.2 vs. Δl_{CHX} = 0.4 ± 0.4 μm; mean ± SEM, p<0.0001, two-tailed Mann-Whitney test). Further analysis of the data revealed that the fraction of Δlength measurements with values less than or equal to zero was significantly higher in the CHX(AC) condition compared to control (44 vs. 12%, respectively; Fig. 2.4C). These findings are evidence that inhibiting local protein synthesis reduces basal axonal growth rate and/or increases axonal retraction. Not surprisingly, CHX(AC) treatment

completely abolished BDNF-induced axonal growth (Fig. 2.4D); essentially identical results were obtained when anisomycin (20 μM) was used instead of CHX. Together these results strongly suggest that local protein synthesis is necessary for BDNF-induced axonal growth in hippocampal neurons.

Figure 2.4 BDNF induces local protein synthesis in hippocampal axons

(**A**) Diagram of experimental protocol: AHA (1mM) was added to axonal compartments of microfluidic cultures (DIV8) for 60 min prior to BDNF (50 ng/mL) or control treatment. (**B**) Protein synthesis was visualized using FUNCAT (arrowheads); higher fluorescence intensity reflects increased AHA incorporation into nascent proteins. Quantification of density of AHA-containing proteins per axonal area; **p<0.005, two-tailed unpaired t-test. (**C**) Top: Schematic of experimental protocol; axonal compartments were pretreated with CHX (10 µg/mL) or vehicle (0.01% DMSO) for 30 min, followed by BDNF (10 ng/mL) or control for 35 ± 5 min. Bottom: Cumulative distributions of Δlength values after CHX(AC) or vehicle (control) treatments; ***Kolmogorov-Smirnov test. (**D**) Representative time-lapse images of distal axon terminals and growth cones. Timestamps are in minutes; BDNF was added at *t*= 0 min. Scale bar, 5 µm. Bottom: Quantification of Δlength per 10-min intervals; n = 12-34 axons per condition. Data is shown as mean ± SEM; *p<0.05, **p<0.005, ***p<0.005, One-way ANOVA with Tukey's *post-hoc* test of multiple comparisons.

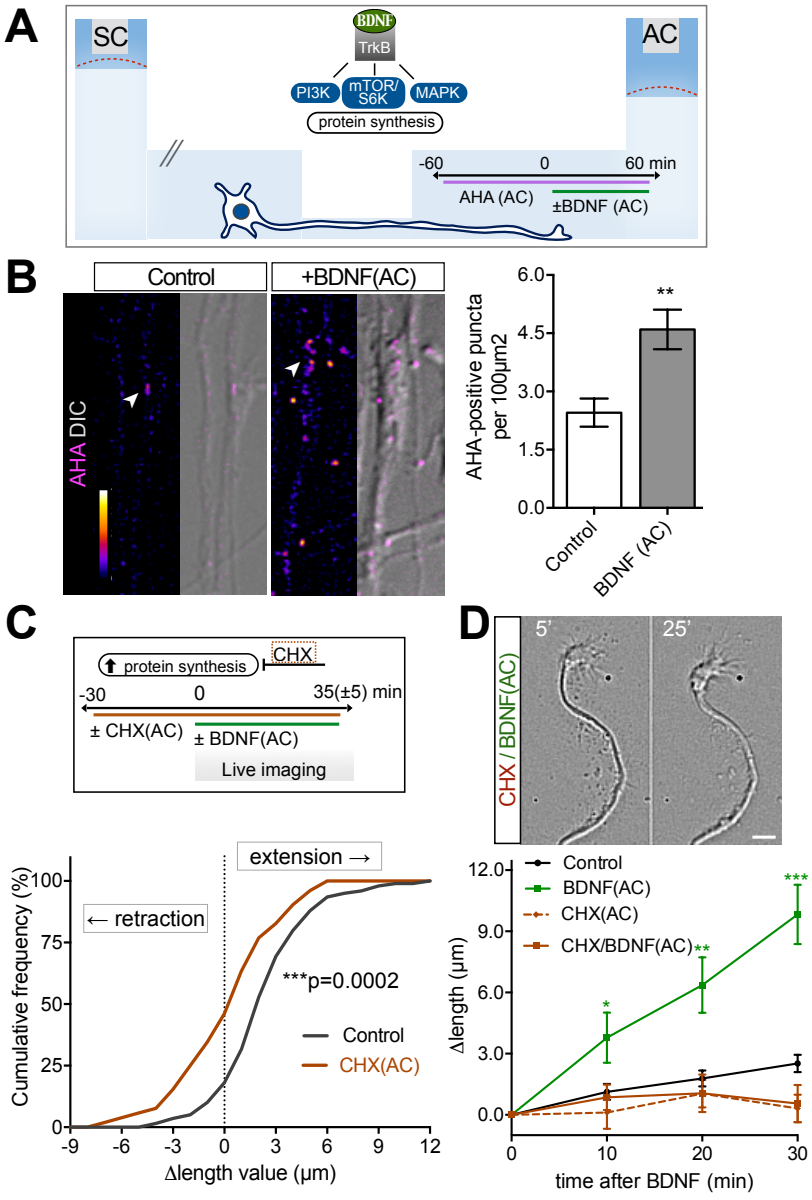
A
SC
AC
BDNF
TrkB
PI3K
mTOR/
S6K
MAPK
protein synthesis
-60
0
60 min
AHA (AC)
±BDNF (AC)
B
Control
+BDNF(AC)
AHA DIC
AHA-positive puncta
per 100µm2
6.0
4.5
3.0
1.5
0.0
**
Control
BDNF (AC)
C
protein synthesis
CHX
-30
0
35(±5) min
± CHX(AC)
± BDNF(AC)
Live imaging
D
5'
25'
CHX / BDNF(AC)
extension →
← retraction
Cumulative frequency (%)
100
75
50
25
0
***p=0.0002
Control
CHX(AC)
-9
-6
-3
0
3
6
9
12
Δlength value (µm)
Control
BDNF(AC)
CHX(AC)
CHX/BDNF(AC)
12.0
9.0
6.0
3.0
0.0
Δlength (µm)
*
**
***
0
10
20
30
time after BDNF (min)

New RNA and protein synthesis in cell bodies sustain BDNF-induced axonal growth

An extensive body of work suggests that Trk receptor activation by neurotrophins elicits a cascade of signaling events underlying 'rapid' cellular responses— e.g. synaptic changes that may occur within seconds— and 'slow' cellular responses, such as growth and survival, which may occur hours to days after signal initiation and are thought to be mediated by transcriptional changes (Harrington and Ginty 2013; Tasdemir-Yilmaz and Segal 2016). Our findings raised some intriguing questions regarding the spatiotemporal regulation of gene expression by BDNF in hippocampal neurons, at the levels of both transcription and translation— particularly as it relates to BDNF-induced axonal growth.

Considering that local BDNF signaling increased axonal growth within minutes, and that axonal protein synthesis appeared to be required for this effect, we next asked whether BDNF-induced transcriptional changes in the nucleus played a role in this fast growth response. To test this, we blocked new RNA synthesis by incubating neuronal cell bodies within the somatodendritic compartment with the transcription inhibitor Actinomycin-D (ActD) for 30 min, then monitored BDNF-induced axonal growth by live imaging (Fig. 2.5A). Interestingly, transcription inhibition in the cell bodies did not have an effect on BDNF-induced axonal growth during the initial 40-min interval following BDNF(AC) treatment (Fig. 2.5B). When cultures were pretreated with ActD(SC), we noticed a significant decrease in axonal growth during the 40-60 min interval after BDNF(AC) addition, compared to cell bodies treated with DMSO as a control (Fig. 2.5B).

In view of these findings, we hypothesized that local BDNF signaling in axons may induce three distinguishable growth responses: (1) an immediate growth response, noticeable within the first 10 min of axonal exposure to BDNF, dependent on active intra-axonal protein synthesis but independent of either mTOR activity or *de novo* transcription; (2) a second period of growth, between 10 to ~60 min after BDNF stimulation, which is dependent on axonal translation *and* local mTOR activity but is also transcription-independent; and finally, (3) a sustained growth response— occurring 60 min or longer after initial exposure to BDNF— which is at least partially dependent on new transcription. To further examine this possibility, we pretreated cell bodies with ActD(SC) for 30 min, and assayed BDNF-induced axonal growth 2 h after BDNF(AC) treatment. Consistent with our hypothesis, transcription inhibition in cell bodies significantly suppressed the sustained axonal growth response induced by BDNF. That is, ActD(SC) treatment significantly reduced the change in axonal length (Δlength) during the 2 h-interval following BDNF(AC) addition, as compared to vehicle (SC)— 22.1 ± 2.6 and 40.6 ± 3.0 μm, respectively (mean ± SEM; Fig. 2.5C). Notably, the average Δlength (2h) recorded in the ActD(SC)/BDNF(AC) condition was still significantly higher than that observed for the control condition without BDNF (22.1 ± 2.6 and 11.5 ± 2.0 μm, respectively; p=0.02). This difference could be explained as a residual effect from the early, transcription-independent growth response induced by BDNF, as we hypothesized earlier. Together, these results suggest that new transcription is required to sustain BDNF-induced axonal growth after the initial 40-min period following BDNF addition.

To confirm that RNA synthesis was inhibited under these experimental conditions, we monitored the levels of select mRNA species in the somatodendritic compartment of microfluidic cultures. To this end, we used quantitative RT-PCR to examine changes in gene expression following ActD(SC) or vehicle treatment. Compared to vehicle control, ActD treatment significantly reduced the relative expression levels of *Map1b* and *Ctnnb1* in the somatodendritic compartment within 60 min (41 ± 11 and 76 ± 2% of control levels, respectively); this effect persisted throughout 4 hours (Fig. 2.5D). In contrast, the expression levels of *Vim*— an mRNA species with a relatively long half-life of ≥ 6 h (Coleman and Lazarides 1992; Lilienbaum et al., 1986)— were just slightly reduced after ActD(SC) treatment (Fig. 2.5D). These results show that ActD treatment effectively suppressed transcription under the conditions employed in our studies.

The need for ongoing transcription to support axonal growth may be due to stimulus-induced changes in the demand for RNA species for axonal transport, new protein synthesis in cell bodies, or both. To determine whether protein synthesis in cell bodies was also necessary for the growth response by BDNF, we pharmacologically inhibited protein synthesis exclusively in the somatodendritic compartment of microfluidic cultures using CHX prior to assessing BDNF-induced axonal growth. To verify that protein synthesis was inhibited by CHX(SC), we used the FUNCAT technique to visualize protein synthesis in neuronal cell bodies. First, we pretreated neurons within the somatodendritic compartment with CHX (5 μg/mL) or vehicle for 30 min, followed by incubation with the amino acid analog AHA (Fig. 2.5F). After fixation, we fluorescently labeled AHA-containing proteins

for quantitative analysis. As expected, CHX(SC) treatment significantly reduced AHA fluorescence in neuronal cell bodies compared to control— 38 ± 5 vs. 100 ± 10%, respectively, indicating that new protein synthesis was indeed suppressed by CHX.

Live-imaging analysis revealed that the significant increase in axonal growth upon BDNF stimulation was unaffected by CHX(SC) treatment during the first 60-min period after axonal exposure to BDNF (Fig. 2.5E). However, sustained BDNF-induced axonal growth (140 min after BDNF addition) was significantly suppressed by CHX treatment compared to vehicle control (22.9 ± 1.7 and 43.7 ± 2.9 µm, respectively; mean ± SEM, $p<0.0001$). This result suggests that, similar to RNA synthesis, protein synthesis in the somatodendritic compartment is not required for early BDNF-induced axonal growth, yet it plays a necessary role in sustaining BDNF-induced axonal growth for longer time periods.

Given our findings that transcription and translation in neuronal cell bodies played a role in sustaining BDNF-induced axonal growth, we wondered whether BDNF signaling from cell bodies could induce axonal growth after longer periods of exposure. To examine this, we extended the period of observation used in earlier studies (Fig. 2.1G) and exclusively treated the somatodendritic compartment with BDNF for 2 h, then assessed axonal growth within the axonal compartment. Interestingly, axonal growth over 2 h was comparable between BDNF(SC) and vehicle-treated control cultures— 11.5 ± 0.6 vs. 12.5 ± 2.5 µm, respectively (average Δlength ± SEM; $p=0.80$, two-tailed *t*-test comparison of BDNF-SC vs control). In other words, longer treatment of cell bodies with BDNF(SC) did not induce axonal growth. Thus, while new RNA and protein synthesis in cell bodies were

required for sustaining BDNF-induced axonal growth, it is necessary for BDNF signaling to be initiated in the distal axons.

Figure 2.5 Transcription and translational responses in cell bodies sustain BDNF-induced axonal growth

(**A**) Diagram of treatment protocol applied to hippocampal neurons grown in microfluidic chambers (DIV7-8). RNA or protein synthesis was inhibited in somatodendritic compartments (SC) using ActD (2μM) or CHX (5μg/mL), respectively, for 30 min, prior to addition of 10 ng/mL BDNF to the axonal compartment (AC). As a control, vehicle (0.01% DMSO) was added to SC for 30 min. (**B**) Axonal growth was monitored by live-imaging before and after BDNF(AC) addition, in the presence or absence of ActD(SC). Change in length (Δlength) was calculated in 10-min intervals for an 80-min recording period. Statistical significance between BDNF(AC) and control is represented by asterisks; significance between ActD(SC)/BDNF(AC) and control is represented by pound signs. *p<0.05, **p<0.005, ***p<0.005, $^{\#}$p<0.05, $^{\#\#}$p<0.005; Kruskal-Wallis test with Dunn's *post-hoc* analysis for multiple comparisons. N.s., not significant. (**C**) Axons were pretreated with ActD(SC) or vehicle, as described in A. Top: phase-contrast images of axons before (left) and after BDNF (AC) treatment for 2 hours (right). Scale bar, 20 μm. Bottom: quantification of Δlength over 2 h period; box-and-whisker plots indicate the median value (center line) and the interquartile range (boxes). n = 18-34 axons per condition from two independent experiments. Statistically-significant difference from control sample is indicated; ***p<0.0001, $^{\#}$p<0.01, One-way ANOVA with Tukey's *post-hoc* test of multiple comparisons. (**D**) Quantitative RT-PCR expression of select mRNAs in the somatodendritic compartment of hippocampal microfluidic cultures before and after ActD(SC) treatment. Top: Diagram of experimental paradigm— RNA lysates were then obtained from SC after ActD (2μM) treatment for the indicated durations, as described in Methods section. Bottom: Relative mRNA expression of Vimentin, ß-catenin and Map1b normalized to GAPDH levels, calculated using ΔC_T method. Data represents $2^{-\Delta\Delta Ct}$ values; mean ± SEM. *p<0.05; two-tailed *t*-test (treatment vs. control). (**E**) BDNF-induced axonal growth was monitored by live-imaging in the presence or absence of CHX(SC), for an 80-min recording period. Change in length 140 min after axonal exposure to BDNF was also calculated. **p<0.001, One-way ANOVA with Tukey's *post-hoc* test of multiple comparisons. (**F**) Protein synthesis was visualized in neuronal cell bodies using FUNCAT. Diagram shows experimental paradigm: SCs were pretreated with CHX (5μg/mL) prior to AHA (1mM) addition. Representative images of AHA fluorescent signal in SCs (pseudo-colored) and quantification of signal intensity, shown as mean ± SEM. n = 12-16 neurons, 2 chambers per condition; ***p<0.0001; unpaired two-tailed *t*-test with Welch's correction.

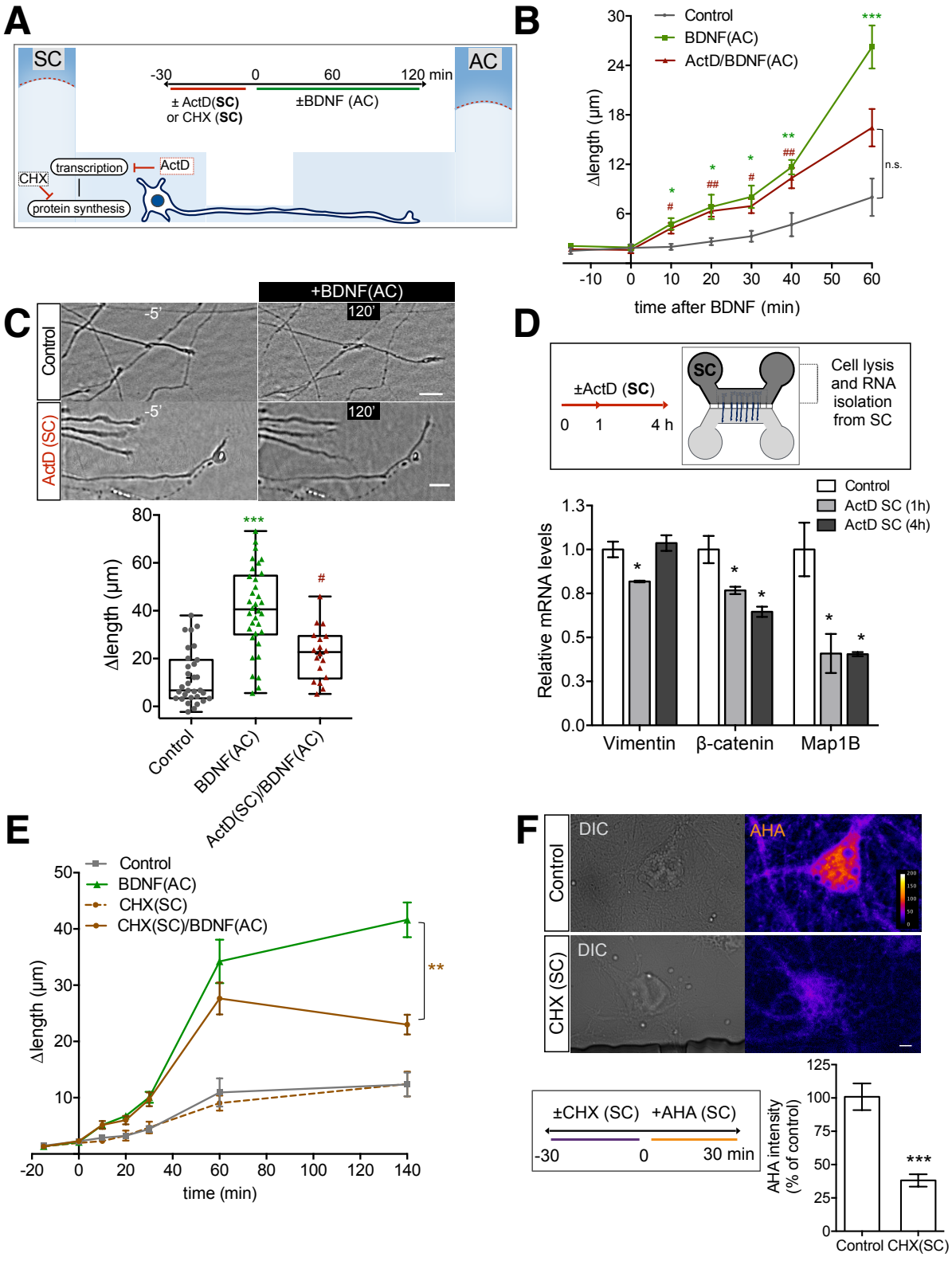
A
SC
AC
-30
0
60
120 min
± ActD(SC)
or CHX (SC)
±BDNF (AC)
transcription
ActD
CHX
protein synthesis
B
Control
BDNF(AC)
ActD/BDNF(AC)
Δlength (μm)
time after BDNF (min)
n.s.
C
+BDNF(AC)
Control
ActD (SC)
-5'
120'
Δlength (μm)
Control
BDNF(AC)
ActD(SC)/BDNF(AC)
D
±ActD (SC)
0
1
4 h
SC
Cell lysis
and RNA
isolation
from SC
Control
ActD SC (1h)
ActD SC (4h)
Relative mRNA levels
Vimentin
β-catenin
Map1B
E
Control
BDNF(AC)
CHX(SC)
CHX(SC)/BDNF(AC)
Δlength (μm)
time (min)
F
Control
CHX (SC)
DIC
AHA
±CHX (SC)
+AHA (SC)
-30
0
30 min
AHA intensity
(% of control)
Control
CHX(SC)

2.3 Discussion

BDNF signals through its receptor TrkB to regulate various aspects of neuronal function. TrkB is present all throughout the neuron in somatodendritic and axonal compartments: within neuronal circuits, these subcellular compartments are spanned by large distances and highly susceptible to their local molecular microenvironment. Given this complex geometry and the wide range of cellular functions that BDNF signaling can regulate, the subcellular location of signal initiation is thought to play an important role in dictating the specificity of BDNF-induced neuronal responses. The detailed nature of the intracellular signaling and molecular events whereby BDNF regulates axonal growth remain poorly understood. In the present study, we investigated the spatiotemporal dynamics of BDNF-induced growth of hippocampal axons after differentiation— when most axonal elongation and/or branching is thought to occur. We provide evidence that BDNF acts locally in hippocampal axons to activate downstream signaling molecules, namely mTOR, and protein synthesis to induce axonal growth within minutes.

Using various neuronal models, a number of previous studies have described a role for BDNF in immature neurite differentiation and growth, but the mechanisms involved remain largely unclear. Most previous studies exploring the effects of BDNF on neurite/ axonal growth have been performed using neuronal mass cultures at developmental stages 1-2 (DIV1-4), where BDNF is bath-applied for durations of 1-3 days, generally added at the time of plating (see Table 1.1). Although these studies have consistently shown that BDNF increases average axonal length, the experimental paradigms that have been commonly used

complicate assessing when and where BDNF exerts its functional effects— it has been particularly difficult to distinguish whether BDNF regulates axonal specification, growth, or both. In one example, Namekata et al. (2012) reported that BDNF promotes axonal outgrowth in cultured hippocampal neurons: axonal length increased by ~45% upon BDNF treatment for 3 days (from DIV 0-3) compared to control— the longest neurites were considered axons and normalized length values were reported as a percentage of control. Despite this seemingly robust effect, these findings need to be interpreted with caution and its various possible interpretations merit further discussion. In one possible scenario, these results could reflect an effect on axonal differentiation exclusively: if BDNF induces or accelerates the process of axonal differentiation at some unspecified point during the treatment duration, newly-differentiated axons will purportedly grow 5-10 times faster than other neurites of the same neuron (Polleux and Snider 2010). Consequently, the average neurite length of such neuronal population— one with a higher fraction of neurons containing differentiated, longer axons— will be higher than that of neurons cultured without BDNF. Alternatively, BDNF may regulate neurite growth rate at various stages before and after axonal specification to aid in both the establishment and maintenance of neuronal polarity.

Here, we investigated BDNF-induced growth of differentiated hippocampal axons (stage 4-5; DIV6-8) employing a microfluidic compartmentalized culture system that allowed us to mimic the scenario when axonal terminals are locally exposed to distant sources of BDNF *in vivo*— e.g. secreted in a paracrine fashion from post-synaptic targets.

Using live-imaging microscopy, we monitored axonal terminal growth before and immediately following BDNF addition to either the axonal or somatodendritic compartments independently**,** for up to 2 h, which allowed us to analyze changes in growth rate within short timescales. Upon exposing distal axons to physiologically-relevant amounts of BDNF, axonal elongation rate greatly increased within the first few minutes and remained elevated for at least 60 min. Interestingly, this increase in elongation rate was only observed when BDNF was applied locally to axons and not when BDNF was applied to the somatodendritic compartment. These findings strongly support the hypothesis that BDNF signaling outcomes are spatially coded. That is, distinct cellular responses are elicited when BDNF signaling originates in the somatodendritic versus axonal compartments. Although our data does not exclude the possibility that BDNF signaling from the somatodendritic compartment might induce distal axonal growth after longer periods of treatment (e.g. days), it provides clear evidence that the subcellular location of signal initiation plays an important role in regulating BDNF-induced axonal growth. Consistent with this notion, a few recent studies described spatial-specific regulation of axonal growth by Netrin-1 and glial-derived neurotrophic factor (GDNF) in compartmentalized mouse cortical or spinal motor neuron cultures (Blasiak et al., 2017; Zahavi et al., 2015).

The spatiotemporal dynamics of BDNF-induced axonal growth are particularly relevant for research attempts aiming to understand the molecular mechanisms underlying growth. If BDNF increases elongation rate within the first hour after initial exposure, there may also be distinct molecular events occurring at various time points and within subcellular

compartments during and after growth. In several previous studies, researchers have studied BDNF-induced signaling events, mainly in short time scales, and correlated these with growth data to understand the molecular mechanisms underlying growth (see Table 2.1). It is important to consider the possibility that molecular events observed days after initial exposure to BDNF may not be directly related to BDNF-initiated growth but instead a reflection of the neuron's attempt to return to its pre-stimulus, quiescent state.

What are the underlying signaling/molecular mechanisms driving this phenomenon?

Our study also provides key insights into the molecular mechanisms that regulate BDNF-induced axonal growth. There is ample evidence substantiating the occurrence and importance of retrograde neurotrophin signaling for overall neuronal function. Prevalent theories suggest that neurotrophin signaling complexes can form in axons but ultimately exert their function through actions in cell bodies (Tasdemir-Yilmaz and Segal 2016). Although the notion that neurotrophins can signal locally to influence specific functions within axons (independent of events occurring in the cell body) has been proposed, evidence supporting this is surprisingly limited— especially in the context of BDNF/TrkB signaling in the CNS. A number of commonly cited studies have shown that neurotrophins can locally activate Trk, ERK and Akt kinases in axons of DRG or SCG neurons using compartmentalized cultures (Atwal et al., 2000; Heerssen et al., 2004; Kuruvilla et al., 2000; Kuruvilla et al., 2004; Watson et al., 2001). It is important to note that in several of these studies TrkB was exogenously introduced to the cultures (Atwal et al., 2000; Heerssen et al., 2004; Watson et al., 2001)— DRGs preferentially express TrkA after embryonic stage E11

(Fariñas et al., 1998) and SCGs do not express TrkB at any developmental stage (Fagan et al., 1996)— and axons were exposed to both NGF and BDNF simultaneously, which may complicate the interpretation of the results. Consistent with findings from the aforementioned studies using compartmentalized cultures of PNS neurons and other studies performed using mass cultures of cortical neurons (Lai et al., 2015; Takei et al., 2001; Takei et al., 2004), we found that axonally-applied BDNF can locally activate endogenous TrkB and members of the mTORC1/S6K signaling pathway in hippocampal axons.

Extensive research has established that mTORC1/S6K signaling plays a central role in the control of cell growth across different tissues (Magnuson et al., 2012); however, its regulation and functions in the various neuronal subcellular compartments remain poorly understood. Our data shows that S6K and mTOR both localize to hippocampal axons and can be locally activated by BDNF, downstream of TrkB activation. S6K activity is thought to be regulated by complex multi-site phosphorylation involving mechanisms that remain largely undefined. Some studies suggest that the phosphorylation of S6K at multiple sites, including Ser-411, serve as priming events for mTORC1-mediated phosphorylation of residue Thr-389, ultimately required for full kinase activation (Dufner and Thomas 1999; Hou et al., 2007). Alternatively, others have proposed that instead of serving as a priming event for eventual phosphorylation by mTORC1 (at T389), phosphorylation of S6K at Ser-411 might serve to regulate substrate specificity (Lai et al., 2015). Here we provide evidence that BDNF acts locally through TrkB to increase S6K (S411) phosphorylation in distal axons. Consistent with this finding, Emdal et al., (2015) identified S6K as part of the

TrkA ‘interactome’ and among the molecules that displayed extensive, sustained activation upon NGF stimulation of neuroblastoma cells. Future studies will have to further explore the TrkB/S6K interaction in hippocampal neurons and the intriguing possibility that S6K phosphorylation and function may be differentially regulated in the various neuronal subcompartments.

The regulation of protein synthesis, particularly to control cell and tissue growth, is by far the best-known function of the mTORC1/S6K signaling pathway. Nevertheless, details concerning the spatiotemporal regulation of protein synthesis by BDNF signaling to support axonal growth remain undefined. Using several biochemical markers for protein synthesis activation— including increased levels of p4EBP1, pS6K, and fluorescently-tagged newly synthesized proteins— we found that axonally-applied BDNF stimulates local translation in hippocampal axons. In addition, the timing of BDNF induced translation parallels the observed increase in axonal growth and pharmacological inhibition of either mTOR or protein synthesis in axons blocked BDNF-induced axonal growth. These observations strongly suggest that local mTOR activity and intra-axonal protein synthesis play an important role in supporting distal axon growth in hippocampal neurons. Notably, inhibition of axonal protein synthesis resulted in a more pronounced disruption of axonal growth— both BDNF-induced and basal growth— than local mTOR inhibition. One plausible explanation is that mTOR activity plays an important role in the signal transduction pathway driving BDNF-induced axonal growth. It is also possible that continual intra-axonal protein synthesis is required for general axonal maintenance and

growth, whereas mTOR-dependent protein synthesis and/or other functions play a role in supporting increased axonal growth induced by specific stimuli.

How is protein synthesis temporally and spatially regulated by BDNF signaling to support axonal growth?

Our results suggest that a BDNF signal originating in axons induces an initial fast growth response mediated by local protein synthesis— most likely relying on a readily accessible pool of axonally-localized mRNAs. Then, a BDNF-induced signal— mediated by the transport of signaling endosomes or through a secondary messenger — communicates with the cell body to induce changes in transcription that appear to be important for a continued growth response. That active transcription is required for sustaining BDNF-induced hippocampal axon growth within such a short timescale was somewhat surprising; previous studies have found that NGF-induced axonal growth in peripheral neurons was transcription-independent during the initial 24h-period after stimulation and appears to require new transcription for a continued growth response 24-48 h after stimulation (Bodmer et al., 2011; Harrington and Ginty 2013). This difference could be due to many factors, e.g neuronal type, developmental age in vitro, trophic factor, ActD concentration used, etc.

The requirement for new transcription to support BDNF-induced continued growth was also surprising because active transcription does not appear to be required for basal axonal growth, based on our own results and others' (Saijilafu et al., 2013). Together, these results further support the theory that for a post-mitotic cell at intermediate developmental

stages, fast transcriptional changes are particularly important for stimulus-induced functions but not necessary for general maintenance (Yosef and Regev 2011). In addition, it is known that BDNF quickly induces transcription of IEGs but it is not necessarily known that this transcriptional response is relevant for growth within such a short timescale. This makes us speculate on the exciting possibilities: BDNF-induced transcriptional changes may be required to either increase levels of mRNAs that are particularly relevant to axonal growth (and are present at low levels in the absence of growth-promoting stimuli), or to replenish the mRNA pool to meet the high protein synthesis demand during active growth.

Acknowledgements: Chapter 2, in full, is currently being prepared for submission for publication of the material. Natera-Naranjo, O and Mobley, W.C. The dissertation author was the primary investigator and author of this material.

Chapter 3:
Characterization of BDNF-induced transcriptional responses

3.1 Introduction

BDNF regulates diverse neuronal functions through highly precise coordination of signaling events, which may occur in different neuronal sub-compartments, with corresponding changes in gene expression. That is, signaling events downstream of BDNF/TrkB elicit transcriptional responses— often through the action of transcription factors such as CREB (Lonze and Ginty 2002; Park and Poo 2012)— to influence the synthesis of mRNAs relevant to the desired neuronal response(s). BDNF signaling can also affect gene expression at the translational level: by rapidly modulating translation rates of available mRNAs, the neuronal proteome can adapt accordingly to achieve specific neuronal responses. For instance, retrograde neurotrophin signaling mediates neuronal survival by promoting the transcription and translation of anti-apoptotic genes, such as members of the *Bcl-2* family (Harrington and Ginty 2013). Similarly, the effects of BDNF on synaptic strengthening (Alder et al., 2003; Messaoudi et al., 2002), spine remodeling (Adasme et al., 2011) and dendritic growth (Finsterwald et al., 2010) have been shown to be mediated by BDNF-induced transcriptional and/or translational changes. The complex spatiotemporal dynamics of BDNF signaling and corresponding regulation of transcriptional and translational events in neurons remain poorly understood.

3.2 Results and Discussion

BDNF rapidly promotes new RNA and protein synthesis in cultured hippocampal neurons

A number of studies have shown that BDNF stimulates protein synthesis in various types of neurons, using brain slices or neuronal mass cultures (Bowling et al., 2016; Genheden et al., 2015; Schratt et al, 2004). We first attempted to confirm this finding in cultured embryonic hippocampal neurons employing the fluorescent un-canonical aminoacid tagging (FUNCAT) technique to visualize new protein synthesis (Dieterich et al., 2010). Briefly, we incubated methionine-starved neurons with the methionine analog AHA (1mM), in the presence or absence of 50 ng/mL BDNF for 60 min (Fig. 3.1A). After fixation, AHA-containing proteins were labeled with a corresponding fluorescent tag and cultures were imaged for analysis. As expected, new protein synthesis significantly increased in neuronal cell bodies after BDNF stimulation compared to controls (219 ± 28 vs 100 ± 12%, mean ± SEM; Fig. 3.1B,C). Analysis of fluorescence in neurites, located at least 60 μm away from cell bodies, revealed an even more pronounced effect: BDNF greatly increased new protein synthesis in neurites compared to control (334 ± 30 vs 100 ± 6%; mean ± SEM; Fig. 3.1D). This effect could be due to fast transport of newly synthesized proteins from cell bodies to neurites. Alternatively, it may reflect BDNF-induced increases in local protein synthesis in dendrites and/or axons.

As discussed in Chapter 1, BNDF has also been shown to induce transcriptional changes in cultured hippocampal neurons within minutes to hours after initial exposure to

BDNF (Alder et al., 2003; Adasme et al., 2011; Melo et al., 2013; Ring et al, 2005). Thus, we next wondered whether the observed BDNF-induced translational response required new transcription. To test this, we incubated neurons with AHA for 30 min in the presence or absence of the transcription inhibitor actinomycin D (ActD, 1μM), then stimulated with BDNF for 10 or 30 min (Fig. 3.1E). New protein synthesis significantly increased in both cell bodies and neurites after 10 or 30 min of BDNF stimulation. However, when transcription was inhibited prior to BDNF stimulation, the increases in protein synthesis in neuronal cell bodies were suppressed (Fig. 3.1F). Quantitative analysis of AHA fluorescence in neurites yielded slightly different results: BDNF stimulation for 10 or 30 min increased new protein synthesis in neurites even when transcription was inhibited by ActD treatment (Fig. 3.1F). These results point to the possibility that BDNF acts through different mechanisms in cell bodies versus neurites. In cell bodies, the translational response induced by BDNF may be closely coupled to a transcriptional response; whereas, BDNF signaling in neurites may induce protein synthesis, possibly locally, without relying on new transcription, at least within the timescale examined here.

Figure 3.1 BDNF promotes new RNA and protein synthesis in cultured hippocampal neurons

(A) Schematic of FUNCAT assay. Hippocampal mass cultures (DIV 6-8) were starved with methionine-free media, then treated with BDNF (50ng/mL) in the presence of AHA (1mM). (**B**) Newly synthesized (AHA-incorporating) proteins were visualized using a fluorescent alkyne tag. Images are pseudo-colored; fluorescence intensity scale is shown on the right. (**C, D)** Quantification of AHA fluorescence intensity in (**C**) cell bodies and (**D**) neurites; ***p<0.0001, two-tailed Mann Whitney test. (**E**) Schematic of experimental paradigm. Neurons were treated with BDNF in the presence of actinomycin D (1 μM) for the specified durations. (**F**,**G**) Quantification of AHA fluorescence intensity; mean ± SEM, shown as percentage of control . n = 7-12 neuronal cell bodies, 18-36 neurites, 2 biological replicates per condition. *p<0.05, **p<0.005, ***p<0.0005; Kruskal-Wallis test with Dunn's *post-hoc* test of multiple comparisons.

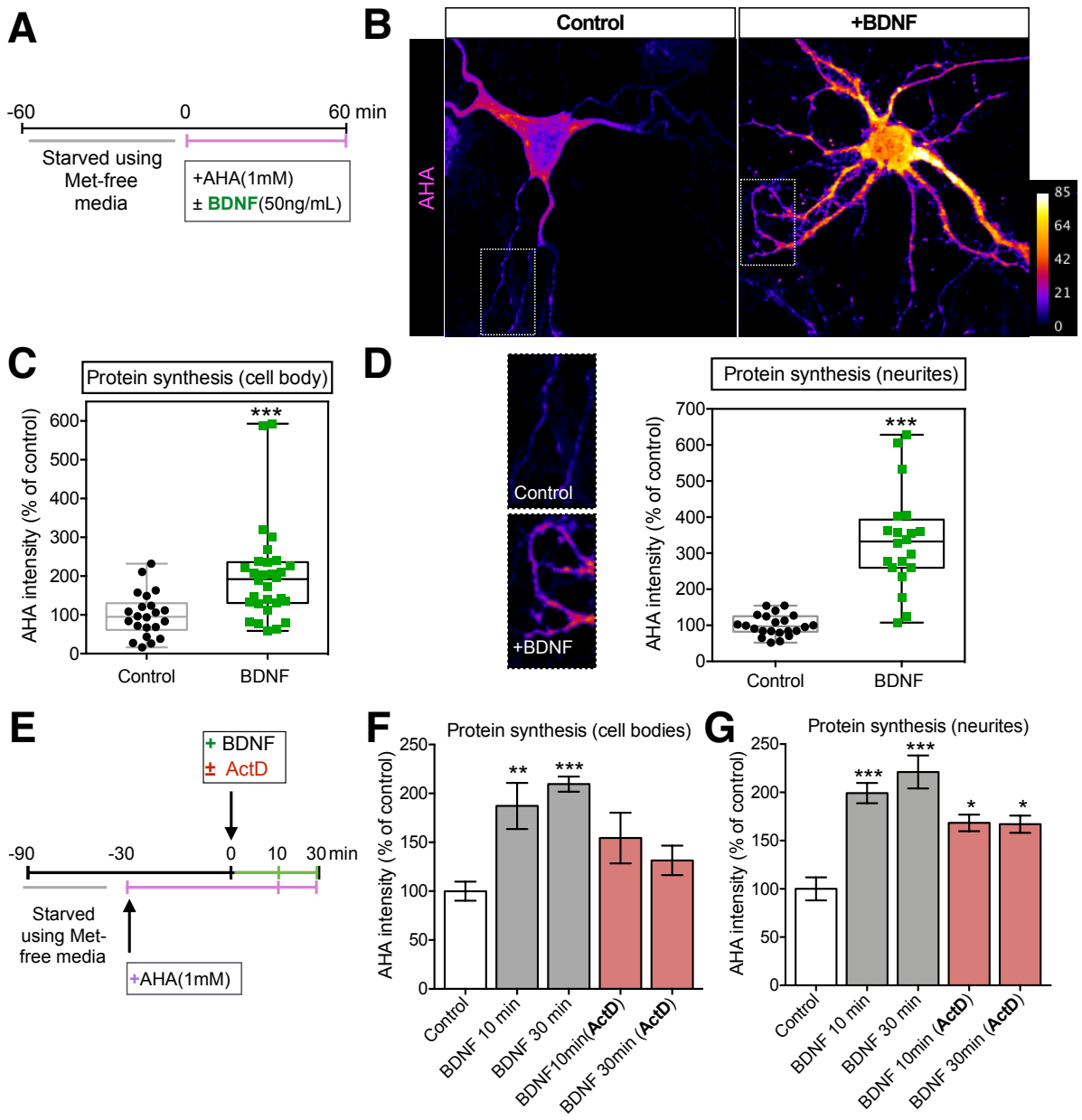
A
-60
0
60 min
Starved using Met-free media
+AHA(1mM)
± BDNF(50ng/mL)
B
Control
+BDNF
AHA
85
64
42
21
0
C
Protein synthesis (cell body)
AHA intensity (% of control)
***
Control
BDNF
D
Control
+BDNF
Protein synthesis (neurites)
AHA intensity (% of control)
***
Control
BDNF
E
+ BDNF
± ActD
-90
-30
0
10
30 min
Starved using Met-free media
+AHA(1mM)
F
Protein synthesis (cell bodies)
AHA intensity (% of control)
**
***
Control
BDNF 10 min
BDNF 30 min
BDNF10min(ActD)
BDNF 30min (ActD)
G
Protein synthesis (neurites)
AHA intensity (% of control)
***
***
*
*
Control
BDNF 10 min
BDNF 30 min
BDNF 10min (ActD)
BDNF 30min (ActD)

Temporal dynamics of BDNF-induced transcription in hippocampal mass cultures

Consistent with previous studies, our findings suggest that BDNF elicits rapid transcriptional and translational responses in hippocampal neuronal mass cultures. To characterize the dynamic transcriptional response to BDNF in hippocampal neurons, we investigated the expression of select transcripts with wide-ranging cellular functions— e.g. signaling, motor-based intracellular transport, oxidative phosphorylation, cytoskeletal/ structural (see Table 3.1)— from samples collected at various time intervals after BDNF stimulation. Among the transcripts investigated, we included putative CREB targets— *Ntrk2*, *Creb1*, *Cox4i1* and *Tubb3* (Impey et al., 2004)— whose expression may be regulated by CREB downstream of BDNF/TrkB signaling.

First, we stimulated hippocampal mass cultures with BDNF (50 ng/mL) for different time periods before harvesting cellular material for RNA extraction (Fig. 3.2A). As revealed by qRT-PCR analysis, the expression pattern of several mRNAs was significantly altered by BDNF treatment. *Creb1* levels significantly decreased upon short stimulation with BDNF (30 and 60 min) and gradually increased (close to control levels) after 90 min of stimulation. BDNF stimulation for longer periods (12 h) significantly induced *Creb1* expression (Fig. 3.2B). In contrast, relative *Ntrk2* (TrkB) levels were greatly reduced after 60 min of BDNF treatment (~70% less than control) and remained down after prolonged BDNF exposure (6 h; Fig. 3.2B). This is consistent with previous reports of TrkB protein downregulation by BDNF in different neuronal populations *in vitro* and *in vivo*, detected as shortly as 2 h after treatment and persisting after longer exposure periods (Knusel et al., 1997; Sommerfeld et

al., 2000; Thoenen and Sendtner 2002). The authors of these studies concluded this effect was unlikely to be mediated by transcriptional changes because of the short timescale in which it was observed. Our results show that TrkB mRNA levels are downregulated as quickly as 60 min after BDNF stimulation; thus, we argue that neurons downregulate TrkB at both mRNA and protein levels in response to BDNF signaling. It is possible that TrkB mRNA and protein downregulation serve as additional means to attenuate BDNF signaling, supplementary to surface receptor internalization, previously discussed in Chapter 1. Interestingly, a similar phenomenon was observed for epidermal growth factor (EGF) signaling in epithelial cells, where EGF receptor (EGFR), a tyrosine kinase receptor, was downregulated within the initial 60-min period after EGF stimulation and its levels remained low 12-24 hours post-stimulation (Golan-Lavi et al., 2017).

The transcriptional profiles of *Mapk1* and *Dnclc1* exhibited similar patterns of change in response to BDNF stimulation: their levels transiently increased 30 min after BDNF stimulation, followed by a decrease 60 min post-stimulation, and returned to control levels after longer exposure periods, in the case of *Mapk1* (Fig. 3.2B). Interestingly, the levels of *Dnclc1* were undetectable in samples obtained from neurons stimulated with BDNF for 6 h (2 biological/4 technical replicates). Although it is possible that *Dnclc1* levels in these particular samples were below the threshold of detection, this seems unlikely because the expression levels of other transcripts examined using these same samples as input were comparable to those of other samples obtained from neurons stimulated for various durations. A plausible alternative, which requires further exploration, is that *Dnclc1*

levels were undetectable 6 h post-stimulation due to sustained repression of *Dnclc1* transcription, similar to the observations for *Ntrk2*. Different from the rest of the genes discussed thus far, *App* levels were unaffected by BDNF stimulation at all time points examined (Fig. 3.2B). These results show dynamic regulation of gene expression after global BDNF stimulation of hippocampal neurons in mass cultures.

Table 3.1: **List of mRNAs evaluated in this study and select previous studies**

†In this study we used embryonic hippocampal neuronal cultures (DIV 7-10); we present the results obtained using mass and microfluidic cultures. For primary neuronal mass cultures, qPCR cycle threshold (C_T) values are presented (mean ± standard deviation; averaged from at least 3 biological/9 technical replicates). For microfluidic chamber cultures, presence of an mRNA species within specified subcellular compartment(s) is denoted by a check-mark (✓). An mRNA was considered 'present' according to the following criteria: a) when it was detected in at least 75% of biological replicates tested (n≥3); **and** (b) there was low variability across technical replicates of the same sample (C_T standard error <1). mRNAs that didn't fit either criteria were mark as 'Und.' (undetected) or labeled with an asterisk if they were reliably detected in less than 50% of biological replicates analyzed; *App* *(1 out of 3), *Creb1* *(3 out of 8), *Stx1a* *(3 out of 7), *Vim* (*1 out of 3). N/A indicates that mRNA species was not evaluated in that category. *Actb* (β-actin); *Cox4i1* (cytochrome c oxidase subunit 4, isoform 1); *Creb1* (cAMP responsive element binding protein); *Ctnnb1* (β-catenin); *Dnclc1* (dynein light chain 1, cytoplasmic); *Gapdh* (glyceraldehyde 3-phosphate dehydrogenase); *Klc1* (kinesin light chain 1); *Map1b* (microtubule-associated protein 1b); *Map2* (microtubule-associated protein 2); *Mapk1* (extracellular signal-regulated kinase 2, Erk2); *Ntrk2* (tropomyosin-related kinase B, TrkB); *Rps23* (ribosomal protein subunit 23); *Stx1a* (syntaxin 1A); *Tubb3* (β-tubulin 3); *Vim* (vimentin).

††Presented here are results from select previous studies performed in axons for comparison. The type of neuronal culture and developmental stage at the time of dissection are specified. Dorsal root ganglion (DRG), superior cervical ganglion (SCG); embryonic (E), post-natal (P), adult (A).

References: 1) Taylor et al., 2009; 2) Gumy et al., 2011; 3) Willis et al., 2005; 4) Cox et al., 2008; 5) Aschrafi et al., 2008

	Results from this study†			Results from previous studies††		
	Mass cultures	Microfluidic cultures (compartment)		Detection in axons (neuron type, developmental stage)		
		Somatodendritic	Axonal			
Gene	C_T (±SD)	C_T range	C_T range	CNS	PNS	Ref.
Actb	20.2 ± 3.9	✓16-18	✓ 28-31	cortical (E)	DRG (E, A)	1, 2, 3
App	22.6 ± 3.8	✓17-22	* 33-34	Und.	DRG (E, A)	2
Cox4i1	N/A	✓ 17-18	✓ 27-30	Und.	DRG (E, A); SCG (P)	2, 3, 5
Creb1	27.7 ± 2.8	✓ 21-23	* 31-35	Und.	DRG (E)	4
Ctnnb1	N/A	✓ 21-24	✓ 29-32	cortical (E)	DRG (E, A)	1, 2
Dnclc1	28.5 ± 4.4	Und.	Und.	cortical (E)	DRG (E, A)	1, 2
Gapdh	19.7 ± 1.1	✓ 16-19	✓ 26-30	cortical (E)	DRG (E, A)	1, 2, 3
Klc1	N/A	✓ 17-19	✓ 33-34	Und.	DRG (E, A)	2
Map1b	N/A	✓ 19-24	✓ 28-31	cortical (E)	DRG (E)	1, 2
Map2	N/A	✓ 17-19	Und.	Und.	Und.	1,2
Mapk1	26.2 ± 4.2	✓ 23-25	✓ 29-30	Und.	Und.	1, 2, 3
Ntrk2	24.2 ± 4.8	✓ 23-25	✓ 29-30	Und.	DRG (E)#	1,2,3
Rps23	23.4 ± 3.9	✓ 21-23	✓ 27-28	cortical (E)	DRG (E, A)	1,2,3
Stx1a	24.7 ±1.3	✓ 19-22	* 33-34	Und.	Und.	1,2,3
Tubb3	N/A	✓ 20-22	Und.	cortical (E)	DRG (E)	1, 2
Vim	N/A	✓ 21-23	* 35-36	Und.	DRG (E, A)	2,3

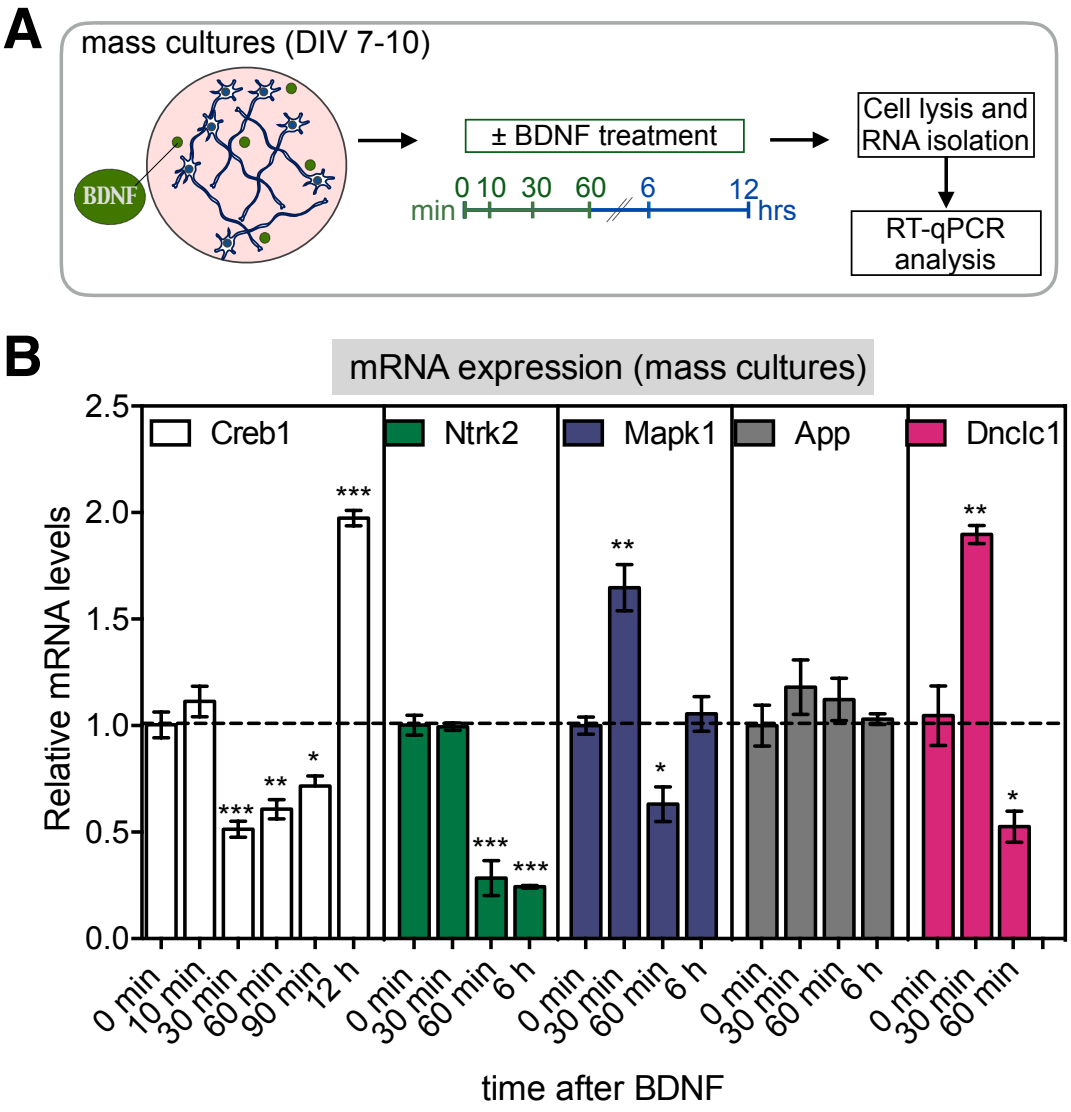

Figure 3.2 BDNF-induced transcriptional response in hippocampal mass cultures

(**A**) Schematic illustration of experimental paradigm. Hippocampal mass cultures were treated with BDNF (50ng/mL) for various time durations; cells were immediately harvested for RNA extraction and gene expression analysis. (**B**) Expression levels of *Creb1*, *Ntrk2*, *Mapk1*, *App* and *Dnclc1* were determined by quantitative real-time PCR (qPCR). mRNA levels were normalized to *Gapdh* and calculated using the ΔC_T method. Data represents $2^{-\Delta\Delta Ct}$ values; mean ± SEM from six replicates (three technical × two biological replicates). *p<0.05, **p<0.005, ***p<0.0005; One-way ANOVA with Tukey's post-hoc test of multiple comparisons.

Axonal BDNF stimulation elicits rapid transcriptional responses in cell bodies

Given their highly polarized morphology, neurons particularly rely on spatial regulation of signaling to generate specific cellular responses. In our previous experiment, we investigated the temporal dynamics of BDNF-induced transcription using neuronal mass cultures, wherein all subcellular compartments, somatodendritic and axonal, were simultaneously exposed to BDNF. However, within neuronal circuits *in vivo*, these subcellular compartments are separated by large distances and generally exposed to different local microenvironments. Thus, we next examined whether a BDNF signal initiating in axons could also elicit fast transcriptional changes in neuronal cell bodies.

To this end, we cultured hippocampal neurons using microfluidic devices that allow fluidic isolation and selective manipulation of the somatodendritic and axonal compartments. To monitor transcriptional changes in cell bodies in response to axonal BDNF signaling, we selectively treated axonal compartments (AC) with BDNF for different time periods, then harvested the cellular material from corresponding somatodendritic compartments (SC) for gene expression analysis (Fig. 3.3A). Previously we showed that BDNF(AC) treatment increases axonal growth within 10 min after exposure, and that transcription in the somatodendritic compartment appears to be necessary for sustaining BDNF-induced axonal growth after 60 min of exposure (Chapter 2, Fig. 2.1 and 2.5). With this in mind, we focused on investigating the expression of a subset of transcripts previously shown to localize to various subcellular neuronal compartments (Table 3.1), including transcripts that have been described to be important for axonal growth and/or regeneration—

namely, *Cox4i1*, *Ctnnb1*, *Actb*, *Vim, Tubb3* (Aschrafi et al, 2008; Costa and Willis 2017; Jung et al., 2012; Minoura et al., 2016), and *Map1b* (Dajas-Bailador et al., 2012, Wang et al., 2015).

After 10 min of BDNF(AC) stimulation, *Creb1* and *Stx1a* expression in the somatodendritic compartment modestly increased compared to control, whereas *Cox4i1* expression significantly decreased at this time point (Fig. 3.3B). After 30 min of BDNF(AC) stimulation, *Stx1a* and *Cox4i1* levels in the SC returned to control levels. Interestingly, *Creb1* expression in the somatodendritic compartment significantly decreased after 60 min of BDNF (AC) stimulation, similar to our observations in mass cultures. One notable distinction was that, in mass cultures, *Creb1* downregulation was already evident after 30 min of global BDNF stimulation, whereas in microfluidic cultures, decreased *Creb1* levels in the SC were first observed after 60 min of axonal BDNF stimulation. [Although the physiological significance of this effect is unclear, one possibility is that *Creb1* expression is transiently downregulated through regulatory feedback mechanisms employed by neurons in response to increased cAMP signaling after BDNF stimulation.] The levels of some of the transcripts examined did not change in response to BDNF. For example, *Klc1* and *Actb* expression in the somatodendritic compartment was unaffected by BDNF(AC) after 10 or 30 min of stimulation (Fig. 3.3 C).

We also examined the transcriptional regulation of select mRNAs after short (30 min) versus long (3 h) exposure of axonal compartments to BDNF. After 30 min of BDNF (AC) stimulation, *Map1b* and *Vim* expression significantly increased in the somatodendritic

compartment compared to control (Fig. 3.3 D). Three hours after BDNF (AC) stimulation, *Vim* levels remained significantly increased, whereas *Map1b* expression returned to control levels. Of note, *Vim* mRNA has previously been shown to display a long half-life, ≥ 6 h (Coleman and Lazarides 1992). Thus, the increase in *Vim* expression observed after 3 h of BDNF stimulation could reflect different scenarios: one possibility is that *Vim* is rapidly upregulated after BDNF stimulation and its levels remain relatively elevated for several hours because of its long half-life. Alternatively, *Vim* expression might be continually upregulated in response to BDNF at least for the initial 3 h after stimulation. In contrast, *Ctnnb1* and *Tubb3* expression was unaltered in the somatodendritic compartment after BDNF stimulation of distal axons for 30 min or 3 h. Together, these results show differential regulation of mRNA levels in cell bodies of hippocampal neurons after BDNF stimulation of distal axons.

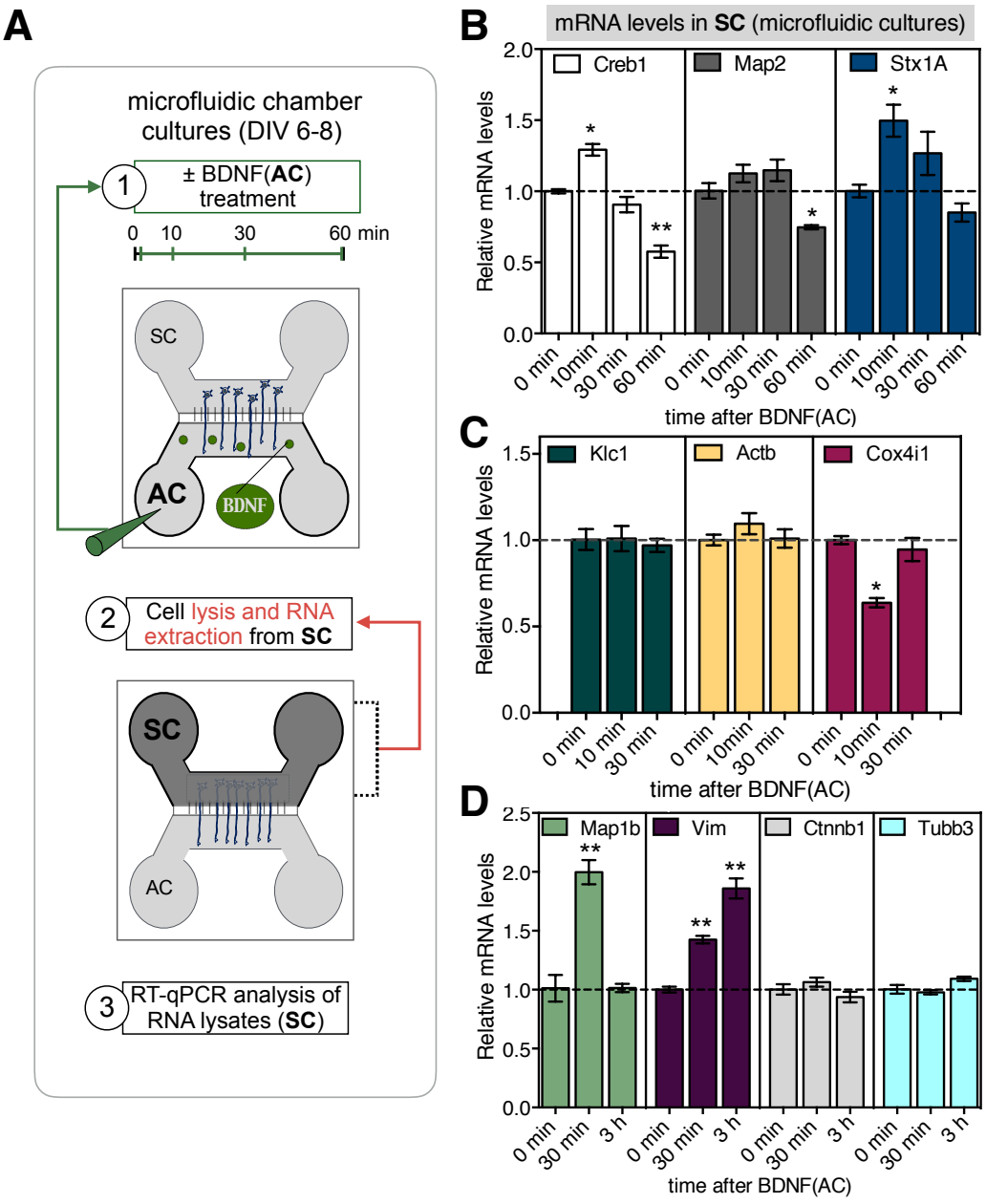

Figure 3.3 Axonally-applied BDNF induces transcriptional changes in the somatodendritic compartment

(**A**) Schematic illustration of experimental paradigm. BDNF was added to axonal compartments of microfluidic cultures; RNA was harvested from corresponding somatodendritic compartments. (**B, C, D**) Expression levels of various mRNAs in the SC were determined by qPCR. Relative mRNA levels were calculated using the ΔC_T method, normalized to *Gapdh*. Data represents $2^{-\Delta\Delta Ct}$ values; mean ± SEM. *p<0.05, **p<0.005, ***p<0.0005; One-way ANOVA with Tukey's post-hoc test of multiple comparisons.

Axonal BDNF stimulation affects intra-axonal mRNA levels

Given the growing evidence pointing to the importance of the axonal transcriptome and its regulation by extracellular stimuli (Jung et al., 2012; Costa and Willis 2017), we asked whether local BDNF signaling also affected axonal mRNA levels. The microfluidic chambers used in this study provided the ideal culture platform to address this question. To this end, we harvested axonal lysates exclusively from axonal compartments of microfluidic chamber cultures after BDNF(AC) stimulation for different time periods (Fig 3.4A). Quantitative PCR (qPCR) analysis revealed the presence of select transcripts in axonal preparations compared to their somatodendritic counterparts (Table 3.1). Consistent with previous findings from studies of other neuronal systems, hippocampal axons were enriched for several mRNAs— including *Actb, Cox4i1, Gapdh, Map1b*— and devoid of dendritic markers such as *Map2* (Table 3.1). Notably, axonal expression of *Creb1*, *Vim* or *Tubb3* could not be confirmed in rat hippocampal neurons at this developmental stage (E18, DIV 6-8)— their corresponding mRNA levels were either too low and/or displayed too much variation across replicates.

Following BDNF(AC) stimulation for specific time periods, RNA was individually isolated from corresponding SC and AC compartments of the same microfluidic cultures. Of the transcripts examined, some displayed different expression patterns in respective compartments. After 10 min of BDNF(AC) stimulation, *Cox4i1* levels transiently decreased in the SC but were unaltered in axonal compartments. 30 min after BDNF(AC) exposure, *Cox4i1* expression in the SC returned to control levels yet it significantly increased in axons

(Fig. 3.3C, 3.4B). The observed increase in *Cox4i1* levels after 30 min of BDNF stimulation could be due to increased mRNA trafficking from the soma, decreased rates of decay, or a combination of both. Importantly, previous studies have shown that the axonal trafficking and translation of *Cox4i1* mRNA is important for axonal elongation and maintenance in sympathetic neurons (Aschrafi et al., 2008; Aschrafi et al., 2010). *Map1b* expression significantly increased in the SC after 30 min of BDNF(AC) and it significantly increased in the AC after 3 h of BDNF(AC) treatment. In contrast, the expression of *Ctnnb1*, *Klc1*, or *Actb* did not significantly change in either compartment after BDNF stimulation (Fig. 3.3D, 3.4C). Differential responses in the two compartments raise the possibility that mRNA levels might be spatially regulated to satisfy the demands of specific subcellular locations. Alternatively, mRNA half-lives might differ in each subcellular compartment.

Although the scope of this study was narrow, it revealed several interesting findings. We show that BDNF induces dynamic changes in gene expression in hippocampal neurons after global or exclusively axonal stimulation. Among the select transcripts examined, we found some similarities in temporal patterns of regulation for a few mRNAs— e.g. *Ntrk2* and *Dnclc1* displayed sustained downregulation after several hours of BDNF exposure. For the most part, each mRNA species exhibited distinct changes in their levels, reflecting the highly dynamic nature of stimulus-induced transcriptional responses. Upon examining mRNA levels from corresponding axonal and somatodendritic compartments of the same cultures, we noticed that changes in the levels of specific mRNAs did not always follow similar patterns in each compartment, suggesting possible differences in post-transcriptional

regulation across subcellular locations. Future studies using specialized techniques for comprehensive transcriptome analysis will help further our understanding of complex BDNF-induced transcriptional responses.

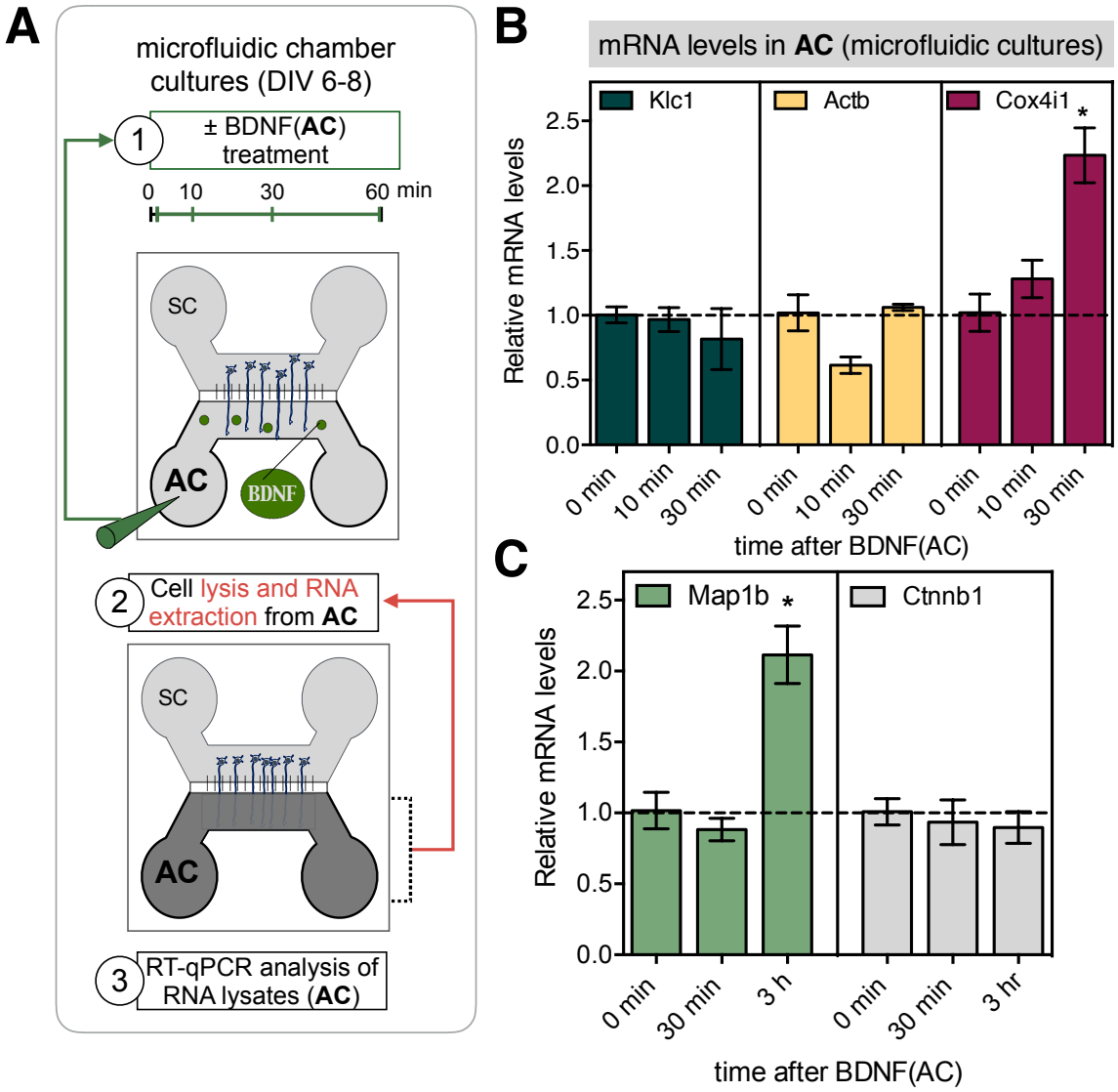

Figure 3.4 Axonally-applied BDNF affects intra-axonal mRNA levels

(**A**) Schematic illustration of experimental paradigm. BDNF was added to axonal compartments of microfluidic cultures; RNA was harvested from axonal compartments. (**B, C**) Expression levels of various mRNAs were determined by qPCR. Relative mRNA levels in axons were calculated using the ΔC_T method, normalized to *Gapdh*. Data represents $2^{-\Delta\Delta Ct}$ values; mean ± SEM. *p<0.05, One-way ANOVA with Tukey's post-hoc test of multiple comparisons.

Chapter 4:
Materials and Methods

4.1 Materials and Methods

Reagents

The following reagents were purchased from Gibco (ThermoFisher): Neurobasal medium, GlutaMAX supplement (100X), B27 supplement (50X), Antibiotic-antimycotic 100X (penicillin/streptomycin/amphotericin B), HEPES (1 M), 2.5% Trypsin solution (10X), Hank's balanced salt solution (HBSS) without calcium or magnesium (10X), methionine-free DMEM. The following reagents were purchased from Sigma-Aldrich: DNAse I, poly-D-lysine (PDL) hydrobromide (70-150 kDa), anisomycin, cycloheximide, actinomycin-D, TBTA, and TCEP. Torin 1 and ANA-12 were purchased from Selleck Chemicals. L-azidohomoalanine (AHA) and AlexaFluor 488-conjugated alkyne were purchased from Invitrogen (ThermoFisher). Corresponding stock solutions were prepared and stored according to manufacturer's indications. The following antibodies were used: rabbit polyclonal anti-phospho-TrkB (Y817, GenScript); mouse monoclonal anti-phospho-S6K1 (S411, Santa Cruz Biotechnology); rabbit polyclonal anti-phospho-mTOR (S2448, Cell Signaling); goat polyclonal anti-phospho-4EBP1 (S65/T70, Santa Cruz Biotechnology).

Animals

All animal procedures were performed in accordance with institutional guidelines and approved by the Institutional Animal Care and Use Committee (IACUC) at the University of California-San Diego. Timed-pregnant *Sprague Dawley* rats were obtained from Charles River Laboratories.

Primary neuronal cultures

Primary cultures of rat embryonic hippocampal neurons were prepared as previously described (Weissmiller et al., 2015). Briefly, brains were harvested from rat embryos at gestational day 18 (E18). Hippocampi were dissected in dissection media (DM) formulated with HBSS (1X), glucose (final concentration adjusted to 0.45% wt/vol), sodium pyruvate (250 μM), HEPES (10 mM) and penicillin/streptomycin/amphotericin B (1X). After dissection, tissue was enzymatically digested with trypsin (0.25% wt/vol in DM) for 15 min at 37º C, then incubated with DNAse I (0.1% vol/vol in DM) for 2 min at room temperature before mechanical trituration. Dissociated hippocampal neurons were resuspended in plating media containing Neurobasal supplemented with 5% fetal bovine serum (FBS), 2% B27-supplement, 1% GlutaMAX, and 1% penicillin/streptomycin/amphotericin B. Cells were plated on PDL-coated glass coverslips and incubated overnight under standard conditions (37ºC, 5% CO_2). After 12-16 h, plating media was replaced with maintenance media prepared with Neurobasal medium supplemented with 2% B27 and 1% GlutaMAX (without antibiotics).

Compartmentalized microfluidic cultures

Compartmentalized cultures of embryonic hippocampal neurons were prepared using two-chamber polydimethylsiloxane (PDMS) microfluidic devices (Xona Microfluidics) assembled onto glass coverslips coated with PDL (3.5μg/cm^2 surface area). Briefly, these

microfluidic devices consist of two main chambers separated by long, thin microgrooves (450 × 10 × 5 μm; L × W × H). Dissociated neurons were seeded on one chamber—hereafter referred to as the somatodendritic compartment— of microfluidic devices at a density of ~4x10^4 cells per device. After 2-4 days *in vitro* (DIV), axons extended through the microgrooves into the second chamber, referred to as the axonal compartment (see schematic diagram in Fig 2.1A). To ensure fluidic isolation between the two compartments, media volume on the axonal compartment (AC) was always maintained ~20% lower than the volume in the somatodendritic compartment (Taylor et al., 2005).

Local treatments of subcellular compartments

Embryonic hippocampal neurons were grown on microfluidic chambers for 6-8 DIV. Prior to BDNF treatment, neurons were incubated with starvation media (Neurobasal supplemented with GlutaMax, without B27) for 2-3 hours; lower media volume on the axonal compartment was maintained throughout the experiment. For selective axonal BDNF application, we added 1-3 μL of BDNF-containing media (final concentration 10 ng/mL) to the AC of microfluidic cultures. For control conditions, we added a similar volume of Neurobasal medium (without BDNF).

Local treatments with chemical compounds (inhibitors, etc) were performed similarly: compounds were selectively added to axonal or somatodendritic compartments, individually. The final working concentrations used for each compound are listed in Table 2.1. To determine these, we considered (manufacturer's suggestions and also) the

compounds' partition coefficients (log *P*), a measurement of hydrophobicity. That is because PDMS— the material that microfluidic devices are made of— has been shown to exhibit high absorption (over 90%) for compounds with logP > 2.62, and low absorption for compounds with logP<2.47 (Wang et al., 2012). High absorption of a compound would reduce their concentration in solution and efficacy. We obtained corresponding log *P* values for each drug/compound using the ChemSpider database; these are listed in Table 4.1. For compounds with high log *P* values, we used working concentrations on the higher end of the manufacturer's suggestion range.

The final concentration of DMSO after dilution was ≤ 0.1% (vol/vol) for experimental and control conditions. After treatments, microfluidic cultures were placed back in the tissue incubator for the specified time durations or immediately subjected to live-imaging microscopy, as indicated.

Table 4.1. Drugs used for local treatments: partition coefficient and concentration

Compound	Partition coefficient (log P)	Working concentration
Actinomycin-D	2.76*	2 mM
AHA	-1.76	1 mM
Alkyne	1.28	2 μM
ANA-12	3.50*	10 μM
Anisomycin	0.97	20 μM
Cycloheximide	0.55	10 μg/mL (35μM)
DMSO	-1.09	≤0.1% vol/vol
Torin 1	5.37*	1 μM

* Compounds with logP values higher than 2.62.

Time-lapse microscopy

For time-lapse imaging of axonal growth, the axonal compartments of microfluidic chamber cultures were imaged using a Leica DMI6000-B inverted microscope equipped with an environmental chamber (37ºC, 5% CO_2) and a motorized X/Y stage. Phase-contrast images were captured every 30-60 s for periods of up to 60 min— starting 15-20 min prior to BDNF addition— using a 40× oil-immersion objective, an EM-CCD camera (Roller-MGi, QImaging) and MetaMorph imaging software.

Quantitative analysis of axonal growth

Time-lapse image series were imported into Fiji software for analysis. To remove large background features and enhance image contrast, we used the 'normalize local contrast' function. We generated time-lapse montages and measured axonal length using the semiautomatic tracing plugin NeuriteTracer. Axons were traced from a stationary point on the axonal shaft to the center of the growth cone. To minimize bias, all axons with visible, non-overlapping growth cones within the image field were traced and included in the analyses. Change in length (Δlength) was calculated in intervals of 5±2 min. For analysis of growth dynamics at shorter time intervals, we used the MtrackJ plugin to track the position of individual growth cones across consecutive frames (every 30 s), starting at t=0.5±1 min after addition of BDNF or control. Instantaneous growth speed was defined as Δlength/ Δtime, e.g. speed at 5 min = Δlength [relative length$_{(6\ min)}$ - relative length$_{(4\ min)}$] / Δtime.

To monitor axonal growth after BDNF treatments lasting 60 min or longer, axonal compartments were imaged before BDNF addition at 20X magnification using the same microscopy setup used for live-imaging. BDNF was applied locally, as described above, and microfluidic cultures were incubated in the tissue incubator for the specified durations. Cultures were then fixed and imaged for axonal growth analysis.

Immunocytochemistry

For immunostaining of microfluidic cultures, neurons were immediately fixed, after treatments, using a pre-warmed 4% para-formaldehyde (PFA)/ 4% sucrose (wt/vol, in PBS) solution for 15 min at room temperature (RT). Fixed cultures were then rinsed thrice with ice-cold PBS (5 min/rinse), permeabilized for 10 min using 0.1% Triton-X in PBS, and incubated with blocking buffer— formulated with goat or horse serum (10% vol/vol) and bovine serum albumin (BSA; 1% wt/vol) in PBS— for 1 h at RT. Neurons were then incubated with primary antibodies (1:100 in blocking buffer; 4ºC overnight) followed by corresponding fluorescently-labeled secondary antibodies (1:500 dilution in PBS; 1 h at RT). Finally, cultures were washed thrice with PBS for 10 min before imaging. For confocal imaging, coverslips were mounted onto glass slides using ProLong Gold antifade mounting reagent (ThermoFisher).

Visualization of nascent protein synthesis

Newly synthesized proteins were labeled for *in situ* visualization using FUNCAT (fluorescent noncannonical amino acid tagging), following the previously described protocol

(Dieterich et al., 2010), with some modifications. First, growth medium from microfluidic neuronal cultures was replaced with pre-warmed methionine-free DMEM supplemented with GlutaMax (1X) and sodium pyruvate (0.22 mM) and cultures were incubated for 2 h in the tissue incubator. Following the starvation period, axonal or somatodendritic compartments (as specified) were incubated with the methionine analog AHA (1 mM) for 1 h at 37ºC. To remove excess AHA, cultures were then briefly washed with ice-cold PBS and immediately fixed using 4% PFA / 4% sucrose in PBS for 15 min. Fixed neurons were rinsed thrice with PBS, permeabilized for 10 min (0.1% Triton-X in PBS), and washed with 3% BSA in PBS.

Newly synthesized proteins were next labeled for visualization using copper-catalyzed azide-alkyne cycloaddition (CuAAC) chemistry: a fluorophore-linked alkyne was added to chemically react with and bind azido moieties in AHA-tagged proteins. A CuAAC reaction mixture was prepared containing 2 μM AlexaFluor488-conjugated alkyne, 200 μM copper (II) sulfate, 400 μM TCEP (a reducing agent to generate the catalytically-active Cu(I) species), and 200 μM TBTA (a triazole ligand that enhances copper's catalytic effect) dissolved in PBS. Permeabilized neuronal cultures were incubated with the CuAAC reaction mixture for 2 h at RT, protected from light. After incubation, cultures were washed thrice for 10 min each with 0.1% Triton-X in PBS, followed by three washes with PBS. Fluorescence images were acquired using a Leica DMI6000-B inverted microscope with a 100×/1.25 NA oil-immersion objective, an EM-CCD camera (QImaging) and MetaMorph software.

High-resolution confocal image capture and analysis

Confocal microscopy was performed using an Olympus IX81 inverted microscope equipped with a Yokogawa CSU-X1-A1 spinning disk confocal scanner, a Hamamatsu EM-CCD camera (1024 ×1024 pixels), and a 100×/1.49 NA oil-immersion objective. Mounted sections were imaged in sequential z planes at intervals of 0.1 μm using the UltraVIEW VoX system (Perking Elmer). 16-bit depth images were acquired in z-stacks with an axial resolution of was 68 nm per pixel. An average of 10-20 randomly selected axonal regions were imaged per microfluidic chamber. Image z-series were analyzed using Fiji.

RNA isolation and real-time quantitative PCR

RNA was isolated using the RNAeasy Micro Kit (Qiagen). After indicated treatments of microfluidic cultures, the medium on the axonal compartment was aspirated, 75μL of lysis buffer were directly added to one AC well and immediately collected from the connecting AC well. Then, the medium on the SC (of the same microfluidic chamber) was aspirated, 150μL of lysis buffer were added to one SC well and collected from the connecting well. Tissue homogenization and RNA extraction were performed according to manufacturer's specifications.

Following RNA extraction, cDNA was synthesized using the QuantiTect Reverse Transcription Kit (Qiagen), in accordance to manufacturer's protocol. The concentration of the generated cDNA was assessed spectrophotometrically using NanoDrop ND-1000. Real-time quantitative PCR (qPCR) analyses were carried out with an Applied Biosystems 7300 PCR system. qPCR reactions were assembled in triplicate using QuantiFast SYBR Green

Master Mix or RT2 SYBR Green Rox qPCR Master Mix (Qiagen), QuantiTect or RT2 qPCR Primer Assays (Qiagen; listed on Table 4**.2**), and ≤100 ng template cDNA (per reaction). Non-template negative controls (for each primer set) and melting curve analyses were included to assess amplification specificity. Quantification of relative gene expression was performed using the comparative threshold (Ct) method. Briefly, mean Ct values for each gene were normalized to *Gapdh* Ct values to generate ΔCt values. Relative mRNA levels were calculated according to the formula: $2^{-\Delta\Delta Ct}$, where $\Delta\Delta Ct = \Delta Ct_{(\text{treated sample})} - \Delta Ct_{(\text{control sample})}$.

Statistical Analysis

Statistical analysis was done using GraphPad Prism software. Prior to performing statistical comparisons between groups, individual data sets were tested for normality using D'Agostino-Pearson and/or Shapiro-Wilk tests. Normally-distributed data were analyzed using parametric tests— two-sample Student's t test or One-way ANOVA, for comparisons between more than two groups. For comparisons between data sets that did not follow a normal distribution, non-parametric tests were used, e.g. Mann-Whitney or Kruskal-Wallis tests. More detailed information, including sample size (n), statistical test used and p values, is provided in the figure legends. Non-significant p values were not reported.

Table 4.2. List of pre-designed qPCR primer sets used in this study

Gene	Primer assay (name)	Catalog number (Qiagen)
Actb	Rn_Actb_1_SG QuantiTect	QT00193473
App	Rn_App_1_SG QuantiTect	QT00177408
Cox4i1	Rn_Cox4i1_1_SG QuantiTect	QT00180761
Creb1	Rn_Creb1_1_SG QuantiTect	QT00191275
Ctnnb1	Rn_Ctnnb1_1_SG QuantiTect	QT01083474
Dnclc1	RT² qPCR Primer Assay for Rat Dynll1	PPR48872B
Gapdh	Rn_Gapd_1_SG QuantiTect	QT00199633
Klc1	Rn_Klc1_1_SG QuantiTect	QT01583610
Map1b	Rn_Map1b_1_SG QuantiTect	QT01607459
Map2	Rn_Map2_1_SG QuantiTect	QT01084244
Mapk1	RT² qPCR Primer Assay for rat Mapk1	PPR48780A
Ntrk2	RT² qPCR Primer Assay for rat Ntrk2	PPR45322B
Rps23	RT² qPCR Primer Assay for Rat Rps23	PPR62140A
Stx1a	Rn_Stx1a_1_SG QuantiTect	QT01083229
Tubb3	Rn_Tubb3_1_SG QuantiTect	QT00188818
Vim	Rn_Vim_1_SG QuantiTect	QT00178724

References

References

Abe, N., Borson, S.H., Gambello, M.J., Wang, F., and Cavalli, V. (2010). Mammalian target of rapamycin (mTOR) activation increases axonal growth capacity of injured peripheral nerves. J Biol Chem *285*, 28034-28043.

Adasme, T., Haeger, P., Paula-Lima, A.C., Espinoza, I., Casas-Alarcón, M.M., Carrasco, M.A., and Hidalgo, C. (2011). Involvement of ryanodine receptors in neurotrophin-induced hippocampal synaptic plasticity and spatial memory formation. Proc Natl Acad Sci U S A *108*, 3029-3034.

Alder, J., Thakker-Varia, S., Bangasser, D.A., Kuroiwa, M., Plummer, M.R., Shors, T.J., and Black, I.B. (2003). Brain-derived neurotrophic factor-induced gene expression reveals novel actions of VGF in hippocampal synaptic plasticity. J Neurosci *23*, 10800-10808.

Amit, I., Citri, A., Shay, T., Lu, Y., Katz, M., Zhang, F., Tarcic, G., Siwak, D., Lahad, J., Jacob-Hirsch, J.*, et al.* (2007). A module of negative feedback regulators defines growth factor signaling. Nat Genet *39*, 503-512.

Ascano, M., Bodmer, D., and Kuruvilla, R. (2012). Endocytic trafficking of neurotrophins in neural development. Trends Cell Biol *22*, 266-273.

Aschrafi, A., Natera-Naranjo, O., Gioio, A.E., and Kaplan, B.B. (2010). Regulation of axonal trafficking of cytochrome c oxidase IV mRNA. Mol Cell Neurosci *43*, 422-430.

Aschrafi, A., Schwechter, A.D., Mameza, M.G., Natera-Naranjo, O., Gioio, A.E., and Kaplan, B.B. (2008). MicroRNA-338 regulates local cytochrome c oxidase IV mRNA levels and oxidative phosphorylation in the axons of sympathetic neurons. J Neurosci *28*, 12581-12590.

Atwal, J.K., Massie, B., Miller, F.D., and Kaplan, D.R. (2000). The TrkB-Shc site signals neuronal survival and local axon growth via MEK and P13-kinase. Neuron *27*, 265-277.

Autry, A.E., and Monteggia, L.M. (2012). Brain-derived neurotrophic factor and neuropsychiatric disorders. Pharmacol Rev *64*, 238-258.

Barde, Y.A., Edgar, D., and Thoenen, H. (1982). Purification of a new neurotrophic factor from mammalian brain. EMBO J *1*, 549-553.

Barford, K., Deppmann, C., and Winckler, B. (2017). The neurotrophin receptor signaling endosome: Where trafficking meets signaling. Dev Neurobiol *77*, 405-418.

Blasiak, A., Lee, G.U., and Kilinc, D. (2015). Neuron Subpopulations with Different Elongation Rates and DCC Dynamics Exhibit Distinct Responses to Isolated Netrin-1 Treatment. ACS Chem Neurosci *6*, 1578-1590.

Bodmer, D., Ascaño, M., and Kuruvilla, R. (2011). Isoform-specific dephosphorylation of dynamin1 by calcineurin couples neurotrophin receptor endocytosis to axonal growth. Neuron *70*, 1085-1099.

Bonni, A., Brunet, A., West, A.E., Datta, S.R., Takasu, M.A., and Greenberg, M.E. (1999). Cell survival promoted by the Ras-MAPK signaling pathway by transcription-dependent and -independent mechanisms. Science *286*, 1358-1362.

Bourgeron, T. (2015). From the genetic architecture to synaptic plasticity in autism spectrum disorder. Nat Rev Neurosci *16*, 551-563.

Bowling, H., Bhattacharya, A., Zhang, G.A., Lebowitz, J.Z., Alam, D., Smith, P.T., Kirshenbaum, K., Neubert, T.A., Vogel, C., Chao, M.V.*, et al.* (2016). BONLAC: A combinatorial proteomic technique to measure stimulus-induced translational profiles in brain slices. Neuropharmacology *100*, 76-89.

Briz, V., Zhu, G., Wang, Y., Liu, Y., Avetisyan, M., Bi, X., and Baudry, M. (2015). Activity-dependent rapid local RhoA synthesis is required for hippocampal synaptic plasticity. J Neurosci *35*, 2269-2282.

Bronfman, F.C., Lazo, O.M., Flores, C., and Escudero, C.A. (2014). Spatiotemporal intracellular dynamics of neurotrophin and its receptors. Implications for neurotrophin signaling and neuronal function. Handb Exp Pharmacol *220*, 33-65.

Bucci, C., Alifano, P., and Cogli, L. (2014). The role of rab proteins in neuronal cells and in the trafficking of neurotrophin receptors. Membranes (Basel) *4*, 642-677.

Campenot, R.B. (1977). Local control of neurite development by nerve growth factor. Proc Natl Acad Sci U S A *74*, 4516-4519.

Cargnello, M., and Roux, P.P. (2011). Activation and function of the MAPKs and their substrates, the MAPK-activated protein kinases. Microbiol Mol Biol Rev *75*, 50-83.

Cazorla, M., Prémont, J., Mann, A., Girard, N., Kellendonk, C., and Rognan, D. (2011). Identification of a low-molecular weight TrkB antagonist with anxiolytic and antidepressant activity in mice. J Clin Invest *121*, 1846-1857.

Chao, M.V. (2003). Neurotrophins and their receptors: a convergence point for many signalling pathways. Nat Rev Neurosci *4*, 299-309.

Chao, M.V., Rajagopal, R., and Lee, F.S. (2006). Neurotrophin signalling in health and disease. Clin Sci (Lond) *110*, 167-173.

Cheng, P.L., Song, A.H., Wong, Y.H., Wang, S., Zhang, X., and Poo, M.M. (2011). Self-amplifying autocrine actions of BDNF in axon development. Proc Natl Acad Sci U S A *108*, 18430-18435.

Chen, Q., Zhou, Z., Zhang, L., Wang, Y., Zhang, Y.W., Zhong, M., Xu, S.C., Chen, C.H., Li, L., and Yu, Z.P. (2012). Tau protein is involved in morphological plasticity in hippocampal neurons in response to BDNF. Neurochem Int *60*, 233-242.

Chiang, G.G., and Abraham, R.T. (2005). Phosphorylation of mammalian target of rapamycin (mTOR) at Ser-2448 is mediated by p70S6 kinase. J Biol Chem *280*, 25485-25490.

Choi, Y.J., Di Nardo, A., Kramvis, I., Meikle, L., Kwiatkowski, D.J., Sahin, M., and He, X. (2008). Tuberous sclerosis complex proteins control axon formation. Genes Dev *22*, 2485-2495.

Cohen, M.S., Bas Orth, C., Kim, H.J., Jeon, N.L., and Jaffrey, S.R. (2011). Neurotrophin-mediated dendrite-to-nucleus signaling revealed by microfluidic compartmentalization of dendrites. Proc Natl Acad Sci U S A *108*, 11246-11251.

Cohen, S. (1960). Purification of a nerve-growth promoting protein from the mouse salivary gland and its neuro-cytotoxic antiserum. Proc Natl Acad Sci USA *46*, 302-311.

Cohen, S., and Levi-Montalcini, R. (1956). A nerve growth-stimulating factor isolated from snake venom. Proc Natl Acad Sci USA *42*, 571-574.

Cohen, S., Levi-Montalcini, R., and Hamburger, V. (1954). A nerve growth-stimulating factor isolated from sarcomas 37 and 180. Proc Natl Acad Sci USA *40*, 1014-1018.

Cohen-Cory, S., and Fraser, S.E. (1995). Effects of brain-derived neurotrophic factor on optic axon branching and remodelling in vivo. Nature *378*, 192-196.

Coleman, T.R., and Lazarides, E. (1992). Continuous growth of vimentin filaments in mouse fibroblasts. J Cell Sci *103 (Pt 3)*, 689-698.

Cosker, K.E., Courchesne, S.L., and Segal, R.A. (2008). Action in the axon: generation and transport of signaling endosomes. Curr Opin Neurobiol *18*, 270-275.

Cosker, K.E., Pazyra-Murphy, M.F., Fenstermacher, S.J., and Segal, R.A. (2013). Target-derived neurotrophins coordinate transcription and transport of bclw to prevent axonal degeneration. J Neurosci *33*, 5195-5207.

Cosker, K.E., and Segal, R.A. (2014). Neuronal signaling through endocytosis. Cold Spring Harb Perspect Biol *6*.

Costa, C.J., and Willis, D.E. (2018). To the end of the line: Axonal mRNA transport and local translation in health and neurodegenerative disease. Dev Neurobiol *78*, 209-220.

Cui, B., Wu, C., Chen, L., Ramirez, A., Bearer, E.L., Li, W.P., Mobley, W.C., and Chu, S. (2007). One at a time, live tracking of NGF axonal transport using quantum dots. Proc Natl Acad Sci U S A *104*, 13666-13671.

Dajas-Bailador, F., Bonev, B., Garcez, P., Stanley, P., Guillemot, F., and Papalopulu, N. (2012). microRNA-9 regulates axon extension and branching by targeting Map1b in mouse cortical neurons. Nat Neurosci.

David, M.D., Yeramian, A., Duñach, M., Llovera, M., Cantí, C., de Herreros, A.G., Comella, J.X., and Herreros, J. (2008). Signalling by neurotrophins and hepatocyte growth factor regulates axon morphogenesis by differential beta-catenin phosphorylation. J Cell Sci *121*, 2718-2730.

Deglincerti, A., Liu, Y., Colak, D., Hengst, U., Xu, G., and Jaffrey, S.R. (2015). Coupled local translation and degradation regulate growth cone collapse. Nat Commun *6*, 6888.

Delcroix, J.D., Valletta, J.S., Wu, C., Hunt, S.J., Kowal, A.S., and Mobley, W.C. (2003). NGF signaling in sensory neurons: evidence that early endosomes carry NGF retrograde signals. Neuron *39*, 69-84.

Dieterich, D.C., Hodas, J.J.L., Gouzer, G., Shadrin, I.Y., Ngo, J.T., Triller, A., Tirrell, D.A., and Schuman, E.M. (2010). In situ visualization and dynamics of newly synthesized proteins in rat hippocampal neurons. Nature Neuroscience *13*, 897-U149.

Dobrowolski, R., and De Robertis, E.M. (2011). Endocytic control of growth factor signalling: multivesicular bodies as signalling organelles. Nat Rev Mol Cell Biol *13*, 53-60.

Dong, Q., Ji, Y.S., Cai, C., and Chen, Z.Y. (2012). LIM kinase 1 (LIMK1) interacts with tropomyosin-related kinase B (TrkB) and Mediates brain-derived neurotrophic factor (BDNF)-induced axonal elongation. J Biol Chem *287*, 41720-41731.

Dufner, A., and Thomas, G. (1999). Ribosomal S6 kinase signaling and the control of translation. Exp Cell Res *253*, 100-109.

Ehlers, M.D., Kaplan, D.R., Price, D.L., and Koliatsos, V.E. (1995). NGF-stimulated retrograde transport of trkA in the mammalian nervous system. J Cell Biol *130*, 149-156.

Emdal, K.B., Pedersen, A.K., Bekker-Jensen, D.B., Tsafou, K.P., Horn, H., Lindner, S., Schulte, J.H., Eggert, A., Jensen, L.J., Francavilla, C*., et al.* (2015). Temporal proteomics of NGF-TrkA signaling identifies an inhibitory role for the E3 ligase Cbl-b in neuroblastoma cell differentiation. Sci Signal *8*, ra40.

Fagan, A.M., Zhang, H., Landis, S., Smeyne, R.J., Silos-Santiago, I., and Barbacid, M. (1996). TrkA, but not TrkC, receptors are essential for survival of sympathetic neurons in vivo. J Neurosci *16*, 6208-6218.

Fan, A., Tofangchi, A., Kandel, M., Popescu, G., and Saif, T. (2017). Coupled circumferential and axial tension driven by actin and myosin influences in vivo axon diameter. Sci Rep *7*, 14188.

Fariñas, I., Wilkinson, G.A., Backus, C., Reichardt, L.F., and Patapoutian, A. (1998). Characterization of neurotrophin and Trk receptor functions in developing sensory ganglia: direct NT-3 activation of TrkB neurons in vivo. Neuron *21*, 325-334.

Fath, T., Ke, Y.D., Gunning, P., Gotz, J., and Ittner, L.M. (2009). Primary support cultures of hippocampal and substantia nigra neurons. Nat Protoc *4*, 78-85.

Finkbeiner, S., Tavazoie, S.F., Maloratsky, A., Jacobs, K.M., Harris, K.M., and Greenberg, M.E. (1997). CREB: a major mediator of neuronal neurotrophin responses. Neuron *19*, 1031-1047.

Finsterwald, C., Fiumelli, H., Cardinaux, J.R., and Martin, J.L. (2010). Regulation of dendritic development by BDNF requires activation of CRTC1 by glutamate. J Biol Chem *285*, 28587-28595.

Genheden, M., Kenney, J.W., Johnston, H.E., Manousopoulou, A., Garbis, S.D., and Proud, C.G. (2015). BDNF Stimulation of Protein Synthesis in Cortical Neurons Requires the MAP Kinase-Interacting Kinase MNK1. Journal of Neuroscience *35*, 972-984.

Geoffroy, C.G., Hilton, B.J., Tetzlaff, W., and Zheng, B. (2016). Evidence for an Age-Dependent Decline in Axon Regeneration in the Adult Mammalian Central Nervous System. Cell Rep *15*, 238-246.

Golan-Lavi, R., Giacomelli, C., Fuks, G., Zeisel, A., Sonntag, J., Sinha, S., Köstler, W., Wiemann, S., Korf, U., Yarden, Y.*, et al.* (2017). Coordinated Pulses of mRNA and of Protein Translation or Degradation Produce EGF-Induced Protein Bursts. Cell Rep *18*, 3129-3142.

Gomis-Rüth, S., Stiess, M., Wierenga, C.J., Meyn, L., and Bradke, F. (2014). Single-cell axotomy of cultured hippocampal neurons integrated in neuronal circuits. Nat Protoc *9*, 1028-1037.

Gong, X., Zhang, L., Huang, T., Lin, T.V., Miyares, L., Wen, J., Hsieh, L., and Bordey, A. (2015). Activating the translational repressor 4E-BP or reducing S6K-GSK3beta activity prevents accelerated axon growth induced by hyperactive mTOR in vivo. Hum Mol Genet *24*, 5746-5758.

Graef, I.A., Wang, F., Charron, F., Chen, L., Neilson, J., Tessier-Lavigne, M., and Crabtree, G.R. (2003). Neurotrophins and netrins require calcineurin/NFAT signaling to stimulate outgrowth of embryonic axons. Cell *113*, 657-670.

Grimes, M.L., Zhou, J., Beattie, E.C., Yuen, E.C., Hall, D.E., Valletta, J.S., Topp, K.S., LaVail, J.H., Bunnett, N.W., and Mobley, W.C. (1996). Endocytosis of activated TrkA: evidence that nerve growth factor induces formation of signaling endosomes. J Neurosci *16*, 7950-7964.

Groth, R.D., and Mermelstein, P.G. (2003). Brain-derived neurotrophic factor activation of NFAT (nuclear factor of activated T-cells)-dependent transcription: a role for the transcription factor NFATc4 in neurotrophin-mediated gene expression. J Neurosci *23*, 8125-8134.

Guo, W., Ji, Y., Wang, S., Sun, Y., and Lu, B. (2014). Neuronal activity alters BDNF-TrkB signaling kinetics and downstream functions. J Cell Sci *127*, 2249-2260.

Gupta, V.K., You, Y., Gupta, V.B., Klistorner, A., and Graham, S.L. (2013). TrkB receptor signalling: implications in neurodegenerative, psychiatric and proliferative disorders. Int J Mol Sci *14*, 10122-10142.

Hanamura, K., Harada, A., Katoh-Semba, R., Murakami, F., and Yamamoto, N. (2004). BDNF and NT-3 promote thalamocortical axon growth with distinct substrate and temporal dependency. Eur J Neurosci *19*, 1485-1493.

Harrington, A.W., and Ginty, D.D. (2013). Long-distance retrograde neurotrophic factor signalling in neurons. Nat Rev Neurosci *14*, 177-187.

Harrington, A.W., St Hillaire, C., Zweifel, L.S., Glebova, N.O., Philippidou, P., Halegoua, S., and Ginty, D.D. (2011). Recruitment of actin modifiers to TrkA endosomes governs retrograde NGF signaling and survival. Cell *146*, 421-434.

Harward, S.C., Hedrick, N.G., Hall, C.E., Parra-Bueno, P., Milner, T.A., Pan, E., Laviv, T., Hempstead, B.L., Yasuda, R., and McNamara, J.O. (2016). Autocrine BDNF-TrkB signalling within a single dendritic spine. Nature *538*, 99-103.

Heerssen, H.M., Pazyra, M.F., and Segal, R.A. (2004). Dynein motors transport activated Trks to promote survival of target-dependent neurons. Nat Neurosci *7*, 596-604.

Hengst, U., Deglincerti, A., Kim, H.J., Jeon, N.L., and Jaffrey, S.R. (2009). Axonal elongation triggered by stimulus-induced local translation of a polarity complex protein. Nat Cell Biol *11*, 1024-1030.

Hoeller, D., Volarevic, S., and Dikic, I. (2005). Compartmentalization of growth factor receptor signalling. Curr Opin Cell Biol *17*, 107-111.

Hofer, M., Pagliusi, S.R., Hohn, A., Leibrock, J., and Barde, Y.A. (1990). Regional distribution of brain-derived neurotrophic factor mRNA in the adult mouse brain. EMBO J *9*, 2459-2464.

Holz, M.K., and Blenis, J. (2005). Identification of S6 kinase 1 as a novel mammalian target of rapamycin (mTOR)-phosphorylating kinase. J Biol Chem *280*, 26089-26093.

Horgan, C.P., and McCaffrey, M.W. (2011). Rab GTPases and microtubule motors. Biochem Soc Trans *39*, 1202-1206.

Hou, Z., He, L., and Qi, R.Z. (2007). Regulation of s6 kinase 1 activation by phosphorylation at ser-411. J Biol Chem *282*, 6922-6928.

Howe, C.L., and Mobley, W.C. (2005). Long-distance retrograde neurotrophic signaling. Curr Opin Neurobiol *15*, 40-48.

Howe, C.L., Valletta, J.S., Rusnak, A.S., and Mobley, W.C. (2001). NGF signaling from clathrin-coated vesicles: evidence that signaling endosomes serve as a platform for the Ras-MAPK pathway. Neuron *32*, 801-814.

Huang, E.J., and Reichardt, L.F. (2003). Trk receptors: roles in neuronal signal transduction. Annu Rev Biochem *72*, 609-642.

Hur, E.M., Saijilafu, Lee, B.D., Kim, S.J., Xu, W.L., and Zhou, F.Q. (2011). GSK3 controls axon growth via CLASP-mediated regulation of growth cone microtubules. Genes Dev *25*, 1968-1981.

Impey, S., McCorkle, S.R., Cha-Molstad, H., Dwyer, J.M., Yochum, G.S., Boss, J.M., McWeeney, S., Dunn, J.J., Mandel, G., and Goodman, R.H. (2004). Defining the CREB regulon: a genome-wide analysis of transcription factor regulatory regions. Cell *119*, 1041-1054.

Ito, K., and Enomoto, H. (2016). Retrograde transport of neurotrophic factor signaling: implications in neuronal development and pathogenesis. J Biochem *160*, 77-85.

Ji, Y., Lu, Y., Yang, F., Shen, W., Tang, T.T., Feng, L., Duan, S., and Lu, B. (2010). Acute and gradual increases in BDNF concentration elicit distinct signaling and functions in neurons. Nat Neurosci *13*, 302-309.

Jia, Y., Zhou, J., Tai, Y., and Wang, Y. (2007). TRPC channels promote cerebellar granule neuron survival. Nat Neurosci *10*, 559-567.

Jovic, A., Howell, B., and Takayama, S. (2009). Timing is everything: using fluidics to understand the role of temporal dynamics in cellular systems. Microfluidics and Nanofluidics *6*, 717-729.

Jung, H.S., Yoon, B.C., and Holt, C.E. (2012). Axonal mRNA localization and local protein synthesis in nervous system assembly, maintenance and repair. Nature Reviews Neuroscience *13*, 308-324.

Kao, H.T., Ryoo, K., Lin, A., Janoschka, S.R., Augustine, G.J., and Porton, B. (2017). Synapsins regulate brain-derived neurotrophic factor-mediated synaptic potentiation and axon elongation by acting on membrane rafts. Eur J Neurosci *45*, 1085-1101.

Kharebava, G., Makonchuk, D., Kalita, K.B., Zheng, J.J., and Hetman, M. (2008). Requirement of 3-phosphoinositide-dependent protein kinase-1 for BDNF-mediated neuronal survival. J Neurosci *28*, 11409-11420.

Kholodenko, B.N. (2006). Cell-signalling dynamics in time and space. Nat Rev Mol Cell Biol *7*, 165-176.

Kim, J.Y., and Jaffrey, S.R. (2016). Separating neuronal compartments gives clues as to local effect of ubiquitin conjugates in synaptogenesis. J Cell Biol *212*, 751-753.

Kim, M.S., Shutov, L.P., Gnanasekaran, A., Lin, Z., Rysted, J.E., Ulrich, J.D., and Usachev, Y.M. (2014). Nerve growth factor (NGF) regulates activity of nuclear factor of activated T-cells (NFAT) in neurons via the phosphatidylinositol 3-kinase (PI3K)-Akt-glycogen synthase kinase 3β (GSK3β) pathway. J Biol Chem *289*, 31349-31360.

Kim, S.R., Kareva, T., Yarygina, O., Kholodilov, N., and Burke, R.E. (2012). AAV transduction of dopamine neurons with constitutively active Rheb protects from neurodegeneration and mediates axon regrowth. Mol Ther *20*, 275-286.

Knusel, B., Gao, H., Okazaki, T., Yoshida, T., Mori, N., Hefti, F., and Kaplan, D.R. (1997). Ligand-induced down-regulation of Trk messenger RNA, protein and tyrosine phosphorylation in rat cortical neurons. Neuroscience *78*, 851-862.

Koch, D., Rosoff, W.J., Jiang, J., Geller, H.M., and Urbach, J.S. (2012). Strength in the periphery: growth cone biomechanics and substrate rigidity response in peripheral and central nervous system neurons. Biophys J *102*, 452-460.

Kuruvilla, R., Ye, H., and Ginty, D.D. (2000). Spatially and functionally distinct roles of the PI3-K effector pathway during NGF signaling in sympathetic neurons. Neuron *27*, 499-512.

Kuruvilla, R., Zweifel, L.S., Glebova, N.O., Lonze, B.E., Valdez, G., Ye, H., and Ginty, D.D. (2004). A neurotrophin signaling cascade coordinates sympathetic neuron development through differential control of TrkA trafficking and retrograde signaling. Cell *118*, 243-255.

Lai, K.O., Liang, Z., Fei, E., Huang, H., and Ip, N.Y. (2015). Cyclin-dependent Kinase 5 (Cdk5)-dependent Phosphorylation of p70 Ribosomal S6 Kinase 1 (S6K) Is Required for Dendritic Spine Morphogenesis. J Biol Chem *290*, 14637-14646.

Lazo, O.M., Gonzalez, A., Ascaño, M., Kuruvilla, R., Couve, A., and Bronfman, F.C. (2013). BDNF regulates Rab11-mediated recycling endosome dynamics to induce dendritic branching. J Neurosci *33*, 6112-6122.

Le Roy, C., and Wrana, J.L. (2005). Clathrin- and non-clathrin-mediated endocytic regulation of cell signalling. Nat Rev Mol Cell Biol *6*, 112-126.

Leal, G., Comprido, D., and Duarte, C.B. (2014). BDNF-induced local protein synthesis and synaptic plasticity. Neuropharmacology *76 Pt C*, 639-656.

Lee, S.I., Zhang, W., Ravi, M., Weschenfelder, M., Bastmeyer, M., and Levine, J.M. (2013). Atypical protein kinase C and Par3 are required for proteoglycan-induced axon growth inhibition. J Neurosci *33*, 2541-2554.

Lemmon, M.A., and Schlessinger, J. (2010). Cell signaling by receptor tyrosine kinases. Cell *141*, 1117-1134.

Levi-Montalcini, R. (1987). The nerve growth factor 35 years later. Science *237*, 1154-1162.

Levi-Montalcini, R., and Booker, B. (1960). Excessive growth of the sympathetic ganglia evoked by a protein isolated from mouse salivary glands. Proc Natl Acad Sci USA *46*, 373-384.

Liao, L., Pilotte, J., Xu, T., Wong, C.C., Edelman, G.M., Vanderklish, P., and Yates, J.R. (2007). BDNF induces widespread changes in synaptic protein content and up-regulates components of the translation machinery: an analysis using high-throughput proteomics. J Proteome Res *6*, 1059-1071.

Lilienbaum, A., Legagneux, V., Portier, M.M., Dellagi, K., and Paulin, D. (1986). Vimentin gene: expression in human lymphocytes and in Burkitt's lymphoma cells. EMBO J *5*, 2809-2814.

Lonze, B.E., and Ginty, D.D. (2002). Function and regulation of CREB family transcription factors in the nervous system. Neuron *35*, 605-623.

Ma, X.M., and Blenis, J. (2009). Molecular mechanisms of mTOR-mediated translational control. Nat Rev Mol Cell Biol *10*, 307-318.

Magnuson, B., Ekim, B., and Fingar, D.C. (2012). Regulation and function of ribosomal protein S6 kinase (S6K) within mTOR signalling networks. Biochem J *441*, 1-21.

Manning, B.D., and Toker, A. (2017). AKT/PKB Signaling: Navigating the Network. Cell *169*, 381-405.

Melo, C.V., Mele, M., Curcio, M., Comprido, D., Silva, C.G., and Duarte, C.B. (2013). BDNF regulates the expression and distribution of vesicular glutamate transporters in cultured hippocampal neurons. PLoS One *8*, e53793.

Mendoza, M.C., Er, E.E., and Blenis, J. (2011). The Ras-ERK and PI3K-mTOR pathways: cross-talk and compensation. Trends Biochem Sci *36*, 320-328.

Messaoudi, E., Ying, S.W., Kanhema, T., Croll, S.D., and Bramham, C.R. (2002). Brain-derived neurotrophic factor triggers transcription-dependent, late phase long-term potentiation in vivo. J Neurosci *22*, 7453-7461.

Minichiello, L. (2009). TrkB signalling pathways in LTP and learning. Nat Rev Neurosci *10*, 850-860.

Minoura, I., Takazaki, H., Ayukawa, R., Saruta, C., Hachikubo, Y., Uchimura, S., Hida, T., Kamiguchi, H., Shimogori, T., and Muto, E. (2016). Reversal of axonal growth defects in an extraocular fibrosis model by engineering the kinesin-microtubule interface. Nat Commun *7*, 10058.

Mita, T., Mayanagi, T., Ichijo, H., Fukumoto, K., Otsuka, K., Sakai, A., and Sobue, K. (2016). Docosahexaenoic Acid Promotes Axon Outgrowth by Translational Regulation of Tau and Collapsin Response Mediator Protein 2 Expression. J Biol Chem *291*, 4955-4965.

Mitchell, D.J., Blasier, K.R., Jeffery, E.D., Ross, M.W., Pullikuth, A.K., Suo, D., Park, J., Smiley, W.R., Lo, K.W., Shabanowitz, J.*, et al.* (2012). Trk activation of the ERK1/2 kinase pathway stimulates intermediate chain phosphorylation and recruits cytoplasmic dynein to signaling endosomes for retrograde axonal transport. J Neurosci *32*, 15495-15510.

Mitre, M., Mariga, A., and Chao, M.V. (2017). Neurotrophin signalling: novel insights into mechanisms and pathophysiology. Clin Sci (Lond) *131*, 13-23.

Mondal, A., Black, B., Kim, Y.T., and Mohanty, S. (2014). Loop formation and self-fasciculation of cortical axon using photonic guidance at long working distance. Sci Rep *4*, 6902.

Mrass, P., Oruganti, S.R., Fricke, G.M., Tafoya, J., Byrum, J.R., Yang, L., Hamilton, S.L., Miller, M.J., Moses, M.E., and Cannon, J.L. (2017). ROCK regulates the intermittent mode of interstitial T cell migration in inflamed lungs. Nat Commun *8*, 1010.

Nagahara, A.H., and Tuszynski, M.H. (2011). Potential therapeutic uses of BDNF in neurological and psychiatric disorders. Nat Rev Drug Discov *10*, 209-219.

Nakamuta, S., Funahashi, Y., Namba, T., Arimura, N., Picciotto, M.R., Tokumitsu, H., Soderling, T.R., Sakakibara, A., Miyata, T., Kamiguchi, H.*, et al.* (2011). Local application of neurotrophins specifies axons through inositol 1,4,5-trisphosphate, calcium, and Ca2+/calmodulin-dependent protein kinases. Sci Signal *4*, ra76.

Namekata, K., Harada, C., Guo, X., Kimura, A., Kittaka, D., Watanabe, H., and Harada, T. (2012). Dock3 stimulates axonal outgrowth via GSK-3β-mediated microtubule assembly. J Neurosci *32*, 264-274.

Nie, D., Di Nardo, A., Han, J.M., Baharanyi, H., Kramvis, I., Huynh, T., Dabora, S., Codeluppi, S., Pandolfi, P.P., Pasquale, E.B.*, et al.* (2010). Tsc2-Rheb signaling regulates EphA-mediated axon guidance. Nat Neurosci *13*, 163-172.

Ozdinler, P.H., and Macklis, J.D. (2006). IGF-I specifically enhances axon outgrowth of corticospinal motor neurons. Nat Neurosci *9*, 1371-1381.

Park, K.K., Liu, K., Hu, Y., Smith, P.D., Wang, C., Cai, B., Xu, B., Connolly, L., Kramvis, I., Sahin, M.*, et al.* (2008). Promoting axon regeneration in the adult CNS by modulation of the PTEN/mTOR pathway. Science *322*, 963-966.

Pazyra-Murphy, M.F., Hans, A., Courchesne, S.L., Karch, C., Cosker, K.E., Heerssen, H.M., Watson, F.L., Kim, T., Greenberg, M.E., and Segal, R.A. (2009). A retrograde neuronal survival response: target-derived neurotrophins regulate MEF2D and bcl-w. J Neurosci *29*, 6700-6709.

Polleux, F., and Snider, W. (2010). Initiating and growing an axon. Cold Spring Harb Perspect Biol *2*, a001925.

Poo, M.M. (2001). Neurotrophins as synaptic modulators. Nat Rev Neurosci *2*, 24-32.
Raiborg, C., and Stenmark, H. (2009). The ESCRT machinery in endosomal sorting of ubiquitylated membrane proteins. Nature *458*, 445-452.

Rangaraju, V., Tom Dieck, S., and Schuman, E.M. (2017). Local translation in neuronal compartments: how local is local? EMBO Rep *18*, 693-711.

Reichardt, L.F. (2006). Neurotrophin-regulated signalling pathways. Philos Trans R Soc Lond B Biol Sci *361*, 1545-1564.

Riccio, A., Pierchala, B.A., Ciarallo, C.L., and Ginty, D.D. (1997). An NGF-TrkA-mediated retrograde signal to transcription factor CREB in sympathetic neurons. Science *277*, 1097-1100.

Ring, R.H., Alder, J., Fennell, M., Kouranova, E., Black, I.B., and Thakker-Varia, S. (2006). Transcriptional profiling of brain-derived-neurotrophic factor-induced neuronal plasticity: a novel role for nociceptin in hippocampal neurite outgrowth. J Neurobiol *66*, 361-377.

Roskoski, R. (2012). ERK1/2 MAP kinases: structure, function, and regulation. Pharmacol Res *66*, 105-143.

Saijilafu, Hur, E.M., Liu, C.M., Jiao, Z., Xu, W.L., and Zhou, F.Q. (2013). PI3K-GSK3 signalling regulates mammalian axon regeneration by inducing the expression of Smad1. Nat Commun *4*, 2690.

Sasi, M., Vignoli, B., Canossa, M., and Blum, R. (2017). Neurobiology of local and intercellular BDNF signaling. Pflugers Arch *469*, 593-610.

Saxton, R.A., and Sabatini, D.M. (2017). mTOR Signaling in Growth, Metabolism, and Disease. Cell *168*, 960-976.

Schratt, G.M., Nigh, E.A., Chen, W.G., Hu, L., and Greenberg, M.E. (2004). BDNF regulates the translation of a select group of mRNAs by a mammalian target of rapamycin-phosphatidylinositol 3-kinase-dependent pathway during neuronal development. Journal of Neuroscience *24*, 7366-7377.

Shimobayashi, M., and Hall, M.N. (2014). Making new contacts: the mTOR network in metabolism and signalling crosstalk. Nat Rev Mol Cell Biol *15*, 155-162.

Skaliora, I., Adams, R., and Blakemore, C. (2000). Morphology and growth patterns of developing thalamocortical axons. J Neurosci *20*, 3650-3662.

Skylaki, S., Hilsenbeck, O., and Schroeder, T. (2016). Challenges in long-term imaging and quantification of single-cell dynamics. Nat Biotechnol *34*, 1137-1144.

Sofroniew, M.V., Howe, C.L., and Mobley, W.C. (2001). Nerve growth factor signaling, neuroprotection, and neural repair. Annu Rev Neurosci *24*, 1217-1281.

Sommerfeld, M.T., Schweigreiter, R., Barde, Y.A., and Hoppe, E. (2000). Down-regulation of the neurotrophin receptor TrkB following ligand binding. Evidence for an involvement of the proteasome and differential regulation of TrkA and TrkB. J Biol Chem *275*, 8982-8990.

Sorkin, A., and von Zastrow, M. (2009). Endocytosis and signalling: intertwining molecular networks. Nat Rev Mol Cell Biol *10*, 609-622.

Suo, D., Park, J., Harrington, A.W., Zweifel, L.S., Mihalas, S., and Deppmann, C.D. (2014). Coronin-1 is a neurotrophin endosomal effector that is required for developmental competition for survival. Nat Neurosci *17*, 36-45.

Takano, T., Wu, M., Nakamuta, S., Naoki, H., Ishizawa, N., Namba, T., Watanabe, T., Xu, C., Hamaguchi, T., Yura, Y.*, et al.* (2017). Discovery of long-range inhibitory signaling to ensure single axon formation. Nat Commun *8*, 33.

Takei, N., Inamura, N., Kawamura, M., Namba, H., Hara, K., Yonezawa, K., and Nawa, H. (2004). Brain-derived neurotrophic factor induces mammalian target of rapamycin-dependent local activation of translation machinery and protein synthesis in neuronal dendrites. J Neurosci *24*, 9760-9769.

Takei, N., Kawamura, M., Hara, K., Yonezawa, K., and Nawa, H. (2001). Brain-derived neurotrophic factor enhances neuronal translation by activating multiple initiation processes: comparison with the effects of insulin. J Biol Chem *276*, 42818-42825.

Tasdemir-Yilmaz, O.E., and Segal, R.A. (2016). There and back again: coordinated transcription, translation and transport in axonal survival and regeneration. Curr Opin Neurobiol *39*, 62-68.

Taylor, A.M., Blurton-Jones, M., Rhee, S.W., Cribbs, D.H., Cotman, C.W., and Jeon, N.L. (2005). A microfluidic culture platform for CNS axonal injury, regeneration and transport. Nat Methods *2*, 599-605.

Terenzio, M., Schiavo, G., and Fainzilber, M. (2017). Compartmentalized Signaling in Neurons: From Cell Biology to Neuroscience. Neuron *96*, 667-679.

Thoenen, H., and Sendtner, M. (2002). Neurotrophins: from enthusiastic expectations through sobering experiences to rational therapeutic approaches. Nat Neurosci *5 Suppl*, 1046-1050.

Thoreen, C.C., Kang, S.A., Chang, J.W., Liu, Q., Zhang, J., Gao, Y., Reichling, L.J., Sim, T., Sabatini, D.M., and Gray, N.S. (2009). An ATP-competitive mammalian target of rapamycin inhibitor reveals rapamycin-resistant functions of mTORC1. J Biol Chem *284*, 8023-8032.

Tsui-Pierchala, B.A., and Ginty, D.D. (1999). Characterization of an NGF-P-TrkA retrograde-signaling complex and age-dependent regulation of TrkA phosphorylation in sympathetic neurons. J Neurosci *19*, 8207-8218.

Valdez, G., Philippidou, P., Rosenbaum, J., Akmentin, W., Shao, Y., and Halegoua, S. (2007). Trk-signaling endosomes are generated by Rac-dependent macroendocytosis. Proc Natl Acad Sci U S A *104*, 12270-12275.

Wang, B., Pan, L., Wei, M., Wang, Q., Liu, W.W., Wang, N., Jiang, X.Y., Zhang, X., and Bao, L. (2015). FMRP-Mediated Axonal Delivery of miR-181d Regulates Axon Elongation by Locally Targeting Map1b and Calm1. Cell Rep *13*, 2794-2807.

Wang, J.D., Douville, N.J., Takayama, S., and ElSayed, M. (2012). Quantitative analysis of molecular absorption into PDMS microfluidic channels. Ann Biomed Eng *40*, 1862-1873.
Wang, L., Liang, Z., and Li, G. (2011). Rab22 controls NGF signaling and neurite outgrowth in PC12 cells. Mol Biol Cell *22*, 3853-3860.

Wang, Y., Su, B., and Xia, Z. (2006). Brain-derived neurotrophic factor activates ERK5 in cortical neurons via a Rap1-MEKK2 signaling cascade. J Biol Chem *281*, 35965-35974.

Watson, F.L., Heerssen, H.M., Bhattacharyya, A., Klesse, L., Lin, M.Z., and Segal, R.A. (2001). Neurotrophins use the Erk5 pathway to mediate a retrograde survival response. Nat Neurosci *4*, 981-988.

Weissmiller, A.M., Natera-Naranjo, O., Reyna, S.M., Pearn, M.L., Zhao, X., Nguyen, P., Cheng, S., Goldstein, L.S., Tanzi, R.E., Wagner, S.L.*, et al.* (2015). A γ-secretase inhibitor, but not a γ-secretase modulator, induced defects in BDNF axonal trafficking and signaling: evidence for a role for APP. PLoS One *10*, e0118379.

Wickramasinghe, S.R., Alvania, R.S., Ramanan, N., Wood, J.N., Mandai, K., and Ginty, D.D. (2008). Serum response factor mediates NGF-dependent target innervation by embryonic DRG sensory neurons. Neuron *58*, 532-545.

Ye, H., Kuruvilla, R., Zweifel, L.S., and Ginty, D.D. (2003). Evidence in support of signaling endosome-based retrograde survival of sympathetic neurons. Neuron *39*, 57-68.

Ye, M., Lehigh, K.M., and Ginty, D.D. (2018). Multivesicular bodies mediate long-range retrograde NGF-TrkA signaling. Elife *7*.

Yin, Y., Edelman, G.M., and Vanderklish, P.W. (2002). The brain-derived neurotrophic factor enhances synthesis of Arc in synaptoneurosomes. Proc Natl Acad Sci U S A *99*, 2368-2373.

Yogev, S., and Shen, K. (2017). Establishing Neuronal Polarity with Environmental and Intrinsic Mechanisms. Neuron *96*, 638-650.

Yosef, N., and Regev, A. (2011). Impulse control: temporal dynamics in gene transcription. Cell *144*, 886-896.

Yoshimura, T., Kawano, Y., Arimura, N., Kawabata, S., Kikuchi, A., and Kaibuchi, K. (2005). GSK-3beta regulates phosphorylation of CRMP-2 and neuronal polarity. Cell *120*, 137-149.

Zahavi, E.E., Ionescu, A., Gluska, S., Gradus, T., Ben-Yaakov, K., and Perlson, E. (2015). A compartmentalized microfluidic neuromuscular co-culture system reveals spatial aspects of GDNF functions. J Cell Sci *128*, 1241-1252.

Zahavi, E.E., Maimon, R., and Perlson, E. (2017). Spatial-specific functions in retrograde neuronal signalling. Traffic *18*, 415-424.

Zahavi, E.E., Steinberg, N., Altman, T., Chein, M., Joshi, Y., Gradus-Pery, T., and Perlson, E. (2018). The receptor tyrosine kinase TrkB signals without dimerization at the plasma membrane. Sci Signal *11*.

Zeng, H., and Sanes, J.R. (2017). Neuronal cell-type classification: challenges, opportunities and the path forward. Nat Rev Neurosci *18*, 530-546.

Zhang, Y., Chopp, M., Liu, X.S., Katakowski, M., Wang, X., Tian, X., Wu, D., and Zhang, Z.G. (2017). Exosomes Derived from Mesenchymal Stromal Cells Promote Axonal Growth of Cortical Neurons. Mol Neurobiol *54*, 2659-2673.

Zhang, Y., Ueno, Y., Liu, X.S., Buller, B., Wang, X., Chopp, M., and Zhang, Z.G. (2013). The MicroRNA-17-92 cluster enhances axonal outgrowth in embryonic cortical neurons. J Neurosci *33*, 6885-6894.

Zheng, J., Shen, W.H., Lu, T.J., Zhou, Y., Chen, Q., Wang, Z., Xiang, T., Zhu, Y.C., Zhang, C., Duan, S.*, et al.* (2008). Clathrin-dependent endocytosis is required for TrkB-dependent Akt-mediated neuronal protection and dendritic growth. J Biol Chem *283*, 13280-13288.

Zhou, B., Cai, Q., Xie, Y., and Sheng, Z.H. (2012). Snapin recruits dynein to BDNF-TrkB signaling endosomes for retrograde axonal transport and is essential for dendrite growth of cortical neurons. Cell Rep *2*, 42-51.

Zweifel, L.S., Kuruvilla, R., and Ginty, D.D. (2005). Functions and mechanisms of retrograde neurotrophin signalling. Nat Rev Neurosci *6*, 615-625.